EXAMINATION OF ESTUARINE SEDIMENT DYNAMICS: INSIGHTS FROM THE LARGE, SHALLOW, ALBEMARLE-PAMLICO ESTUARINE SYSTEM, NC, U.S.A.

by

Devon Olivola Eulie

Dissertation Co-Advisor: D. Reide Corbett, PhD

Dissertation Co-Advisor: J.P. Walsh, PhD

Major Department: Coastal Resources Management

ABSTRACT

This dissertation investigated the dynamics of estuarine shorelines in the Albemarle-Pamlico Estuarine System (APES). Shoreline change is influenced by human activities (e.g., shoreline modification), and natural processes (e.g., waves, storms, and sea-level rise) on variable temporal and spatial scales in the coastal zone. This research examined the spatio-temporal dynamics of shoreline change, the drivers of that change, and the role of shoreline erosion in the sediment dynamics of the larger estuarine system. Historical rates of change were found to be comparable to previous studies at -0.5 ± 0.07 m yr^{-1}. Decadal and sub-annual rates of change were highly variable over the study, both spatially and temporally. However, linear regression models indicate that the large changes in shoreline position observed in high-frequency (bi-monthly) surveys are captured within the long-term (historical) average rate of shoreline change. Simulations from a coupled hydrodynamic and wave model indicate that waves and storms (hurricanes) are important drivers of shoreline change. Wave energy along

different shorelines was found to be dependent on shorezone characteristics such as shoreline orientation, wind direction and fetch, and nearshore bathymetry.

The role of shoreline erosion in the sediment dynamics of the larger estuarine system was also investigated for a region of the APES, the Tar-Pamlico estuary. Shoreline erosion and shoreline modification were examined within the estuary in order to explore the significance of erosion as a source of fine sediment to the estuary. Sediment storage was also evaluated for the Tar-Pamlico estuary using rates of sediment accumulation determined from the radionuclide tracers of ^{210}Pb and ^{137}Cs. A fine sediment budget was constructed for the Tar-Pamlico estuary. The budget indicates that eroding wetland shorelines represent a significant (43% of total fine sediment input) source of material to the estuary. Also, the majority of fine sediment is retained within zones of accumulation within the estuary, with only about 7% potentially exported to the adjacent Pamlico Sound.

Overall, this research highlights the dynamic process of estuarine shoreline change, and the role of that change in the functioning of the larger estuarine system. Coastal managers need to incorporate an understanding and accommodation of these processes into future management plans for North Carolina's estuarine shorelines.

EXAMINATION OF ESTUARINE SEDIMENT DYNAMICS: INSIGHTS FROM THE LARGE, SHALLOW, ALBEMARLE-PAMLICO ESTUARINE SYSTEM, NC, U.S.A.

A Dissertation

Presented To the Faculty of the Institute for Coastal Science and Policy

East Carolina University

In Partial Fulfillment of the Requirements for the Degree

Coastal Resources Management

Primary Concentration in Coastal Geosciences

Secondary Concentrations in Coastal & Estuarine Ecology and Social Science & Coastal Policy

By

Devon Olivola Eulie

May, 2014

EXAMINATION OF ESTUARINE SEDIMENT DYNAMICS: INSIGHTS FROM THE LARGE, SHALLOW, ALBEMARLE-PAMLICO ESTUARINE SYSTEM, NC, U.S.A

by

Devon Olivola Eulie

APPROVED BY:

CO-DIRECTOR OF
DISSERTATION/THESIS: _____
(D. Reide Corbett, PhD)

CO-DIRECTOR OF
DISSERTATION/THESIS: _____
(J.P. Walsh, PhD)

COMMITTEE MEMBER: _____
(Thomas R. Allen, PhD)

COMMITTEE MEMBER: _____
(Ryan P. Mulligan, PhD)

COMMITTEE MEMBER: _____
(Terry West, PhD)

CHAIR OF THE DEPARTMENT
OF COASTAL RESOURCES MANAGEMENT: _____
(Hans Vogelsong, PhD)

DEAN OF THE
GRADUATE SCHOOL: _____
(Paul J. Gemperline, PhD)

ACKNOWLEDGEMENTS

I would like to thank the many people who have contributed to the completion of this dissertation. Foremost, I thank my advisors, Drs. Reide Corbett and J.P. Walsh, for providing me with this incredible opportunity. Without their constant support and patience during my time at East Carolina University this work would not have been possible. I would also like to thank my dissertation committee, Tom Allen, Ryan Mulligan, and Terry West for their support. I could not have completed this work without their assistance and guidance. I would especially like to thank Ryan Mulligan for spending countless hours on long-distance phone meetings.

I would also like to thank Dr. Hans Vogelsong, Director of the Coastal Resources Management Program, as well as the staff and faculty of the Institute for Coastal Science and Policy; Dr. John Rummel, Ms. Kay Evans, and Ms. Cindy Harper. I am very grateful to the assistance and support of John Woods and Jim Watson, without whom much of this research could not have been completed. I would also like to thank Dr. Chester Jackson for his academic advice and for providing me with his program AMBUR, which was instrumental in the completion of this work. Thank you to the Albemarle-Pamlico National Estuary Program, the North Carolina Division of Coastal Management, and the Institute for Coastal Science and Policy for providing funding for this research. Also, thanks to Kevin Bischof (Goose Creek State Park), Dale Davis (Gull Rock Gameland), and Bo Dame (Kitty Hawk Estuarine Research Reserve) for their permission and assistance in utilizing the coastal areas under their management for research. A special thanks also to Dr. Lauriston King, the first director of the CRM program.

I was honored to receive assistance in the collection of field data from many undergraduate and graduate students during the course of this research; Stephanie Balbuena, Brian Burgess, Robbie Broda, Ian Conery, Michelle Covi, Jen Cudney, Andrew Dietsche, Anne Ditlevson, Andrea Dell'Apa, Scott Elkins, Nate Gwyn, Joey Kiker, Cecilia Krahforst, Kelli

Moran, William Rouse, Casey Smith, Eric Thornton, and David Young. I am especially grateful for the moral support and advice of Cecilia Krahforst, Michelle Covi, Reanna Camp, David Lagomasino, Kat Marciniak, and my coffee companions, Maheanai Kaneshiro-Pineiro and Joey Kiker. Finally, I could not have completed this degree without the incredible support and love of my family, my parents, Mark and Joan Olivola; my brother, Matt Olivola; my friend and sister-in-law, Sarah Olivola. I especially thank my wonderful husband, Evan Eulie, for his incredible support and love. This would have been impossible without his unconditional support while I completed this degree.

TABLE OF CONTENTS

CHAPTER 1

Introduction

1.0 Research Significance

Coastal zones are important areas that encompass a range of terrestrial and aquatic ecosystems that provide essential goods and services to both humans and the larger ecosystem. Humans utilize the coastal zone for recreation, resource extraction, transportation, and benefit directly and indirectly from the biophysical processes that operate along the coast. Over 50% of the United States population lives within the coastal zone and directly utilizes its resources (Crossett et al. 2004). Over the last century the rate of development has steadily increased (Camfield and Morang 1996). Many people rely on resources such as aquatic life (commercial and recreational fishing) and less tangible things such as beach serenity and striking viewscapes (tourism). Ecologically, the coastal zone represents a transition between marine and terrestrial systems and is an area vulnerable to change, both natural and anthropogenic (Poulter et al., 2009). As our utilization of the coast increases, there is greater potential for conflict between different stakeholders (Charlier and De Meyer 1998). Also, the emergence of more uses for coastal resources (e.g., off-shore wind farms) and awareness of future issues (e.g., sea-level rise) creates new problems for coastal managers, and in many cases, policy has yet to develop addressing these challenges (Charlier and De Meyer 1998).

North Carolina includes thousands of miles of oceanic, estuarine, and riverine shoreline in twenty counties designated as "coastal" or CAMA (Coastal Area Management Act) counties (Deaton et al. 2010; Geis and Bendell 2010). These include the beaches of the Outer Bank, extensive wetlands (marshes and swamps), and a growing number of engineered shorelines (Corbett et al. 2008; Poulter et al. 2009). Over the last several decades most CAMA counties have steadily grown in population (Beatley et al. 2002; Stuart 2010). Census data shows that from 1990 to 2000, 18 of the State's CAMA counties gained in population, and 12 exhibited at

least a 10% growth (Stuart 2010). Impressively, five of these counties, all part of the Outer Banks coastal zone, experienced a 30% or more growth in population (Stuart 2010). In comparison, the national average increase in the population of coastal counties was about 12% (Beatley et al. 2002). With this increase in the coastal population comes the expansion of coastal infrastructure. As more high-value and dense development occurs, the costs associated with both protecting and recovering from the impacts of coastal hazards such as shoreline erosion, sea-level rise, and hurricane winds, also rises (Beatley et al. 2002). A study by the Heinz Center estimated that the cost of property loss due to coastal erosion alone was $500 million per year nationally (NRC 2007).

Ocean shoreline erosion has long been recognized as an important coastal issue in North Carolina, and more recently, erosion of the estuarine shoreline has been identified as a significant concern (Corbett et al. 2008; Riggs and Ames 2003). Research in estuaries has documented zones of accretion and rates of erosion as high as over seven meters per year (Bellis et al. 1975; Corbett et al. 2008; Cowart 2011; Riggs 2001; Riggs and Ames 2003). Early studies in North Carolina identified possible responses or policies that could mitigate future shoreline erosion and the impact of development on the coastal zone (i.e., see recommendations in Bellis et al. 1975). North Carolina was the first coastal state to participate in the Coastal Zone Management Program, and their Coastal Area Management Act went into effect in 1974 (NOAA 2010). North Carolina is also one of the few coastal states with a regulatory ban on the building of permanent stabilization structures on the ocean shoreline (Christie 1994; Kittinger and Ayers 2010; Nordstrom 1992). However, no such ban exists for the estuarine shoreline, and over the years, there has been extensive modification. A report from the North Carolina Division of Coastal Management calculated the percent of estuarine shoreline that is modified or “hardened”

in the twenty CAMA counties at 5%, and in seven of the twenty counties, the average is over 5% (McVerry 2012). In comparison, 50 to 75% of the shoreline is modified by structures in New Jersey, San Diego, and the Chesapeake Bay (Erdle et al. 2006). However, the growing modification of the estuarine shoreline in North Carolina should be viewed as a precursor to the heavily engineered shore environment seen elsewhere (Erdle et al. 2006).

The purpose of this dissertation research is to investigate the dynamics of estuarine shoreline change in the large, shallow, Albemarle-Pamlico Estuarine system (APES) of North Carolina with the goal of informing management decisions. Specific objectives were to: 1) explore the utility of new remote sensing techniques for observing rapid shoreline change, 2) examine the temporal and spatial variability of estuarine shoreline change and evaluate drivers of that change, 3) determine the significance of shoreline erosion as a source of fine sediments to the estuarine system, and 4) identify the potential impacts of shoreline hardening on the system and the implications for future coastal management in North Carolina.

2.0 Estuarine Shorelines

The land-water interface is a complex area where terrestrial and marine processes interact with environments. This region has been designated by some as the "shore zone" and extends from an upland boundary (e.g., vegetation line) to a seaward limit (e.g., water depth), and can vary depending on how these limits are defined and controlling processes. The boundaries are commonly set by a combination of government law and geomorphic features or processes (Fig. 1; Christie 1994; NRC 2007). From a geomorphic perspective, the shore zone may be defined by

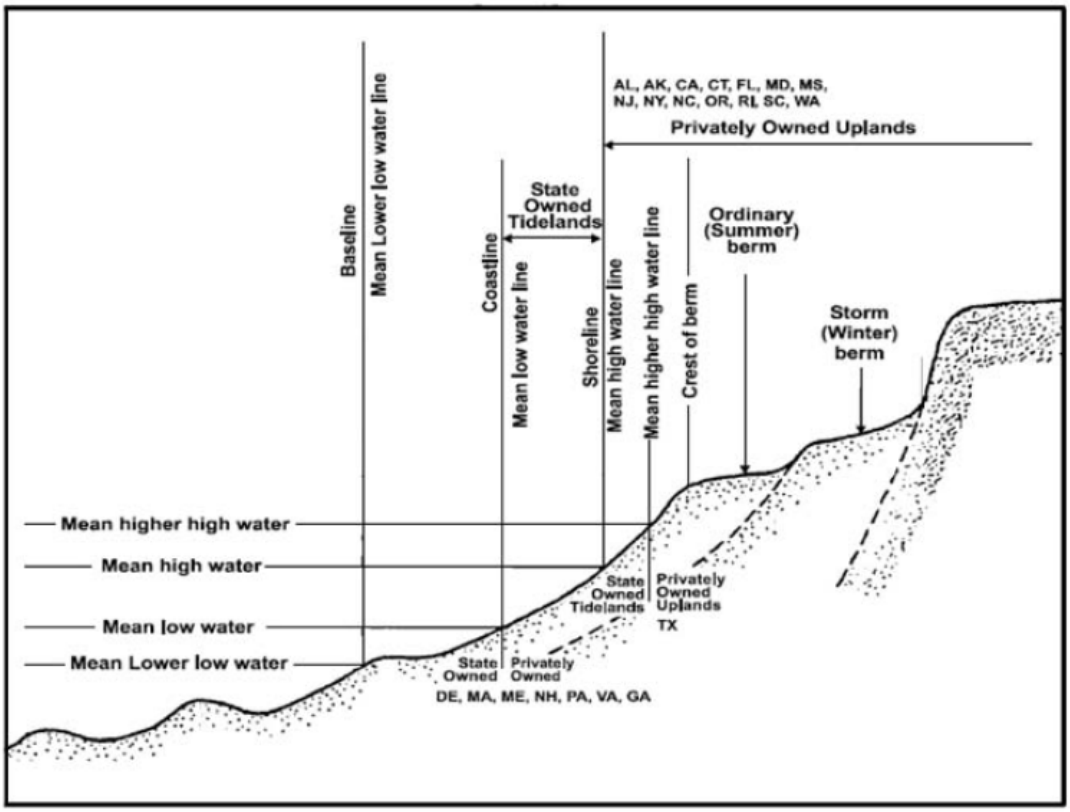

Figure 1 Definitions of nearshore zones and legal ownership for a typical coastal zone. The common legal demarcation between private and public lands, the "shoreline," is usually taken to be the intersection of the mean high water line with the beach profile. But temporal variation of the beach profile and even of the sea-level complicates this interpretation (Modified from NOAA 2001; from NRC 2007).

tidal range, mean water level, or features such as depth contours, dunes, and vegetation (Coyne et al. 1999; French 2001; French 2003; NRC 2007; Nordstrom 1992). In the Netherlands the shore zone is defined by integrating around the mean shoreline position between the -5 meter and +3 meter contours relative to their sea-level datum (Fig. 2; NRC 2007). By defining their shoreline as an area instead of a contour, the Netherlands has integrated an automatic easement into their shoreline definition; this is a strategy that some states, such as South Carolina, have also adopted (SCDHEC-OCRM 2010).

Within the shore zone, a specific position of the actual land-water interface is termed the "shoreline". The exact location of the shoreline can change due to astronomical and meteorological tides, storm surges, sea-level changes, and variations in land elevation (e.g., subsidence and uplift; Bellis et al. 1975; Camfield and Morang 1996; Esteves et al. 2006; List et al. 2006; Pajak and Leatherman 2002; Riggs and Ames 2003). In order to characterize fluctuations over time or utilize shoreline information in policies and development plans, the location of the shoreline must first be carefully defined (Boak and Turner 2005). As with the limits of the shore zone, there are many ways to define shoreline position, such as the mean and instantaneous shoreline positions. A mean shoreline may be derived from an average water-level statistic such as the mean high water line over the 19.2 year tidal epoch (Ali 2010; Byrne 2010; Christie 2009; NRC 2007). This is also sometimes termed a tide-coordinated shoreline where the average intersection of a tidal level is defined in reference to some vertical datum (Ali 2010; NRC 2007). This type of shoreline is most commonly used for regulatory purposes (Byrne 2010; Christie 2009). An instantaneous shoreline represents a single snapshot of the position at a specific time (Ali 2010; Byrne 2010; Christie 2009). This is the type of shoreline that is derived from aerial or satellite images and is not necessarily in reference to a vertical datum (Ali 2010,

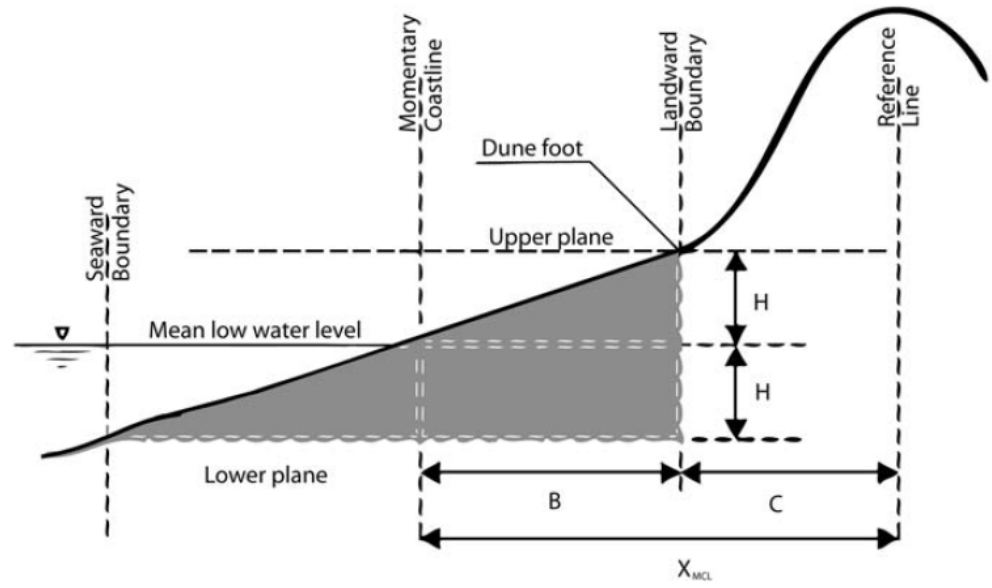

Figure 2 The definition of the open-coast shoreline in the Netherlands is called the Momentary Coastline (MCL) and is found as the total area of beach lying between -5 meters and +3 meters from NAP (Normaal Amsterdams Peil, i.e., Netherlands' reference for sea-level) divided by 8 meters. This quantity integrates detailed profile fluctuations that would otherwise confuse estimation based on a more traditional shoreline location (from NRC 2007).

Camfield and Morang 1996). It is important to note that most studies of shoreline change use the instantaneous shoreline rather than the mean shoreline; however, the goal is to have the instantaneous shoreline represent a mean shoreline, so tide-coordinated images or other evaluations may be made.

Shorelines have varied geomorphology that is influenced by antecedent coastal geometry, climate, and more recently human alteration (Bellis et al. 1975; Nordstrom 1992; Riggs and Ames 2003). Physical processes are also key determinants of shoreline morphology. At a continental or regional scale, coastlines are divided into rocky, soft, and organic shorelines (Nordstrom 1992). This dissertation focuses on "soft" sediment and organic shorelines, the types commonly found in the southeastern United States and particularly in northeastern North Carolina. These shore types are common in estuaries and ocean embayments where sediment has accumulated because of the limited influence of ocean swell (NRC 2007; Roman and Nordstrom 1996). As a result of the limited ocean influence, sheltered coastlines are more varied and develop features characteristic of low-energy environments such as extensive mudflats and wetlands (NRC 2007; Riggs and Ames 2003; Whitehouse et al. 2000). These systems are heavily influenced by local-scale, shallow-water, sediment transport processes (NRC 2007, Nordstrom 1992). The sediments that compose these shorelines are also local and often formed in-situ (through physical or biological processes), transported from adjacent areas, or exported from nearby rivers (NRC 2007; Riggs and Ames 2003). The type and composition of the sediments along these shorelines is important for discussions of shoreline change. Grain-size and sediment composition impact the susceptibility of shorelines to erosive forces and the potential for eroded material to be transported.

Sediment shorelines such as bluffs and banks are prevalent in the Southeast and are one of the most common types of shorelines used for recreation or other human activities due to accessibility (Nordstrom 1992; NRC 2007; Riggs and Ames 2003). Most commonly they are low sediment banks or estuarine pocket beaches composed of unconsolidated, coarse to fine sands (Bellis et al. 1975; Nordstrom 1992; Nordstrom and Jackson 2012; NRC 2007; Riggs and Ames 2003). These are essentially shoreline accumulations that have been shaped by wave action, along-shore currents, and storm surges (Nordstrom 1992; NRC 2007; Roman and Nordstrom 1996). Local material is eroded from other shorelines such as high bluffs or inlets and transported to areas of lower energy where they deposit, and can accumulate depending on conditions (Nordstrom and Jackson 2012; Riggs and Ames 2003; Runyan and Griggs 2003). These sediments can also accumulate in embayments along organic shorelines such as marshes and form small pocket beaches (Nordstrom 1992; Riggs and Ames 2003; Roman and Nordstrom 1996). Studies suggest that the profile of these beaches and the direction of sediment transport are driven by the locally generated wave climate and the pre-existing shore slope (Jackson et al. 2002; Nordstrom and Jackson 1992; Makaske and Augustinus 1998; Riggs and Ames 2003). Sediment bank coasts can also exhibit features such as nearshore bars and shoals from material transported both along- and across-shore (Nordstrom and Jackson 2012; NRC 2007; Pilkey et al. 2009). Research also suggests that these nearshore features can affect further shoreline erosion; once formed, bars act to force waves to break off-shore and lessen the erosive energy reaching the actual shoreline (Bellis et al. 1975; Nordstrom 1992; NRC 2007). However, if these features are removed either through large storms or human activities, then the shoreline is once again exposed to the full force of waves and currents.

Organic shorelines include wetlands such as marshes and swamps, as well as tidal flats (Bellis et al., 1975; Mitsch and Gosslink 2000; Riggs and Ames 2003; Roman and Nordstrom 1996). They occur on low-energy shorelines where the gradient is small, and the mud content can be high, where fine sediments are available (Coyne et al. 1999; NRC 2007; Riggs and Ames 2003). Wetlands by definition are areas of biological growth and often have a greater organic component due to the presence of extensive root mats, leaf litter, and other decomposing organic material supplied by vegetation (Mitsch and Gosslink 2000; NRC 2007; Riggs and Ames 2003). The organic matter and fine sediments create a more cohesive substrate makes these types of shorelines more resistant to erosion by waves than unconsolidated sandy shores (Cowart et al. 2011; Roman and Nordstrom 1996).

In North Carolina, marsh areas expanded as sea-level stabilized around 6,000 to 8,000 years ago (Riggs and Ames 2003). Underlying them is generally peat and muddy sediment approximately a meter or more thick, and overlying sandy marine deposits (Bellis et al. 1975). Wave erosion in many areas has created a distinct scarp in the profiles that transition to sandy sediments on the bottom just offshore (Bellis et al. 1975). Where the tidal range is sufficient, there can be vegetated or un-vegetated extensive muddy intertidal flats (Mitsch and Gosslink 2000).

Along the upper tributaries of estuaries and protected embayments are swamp forest wetlands vegetated with hydrophilic trees and scrub brush (Mitsch and Gosslink 2000; Riggs and Ames 2003). The trees, commonly cypress in coastal North Carolina, are sensitive to water-level fluctuations and salinity (Bellis et al. 1975; Mitsch and Gosslink 2000). Extensive inundation can create a fringe of dead trees, debris, and relict root systems at the shoreline that can act to

armor these shorelines against wave attack (Bellis et al. 1975). These features also serve as obvious indicators of shoreline erosion (Bellis et al. 1975; Leatherman 2003; Schwimmer 2001).

3.0 Dynamics of Sediment Transport and Shoreline Erosion

3.1 Sediment Budgets and Littoral Cells

Ultimately, the position of the shoreline is determined by sea-level (French 2003; French 2001; NRC 2007). However, on a smaller scale (regional and smaller) the shoreline position changes over time due to geomorphic processes and human intervention (Camfield and Morang 1996). Movement can be cyclical and occur over timescales from hours to millennia (Camfield and Morang 1996). Different stresses are capable of supplying, transporting, and eroding material from the shore. As long as transport of sediment in and out of the system is balanced (i.e., steady state), there may be change in the shoreline position or profile, but no net change in sediment volume in the system (Fig. 3; French 2001; NRC 2007; Rosati 2005). This balance is calculated using a sediment budget:

$$\sum Q_{source} - \sum Q_{sink} - \Delta V + P - R = Residual \qquad \text{Equation 1}$$

where the total sources ($Q_{sources;}$ e.g., longshore transport from adjacent cells) and sinks ($Q_{sinks;}$ e.g., longshore transport out of the cell) that control total sediment volume for the littoral cell are quantified, along with the net change in shoreline sediment volume (ΔV), and the anthropogenic placement (P) or removal (R) of material on or off the shoreline (Fig. 3; Rosati 2005). The resulting residual represents the balance of sediment (Rosati 2005). If the residual is zero then the inputs and outputs are considered balanced (French 2001; Rosati 2005). A residual other

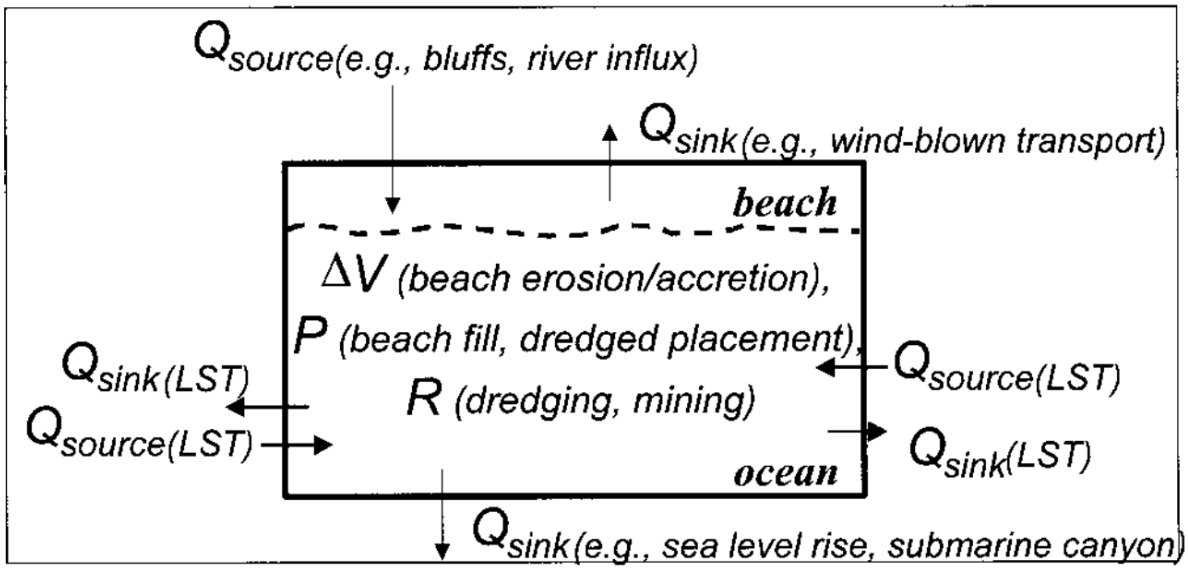

Figure 3 Sediment budget parameters for a coastal cell. Q_{sink} and Q_{source} represent pathways for sediment transport in and out of the budget cell. Volumetric changes of sediment within the cell are represented by *P*, *R*, and ΔV (from Rosati 2005).

than zero indicates an alongshore gradient in sediment transport in the system and consequently, a volume change (Rosati 2005).

This equation is typically applied to individual littoral cells or lengths of coastline where sediment transport processes are considered to be independent of adjacent areas (NRC 2007; Patsch and Griggs 2006). Boundaries between littoral cells tend to be geomorphic features such as spits, islands, or headlands (Bowan and Inman 1966; Dolan et al. 1987; Rosati 2005). Littoral cells on protected coastlines are much smaller than in the coastal ocean due to the complexity of shoreline geometry and presence of obstacles (natural or man-made) that interrupt alongshore currents (Komar 1983; Nordstrom 1992; NRC 2007; Roman and Nordstrom 1996). The concept of the littoral cell is important when an action (e.g., development) alters transport, or the sources and sinks of a cell. A clear example is the construction of a structure, such as a groin, that interrupts longshore transport within a littoral cell, creating a change in the pattern of accumulation and erosion in the cell or adjacent area (French 2001; NRC 2007; Roman and Nordstrom 1996). Logically, segments of shoreline cannot be considered independent of adjacent areas (Roman and Nordstrom 1996).

Sediments are supplied to the coast primarily through river discharge, direct run-off, erosion of adjacent shorelines, transport in the coastal zone, and to a minor extent, aeolian transport (Ali 2010; NRC 2007; Roman and Nordstrom 1996). Erosion of adjacent shorelines and the along-shore transport of that material is especially important as a sediment source for some estuarine shorelines. River discharge is another significant source of material to the coastal zone (Ali 2010; NRC 2007; Roman and Nordstrom 1996). In many areas, this has been reduced over the last 100 years due to damming and channel alteration (Ali 2010; NRC 2007; Roman and Nordstrom 1996). On back-barrier shorelines, overwash events also can be important but

episodic sources of sediment (Ali 2010; Camfield and Morang 1996; NRC 2007; Roman and Nordstrom 1996). However, with increased development and armoring of the oceanfront shoreline, it is difficult for material to reach the back-barrier even during periods of high storm surge (Ali 2010; NRC 2007; Roman and Nordstrom 1996).

3.2 Mechanisms of Shoreline Erosion

The erodibility of a given shoreline is a function of many factors, including wave energy (determined by fetch and water depth), shoreline composition and morphology, vegetation, nearshore littoral processes, and sediment supply (Ali 2010; Bellis et al. 1975; Corbett et al. 2008; French 2003; NRC 2007; Phillips 1986; Riggs 2001; Riggs and Ames 2003; Rosen 1980). Human activities such as shoreline hardening can modify any of these parameters and impact the rate of erosion (Ali 2010; Bellis et al. 1975; NRC 2007; Roman and Nordstrom 1996). At a regional scale many of the mechanisms controlling shoreline erosion may function similarly (Jackson and Nordstrom 1992). However, at a local level these mechanisms can be controlled by fine scale, site specific factors (Jackson and Nordstrom 1992; Nordstrom and Jackson 2012). Local controls include shoreline orientation, longshore currents, shoreline sinuosity or geometry, and nearshore bathymetry (Cooper et al. 2007; Jackson and Nordstrom 1992; Nordstrom 1992; Nordstrom and Jackson 2012; Phillips 1986).

Waves introduce energy to the coastal zone and can drive intertidal and subtidal erosion in some places and deposition in others (French 2001; Komar 1983; Nordstrom 1992; NRC 2007; Roman and Nordstrom 1996). The amount of wave energy impacting the shorezone along sheltered shorelines is a function of the fetch (French 2001; Komar 1983; Munk 1950; Sorensen, 2006). In sheltered and shallow estuarine shorelines, fetch and depth are the main limits to wave

growth and therefore a significant control on erosion and sediment transport (Komar 1983; Nordstrom and Jackson 2012; NRC 2007; Smith et al. 2001). As fetch and depth increase, so does the potential wave energy (Komar 1983; Nordstrom and Jackson 2012, NRC 2007). Along a given shoreline, orientation relative to the prevailing wind (and wave) direction also controls wave energy (Lorang et al. 1993; Nordstrom and Jackson 2012). For examples, a study in Scotland by Pierce (2004) observed a maximum wave height of 0.94 m when storm winds were oriented with the long-axis of a loch (33 km), and wave heights of less than 0.1 m under similar storm conditions but with wind from the most fetch-limited (7 km) direction. Maximum depth in the loch was 152 m, indicating that fetch, instead of depth, was limiting wave growth in the loch (Pierce 2004).

Waves that develop in shallow areas (e.g., estuaries) are generally smaller, steeper, and have shorter periods than ocean waves (less than 4-5 seconds; French 2001; Jackson et al. 2002; Kamphuis 2012; Komar 1983; Nordstrom 1992; Nordstrom and Jackson 2012; NRC 2007; Roman and Nordstrom 1996). In the study by Pierce (2004), wave periods of 1 to 2 seconds were most common. It should be noted that other environmental factors, such as wind and tides, can also impact wave climate in estuarine or lacustrine systems by altering water-levels (Lorang et al. 1993; Luettich et al. 2000). Increased water-level due to meteorological forcing can result in greater wave energy as well as flooding of the shore face and lead to erosion (Lorang et al. 1993).

Along sandy estuarine shores, the energy of breaking waves shapes shoreline morphology through the across- and along-shore movement of sediment in a manner similar to oceanfront shorelines. During periods of high wave energy the direction of transport is offshore; however, due to the relatively low wave energy (in comparison to oceanfront shorelines) much of this

material may only move between the upper and lower shore face (Jackson et al. 2002; Nordstrom and Jackson 1992; Nordstrom and Jackson 2012). During periods of low wave energy there is net onshore movement of sediment and building of berm and foreshore elevation (Komar 1983; Nordstrom and Jackson 2012). Along oceanfront shorelines these beach profiles are commonly linked with (and referred to as) seasonal cycles (e.g., summer or winter) in wave energy regime or the passage of individual storms (Brown et al. 1999; Komar 1983).

Along muddy shorelines the interaction between waves and nearshore sediments is a little different than what occurs along sandy estuarine shorelines. Fine, muddy sediments may be eroded when bed shear stress exceed cohesive forces (Wells and Kemp 1984). The highly porous and often bioturbated muddy bottom also creates more frictional interaction with wave orbitals which results in greater wave attenuation in the nearshore zone (Wells and Kemp 1984). Research by Wells and Kemp (1984) found that along coastlines of Louisiana and Surinam that the presence of fluid muds in nearshore environment attenuated over 90% of wave energy. The presence of fluid mud deposits and other muddy cohesive features such as extensive mudflats can therefore provide protection to the shoreline by significantly reducing incoming wave energy (Wells and Kemp 1984).

In contrast to erosion along sandy shorelines, marshes typically eroded through a process where waves undercut the marsh platform along the shoreline (Finkelstein and Hardaway, 1988; Schwimmer, 2001). As marshes tend to have exposed scarps at the edge of the marsh platform the subsurface is exposed to wave attack (Finkelstein and Hardaway 1988; Phillips 1986; Schwimmer 2001). Over time the weight of the unsupported root mat causes slumping (Fig. 4b). Schwimmer (2001) described a common morphology of an eroding marsh shoreline as a series of clefts and necks where waves have undercut the marsh until segments slumped into the

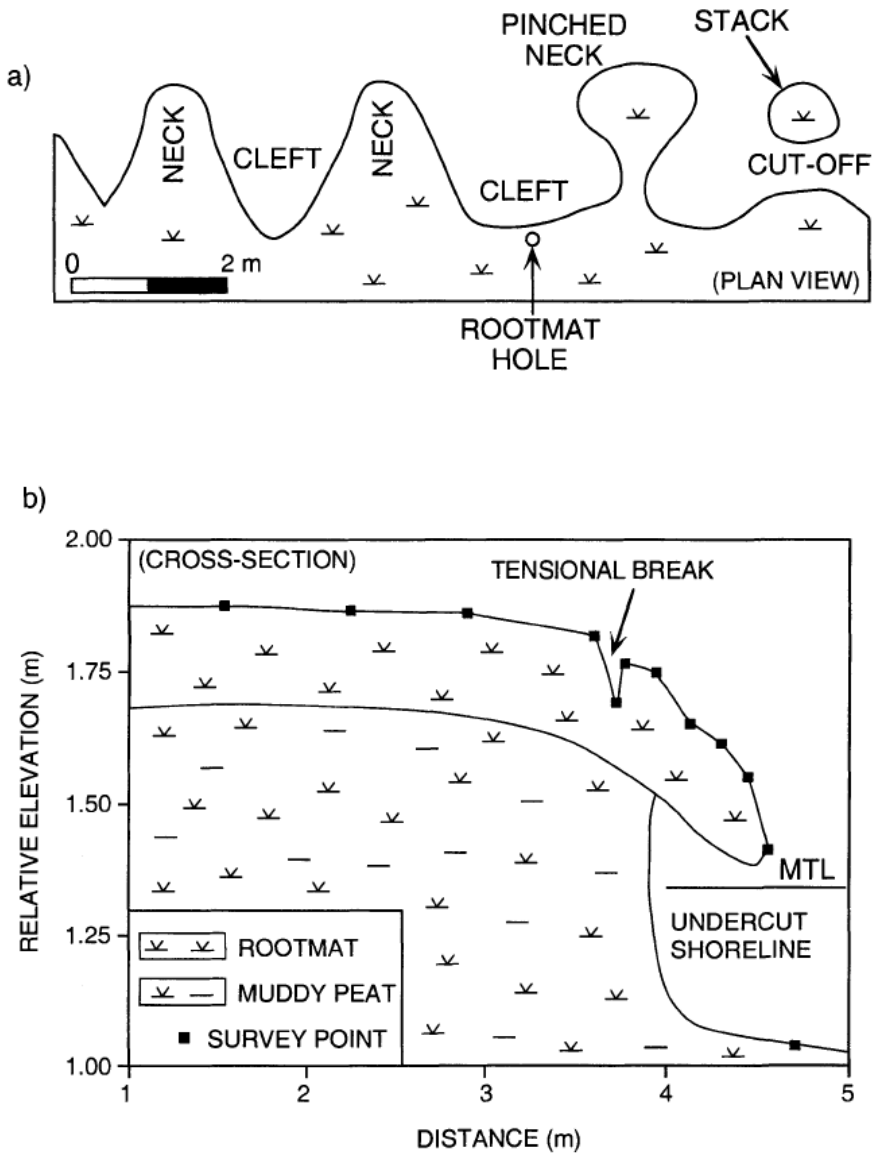

Figure 4 Morphological characteristics of an eroding marsh shoreline; a) plan view, b) cross-section (from Schwimmer 2001).

water forming clefts (Fig. 4a). Eventually, wave energy focused in the clefts erodes away the base of the neck (pinched neck, Fig. 1.4a) until it separates from the shore entirely, effectively returning the shoreline to a more smooth geometry (Schwimmer 2001). In Schwimmer (2001) it was found that there was a correlation between wave power (P) and the rate of marsh erosion, emphasizing the role of waves in shaping marsh shorelines. Some of the material eroded from the marsh edge has also been shown to be transported onto the adjacent marsh surface, becoming a significant source of sediment for vertical accretion (Pethick and Reed 1988). Vegetation also plays an important role in marsh shoreline change. Beaches can respond quickly to changes in wave energy through adjustment of their cross-shore profile; however, marshes build elevation slowly through the accumulation of fine sediment and organic matter (Mitsch and Gosselink 2000; Reed 1990; Stumpf 1983). The type of wetland vegetation impacts the rate of peat production and the trapping of sediment by reducing flow velocities to facilitate the settling of suspended particles (Leonard et al. 2002; Phillips 1986).

Large coastal storms such as hurricanes or nor'easters can result in potentially dramatic shoreline erosion over a very short time period (Camfield and Morang 1996; Dolan et al. 1978; Phillips 1999). Along the mid-Atlantic in 1962 the "Ash Wednesday Storm" caused extensive ocean overwash and eroded beaches and dunes established over 30 years prior (Dolan et al. 1988). Storm surge associated with these episodic events increases wave run-up and brings breaking waves further up the shoreface (Dolan et al. 1978). Studies have shown that the increased sediment mobilization associated with storms also contributes to enhanced sediment exchange between estuarine environments (Reed 1989; Roman and Nordstrom 1996). In the future changes in the frequency and magnitude of these storms could impact rates and patterns of shoreline erosion, especially where modification of the shoreline has occurred (Camfield and

Morang 1996). Finally, where barrier islands are present in the coastal zone, their evolution and processes (e.g., overwash and inlet dynamics) also impact the estuarine shoreline (Riggs and Ames 2003).

4.0 Dissertation Overview

With the exception of Chapters 1 and 5, all the chapters in this thesis are formatted as individual publications. Chapter 1 consists of introduction and background material for the thesis. Chapter 2 has already been published, but for the purpose of this thesis was reformatted to match the rest of the document. Chapters 3 and 4 present new research, and Chapter 5 focuses on the management applications of this work.

This research examined the spatio-temporal dynamics of estuarine shoreline change, as well as the role of waves and storms as drivers of that change, and evaluated the importance of shoreline erosion as a source of fine sediments to the larger Albemarle-Pamlico Estuarine System (APES). The spatial and temporal dynamics of shoreline change were evaluated at five study sites across the APES using a combination of aerial imagery and in-situ shoreline surveys (Chapters 2 and 3). The application of a balloon-aerial-photography system for capturing high-resolution, cost-efficient, and timely imagery of the shorezone was also examined (Chapter 2). This imagery, coupled with measures from a high-accuracy, real-time kinematic GPS, enable the observation of rapid changes in the shoreline position and collection of ancillary environmental data (Chapter 3).

More specifically, in Chapter 3 shoreline change was determined for a range of temporal periods or 'eras', from a historical period of 50 years to bi-monthly surveys utilizing the methods assessed in Chapter 2. Waves and storms are explored as the main drivers of shoreline change. Waves generated by local weather patterns and storm events were examined for the sub-annual

shoreline eras using a coupled hydrodynamic and wave model. Shoreline orientation, wind direction, and water depth on wave energy were also investigated using the coupled hydrodynamic and wave model (Chapter 3).

Chapter 4 explores the importance of wetland shoreline erosion as a source of fine sediments to the Tar-Pamlico sub-estuary, a tributary of the APES. To examine these dynamics, a fine sediment budget was constructed for the Tar-Pamlico estuary. Rates of shoreline change and sediment accumulation using radionuclide tracers were determined for the study area. Erosion rates for the shorelines classified as wetlands (i.e., swamp and marsh shorelines) were used, along with elevation and bulk density estimates, to calculate the mass of sediment supplied to the estuary. Export was estimated based on supply and storage. These observations provided information on system functioning.

Chapter 5 provides a summary and synthesis of this research and its implications for future coastal management in North Carolina.

REFERENCES

Ali, T.A., 2010. Analysis of shoreline-changes based on the geometric representation of the shorelines in the GIS database. Journal of Geography and Geospatial Information Science 1, 1-16.

Beatley, P.W., Brower, D.J., Schwab, A.K., 2001. An Introduction to Coastal Zone Management, Second ed. Island Press, New York.

Bellis, V., O'Conner, M.P., Riggs, S.R., 1975. Estuarine shoreline erosion in the Albemarle-Pamlico region of North Carolina. UNC Sea Grant Publication, North Carolina State University, Raleigh, North Carolina.

Byrne, J.P., 2010. Rising seas and common law baselines: a comment on regulatory takings discourse concerning climate change. Georgetown Law Faculty Publications and Other Works, Georgetown University.

Camfield, F.E., Morang, A., 1996. Defining and interpreting shoreline change. Ocean and Coastal Management 32(3), 129-151.

Charlier, R.H., De Meyer, C.P., 1998. Coastal Erosion: Response and Management. Springer, New York.

Christie, D.R., 1994. Coastal and Ocean Management Law. West Publishing, St. Paul.

Christie, D.R., 2009. Of beaches, boundaries, and SOBs. Journal of Land Use and Environmental Law 25, 1-75.

Cooper, J.A.G., Lewis, D.A., Pilkey, O.H., 2007. Fetch-limited barrier islands: overlooked coastal landforms. GSA Today 17(3), 4-9.

Corbett, D.R., Walsh, J.P., Cowart, L., Riggs, S.R., Ames, D.V., Culver, S.J., 2008. Shoreline change within the Albemarle-Pamlico Estuarine System, North Carolina. East Carolina University.

Cowart, L., Corbett, D.R., Walsh, J.P., 2011. Shoreline change along sheltered coastlines: insights from the Neuse River Estuary, NC, USA. Remote Sensing 3, 1516-1534.

Coyne, M.A., Fletcher, C.H., Richmond, B.M., 1999. Mapping coastal erosion hazard areas in Hawaii: observations and errors. Journal of Coastal Research 28, 171-184.

Crossett, K.M., Culliton, T.J., Wiley, P.C., Goodspeed, T.R., 2004. Population trends along the coastal United States: 1980-2008.

Deaton, A.S., Chappell, W.S., Hart, K., O'Neal, J., Boutin, B., 2010. North Carolina Coastal Habitat Protection Plan. North Carolina Department of Environment and Natural Resources, Division of Marin Fisheries, North Carolina.

Dolan, R., 1971. Coastal landforms: crescentic and rhythmic. Geologic Society of America Bulletin 82, 177-180.

Dolan, R., Hayden, B., Heywood, J., 1978. Analysis of coastal erosion and storm surge hazards. Coastal Engineering 2, 41-53.

Dolan, R., Lins, H., Hayden, B., 1988. Coastal storms. Journal of Coastal Research 4, 417-433.

Erdle, S.Y., Davis, J.L.D., Sellner, K.G., 2006. Management, Policy, Science, and Engineering of Nonstructural Erosion Control in the Chesapeake Bay. Living Shoreline Summit, Williamsburg, Virginia.

Esteves, L.S., Williams, J.J., Dillenburg, S.R., 2006. Seasonal and interannual influences on the patterns of shoreline change in Rio Grande de Sul, Southern Brazil. Journal of Coastal Research 22, 1076-1093.

Finkelstein, K., Hardaway, C.S., 1988. Late Holocene sedimentation and erosion of estuarine fringing marshes, York River, Virginia. Journal of Coastal Research 4, 447-456.

French, P.W., 2001. Coastal Defense: Processes, problems and solutions. Routledge, London.

French, P.W., 2003. Coastal and Estuarine Management. Routledge, London.

Jackson, N.L., Nordstrom, K.F., 1992. Site specific controls on wind and wave processes and beach mobility on estuarine beaches in New Jersey, U.S.A. Journal of Coastal Research 8(1), 88-98.

Jackson, N.L., Nordstrom, K.F., Eliot, I., Masselink, G., 2002. Site specific controls on wind and wave processes and beach mobility on estuarine beaches in New Jersey, U.S.A.. Journal of Coastal Research 8, 88-98.

Kamphuis, J.W., 2012. Introduction to Coastal Engineering and Management. World Scientific, New Jersey.

Kana, T.W., 1988. Beach erosion in South Carolina. South Carolina Sea Grant Consortium, Charleston, South Carolina.

Kittinger, J.N., Ayers, A.L., 2010. Shoreline armoring, risk management, and coastal resilience under rising seas. Coastal Management 38, 634-653.

Komar, P.D., 1971. Nearshore cell circulation and the formation of giant cusps. Geological Society of America Bulletin 82, 2643-2650.

Komar, P.D., 1983. Beach processes and erosion, in: Komar, P.D., Moore, J.R. (eds), CRC Handbook of Coastal Processes and Erosion. CRC Press Inc., Boca Raton, Florida.

Leatherman, S.P., 2003. Shoreline change mapping and management along the U.S. East Coast. Journal of Coastal Research SI38, 5-13.

Leonard, L.A., Wren, A., Beavers, R.L., 2002. Flow dynamics and sedimentation in *Spartina alterflora* and *Phragmites austrailis* marshes of the Chesapeake Bay. Wetlands 22, 415-424.

Leuttich, R., Carr, S.D., Reynolds-Fleming, J., Fulcher, C.W., McNinch, J.E., 2000. Semi-diurnal seiching in a shallow, micro-tidal lagoonal estuary. Continental Shelf Research 22(11-13), 1669-1681.

List, J.H., Farris, A.S., Sullivan, C., 2006. Reversing storm hotspots on sandy beaches: spatial and temporal characteristics. Marine Geology 226, 261-279.

Lorang, M.S., Komar, P.D., Standford, J.A., 1993. Lake level regulation and shoreline erosion on Flathead Lake, Montana: a response to the redistribution of annual wave energy. Journal of Coastal Research 9, 494-508.

Makaske, B., Augustinus, P.G.E.F., 1998. Morphologic changes of a micro-tidal, low wave energy beach face during a spring-neap tide cycle, Rhone-Delta, France. Journal of Coastal Research 14(2), 632-645.

Munk, W.H., 1950. Origin and generation of waves. Conference on Coastal Engineering, Council on Wave Research, Long Beach, California.

Nielsen, P., 1992. Coastal bottom boundary layers and sediment transport. World Scientific, New Jersey.

NOAA, 2010. Ocean and Coastal Management in North Carolina. Office of Ocean and Coastal Resource Management.

Nordstrom, K.F., 1977. Bayside beach dynamics: implications for simulation modeling on eroding, sheltered, tidal beaches. Marine Geology 25, 333-342.

Nordstrom, K.F., 1992. Estuarine Beaches. Elsevier Applied Science, New York.

Nordstrom, K.F., Jackson, N.L., 2012. Physical processes and landforms on beaches in short fetch environments in estuaries, small lakes, and reservoirs: a review. Earth-Science Reviews 111, 232-247.

NRC, 2007. Mitigating Shoreline Erosion along Sheltered Coasts. National Academies Press, Washington.

Pajak, M.J., Leatherman, S., 2002. The high water line as shoreline indicator. Journal of Coastal Research 18(2), 329-337.

Patsch, K., Griggs, G., 2006. Littoral cells, sand budgets, and beaches: understanding California's shoreline. California Coastal Sediment Management WorkGroup, University of California, Santa Cruiz, California.

Pethick J., and Reed, D.J., 1988. Coastal protection in an area of salt marsh erosion. Proceedings of Coastal Sediments '87, American Society of Civil Engineers, New York.

Pierce, L.R., 2004. Lake waves, coarse clastic beach variability and management implications, Loch Lomond, Scotland, UK. Journal of Coastal Research 20(2), 562-585.

Phillips, J.D., 1986a. Coastal submergence and marsh fringe erosion. Journal of Coastal Research 2, 427-436.

Phillips, J.D., 1986b. Spatial analysis of shoreline erosion, Delaware Bay, New Jersey. Annals of the Association of American Geographers 76.

Phillips, J.D., 1999. Event timing and sequence in coastal shoreline erosion: Hurricanes Bertha and Fran and the Neuse Estuary. Journal of Coastal Research 15, xx-616.

Pilkey, O., Hume, T.M., 2001. The shoreline erosion problem: lessons from the past. Water and Atmosphere 9, 22-23.

Poulter, B., Feldman, R.L., Brinson, M.M., Horton, B.P., Orbach, M.K., Pearsall, S.H., Reyes, E., Riggs, S.R., Whitehead, J.C., 2009. Sea-level rise research and dialogue in North Carolina: creating windows for policy change. Ocean and Coastal Management 52, 147-153.

Reed, D.J., 1989. Patterns of sediment deposition to subsiding coastal salt marshes, Terrebonne Bay, Louisiana: the role of winter storms. Estuaries 12, 222-227.

Reed, D.J., 1990. The impact of sea-level rise on coastal salt marshes. Progress in Physical Geography 14, 24-40.

Riggs, S.R., 2001. Shoreline erosion in North Carolina Estuaries. North Carolina Sea Grant Publication, Raleigh, North Carolina.

Riggs, S.R., Ames, D.V., 2003. Drowning the North Carolina coast: sea-level rise and estuarine dynamics. North Carolina Sea Grant, North Carolina.

Rogers, S., Skrabal, T.E., 2001. The Soundfront Series: Managing erosion on estuarine shorelines. UNC-SG-01-12, North Carolina.

Roman, C.T., Nordstrom, K.F., eds., 1996. Estuarine Shores: Evolution, Environments and Human Alterations. John Wiley & Sons, London.

Rosati, J.D., 2005. Concepts in sediment budgets. Journal of Coastal Research 21(2), 307-322.

Rosen, P.S., 1980. Erosion susceptibility of the Virginia Chesapeake Bay shoreline. Marine Geology 34, 42-45.

Runyan, K., Griggs, G.B., 2003. The effects of armoring seacliffs on the natural sand supply to the beaches of California. Journal of Coastal Research 19, 336-347.

SCDHEC-OCRM, 2010. Adapting to shoreline change: A foundation for improved management and planning in South Carolina. Shoreline Change Advisory Committee.

Schwimmer, R.A., 2001. Rates and processes of marsh shoreline erosion in Rehoboth Bay, Delaware, USA. Journal of Coastal Research 17, xx-672.

Smith, M.J., Stevens, C.I., Gorman, R.M., McGregor, J.A., Neilson, C.G., 2001. Wind-wave development across a large shallow intertidal estuary: a case study of Manukau Harbor, New Zealand. New Zealand Journal of Marine and Freshwater Research 35, xx-985.

Sorensen, 2006

Stuart, A.W., 2010. The North Carolina Atlas.

Stumpf, R.P., 1983. The process of sedimentation on the surface of a salt marsh. Estuarine, Coastal and Shelf Science 17, 495-508.

Wells, J.T., Kemp, G.P., 1984. Interaction of surface waves and cohesive sediments: field observations and geologic significance, in: Mehta, A. (ed.), Estuarine Coastal Sediment Dynamics. Springer-Verlag, New York.

Whitehouse, R., Soulsby, R., Roberts, W., 2000. Dynamics of Estuarine Muds. Thomas Telford Publishing, London.

CHAPTER 2

High-resolution Analysis of Shoreline Change and Application of Balloon-based Aerial Photography, Albemarle-Pamlico Estuarine System, North Carolina, USA

Abstract

Previous studies of shoreline erosion have relied on satellite imagery or airplane-based aerial photography, which can be costly, of limited availability, and of restricted resolution. These factors limit the usefulness of such imagery for detailed shoreline-change measurements that require frequent observations with high spatial accuracy. Easily deployed balloon-based photography systems can provide high spatial and temporal resolution images at relatively low cost. This study utilized an Aerostat balloon photography system along with real-time kinematic (RTK) GPS to observe sub-annual changes in the shoreline position of the Albemarle-Pamlico Estuarine System (APES), North Carolina, USA. The fine (0.03 m-pixel) resolution of Aerostat images is ideal for mapping shoreline areas although limited in spatial extent. Features digitized from these images compare well in position (0.5 ± 0.5 m) and accuracy (± 0.4 m) to in-situ RTK-GPS surveys. The balloon system is best utilized concurrently with RTK-GPS surveys to obtain the highest possible georectification accuracy. Results demonstrate that this method is well-suited to high-accuracy analysis of shoreline positions over short timescales (annual to sub-annual), and that the balloon images provide a valuable spatial context for any measured changes. Preliminary analysis of shoreline change across the APES highlights great spatial and temporal complexity. Annualized rates of change reached >30 m/yr but average net changes were modest for survey periods (-0.5 m to 0.04 m). Tropical weather systems (e.g., Hurricane Earl) can be key drivers of the observed shoreline response, and the associated sediment dynamics likely have important ecological (e.g., submerged-aquatic-vegetation and water quality) ramifications.

1.0 Introduction

Remote sensing via satellites and aerial photography is regularly utilized to capture and study spatial information such as the land-water boundary, submerged-aquatic-vegetation (SAV) distribution, and land-cover attributes. More specifically, the shoreline position has been determined historically by mapping from remotely sensed imagery or other map sources (e.g., NOS T-sheets), in-situ survey methods or a combination of these approaches (Dolan et al. 1978; Crowell et al. 1991; Crowell et al. 1993; Graham et al. 2003; Langley et al. 2003; Wang and Allen 2008). Airplane-acquired aerial photography has been the most commonly utilized tool for shoreline-change studies due to its availability (digital and hardcopy), wide spatial coverage, and reduced cost (in comparison to in-situ surveys). However, these images are typically acquired only every few or more years, and the collection of additional imagery is costly, precluding higher frequency observations. Additionally, while spatial coverage may be moderate (i.e., ~10 km^2 coverage), the spatial resolution is often mediocre (0.5 m pixel size is most common) depending on the age and quality of the imagery (Table 1). As a result, airplane-based imagery in most cases can only be used to determine meter-scale changes in shoreline location (Crowell et al. 1991; Smith et al. 2009). The low resolution also impacts the ability to obtain environmental information, such as shoreline vegetation composition or the presence of hard structures, that may provide valuable insight into shoreline change processes and other studies of small-scale biogeomorphic features (Miyamoto et al. 2004; Boak and Turner 2005; Massada et al. 2008).

The advent of relatively inexpensive and easily used balloon photography or other self-deployed (e.g., a remote controlled hexacopter or the helikite) systems facilitates the acquisition of high-frequency, high-resolution, aerial imagery (Miyamoto et al. 2004; Boak and Turner 2005; Massada et al. 2008; Smith et al. 2009). Furthermore, these systems can be rapidly

Table 1 Summary of image attributes for different remote-sensing methods. The asterisk indicates imagery used in this study. Uncertainty is provided by image metadata and is calculated for the Aerostat.

Aerial Image Type	Pixel Size (m)	Horizontal Uncertainty (m)
1 m DOQQs	1.00 (3.28 ft)	+/- 7.0
(400 ft) scale orthophotos*	0.30 (1 ft)	+/- 2.4
(200 ft) scale orthophotos	0.15 (0.5 ft)	+/- 1.2
(100 ft) scale orthophotos	0.08 (0.25 ft)	+/- 0.6
Aerostat images*	0.03 (0.1 ft)	+/- 0.3

deployed at a relatively low cost. The main objectives of this paper are to (1) illustrate the utility of a balloon-aerial photography system for making detailed shoreline-change observations and (2) conduct a preliminary analysis of high-resolution spatial and temporal changes in estuarine shoreline character.

2.0 Materials and Procedures

A pilot study of high-resolution estuarine shoreline change was conducted at two sites within the Albemarle-Pamlico Estuarine System (APES) of North Carolina (USA) for a one-year period (Fig. 1A). These sites were utilized to evaluate any methodological issues and/or change similarities in different settings. One site was located in the Palmetto-Peartree Preserve (PPP) adjacent to Albemarle Sound in Tyrrell County (Fig. 1B). This site consists of a sediment bank shoreline characterized by scattered woody debris, tree stumps, and some fringing grasses. The second site was in the Gull Rock Gamelands (GRG) located along Pamlico Sound in Hyde County (Fig. 1C). Site GRG is a marsh shoreline characterized by a subaqueous vertical scarp (generally <1 m) and an erosional morphology analogous to that described by Schwimmer et al. (2001), with cleft-and-neck formations, undercutting, and pockets of sandy shoreline. The site is backed by a man-made canal system.

The project utilized an Aerostat balloon photography system sold by Aerial Products (hereafter referred to as the "Aerostat"). The system consists of a 7.2 m^3 Kingfisher Aerostat polyurethane helium balloon fitted with a custom remote-controlled gimbal mount that holds a digital SLR camera (Fig. 2). The camera and gimbal mount are controlled wirelessly using the Futaba remote-operation station with an integrated 18-cm (7-inch) LCD screen. The camera used in this work was a Canon Rebel T2i (EOS 550D camera body, 18.0 megapixel) with an

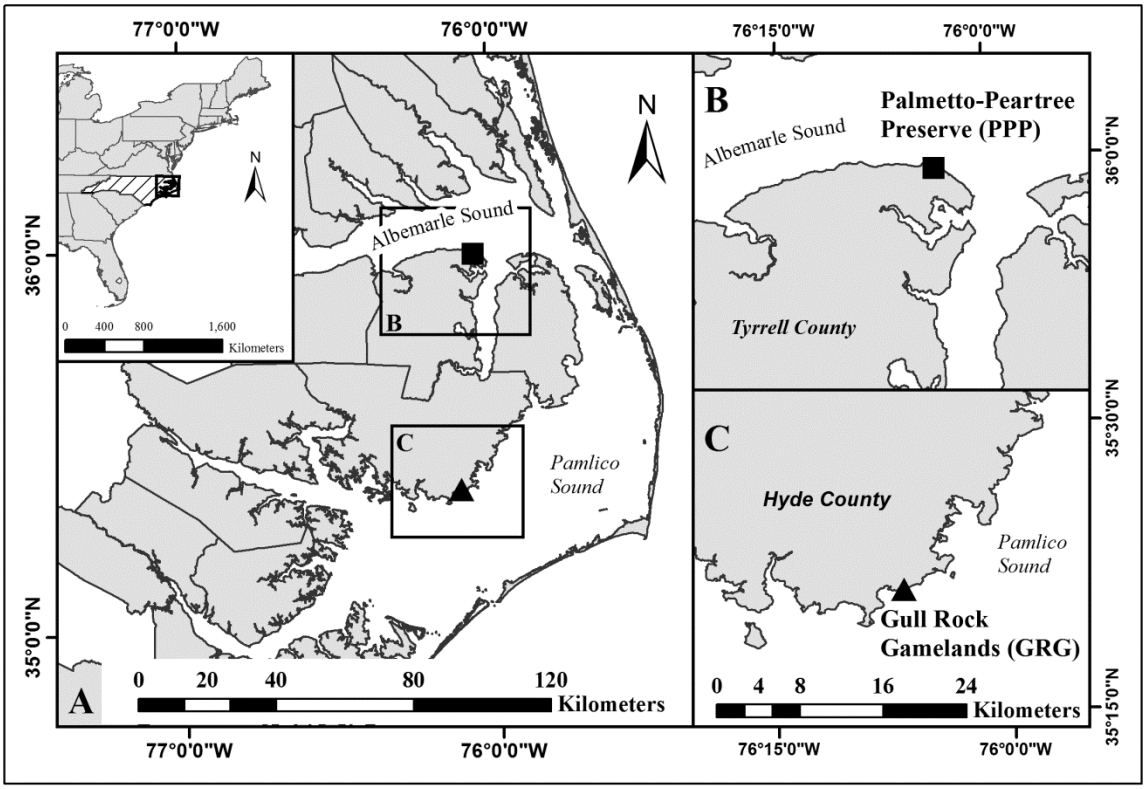

Figure 1 Maps of study sites. A) regional overview map; B) the Palmetto-Peartree Preserve (PPP) site in Tyrrell County and C) the Gull Rock Gamelands (GRG) site in Hyde County. Note, the boundary boxes for (B) and (C) are shown in (A).

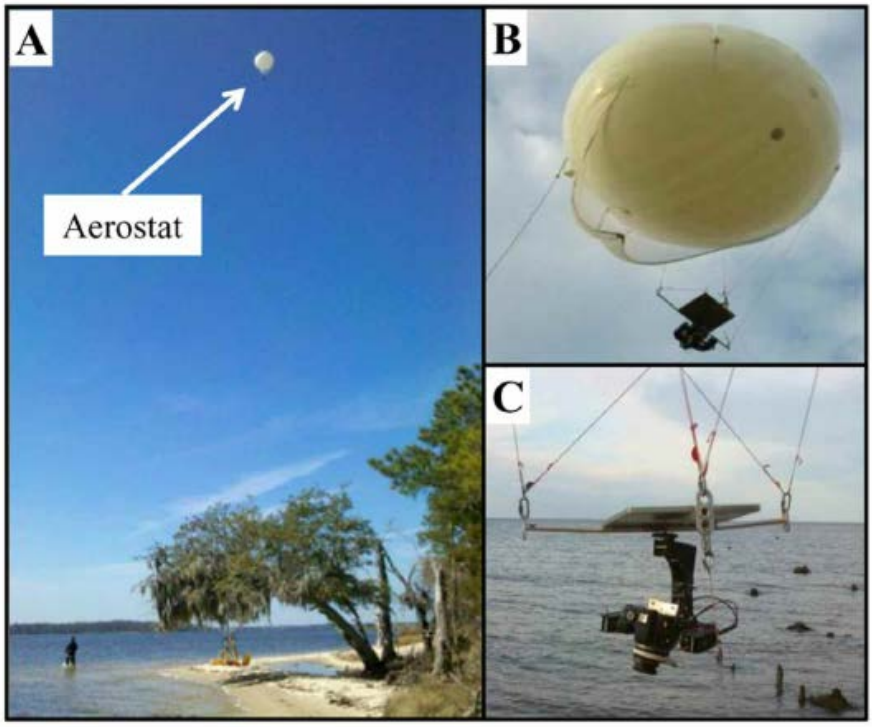

Figure 2 The Aerostat balloon photography system. A) Aerostat system deployed; B) close-up of Aerostat system; C close-up of camera mounted on remote controlled gimbal platform.

EF-S 18-55 mm lens with digital image stabilizer. Images were acquired with a 1/1250 s shutter speed, auto ISO, auto focus, and 4.5 aperture. The total cost of the system was approximately $8,000. Helium was obtained from a local supplier at $45 per tank, with a complete fill of the balloon requiring 2 tanks. While the Aerostat system is more expensive than homemade kite and balloon systems, it is well-designed and significantly cheaper than acquiring imagery by airplane or helicopter. It is noted here that recently developed remote-controlled flying devices (e.g., the hexacopter) may provide a similarly stable, economical photographic platform to that of the balloon.

The study sites were prepared in advance for aerial-image acquisition with the installation of a network of ground control points (GCPs) to facilitate image georeferencing (Thieler and Danforth 1994; Hughes et al. 2006). Testing conducted in a campus parking lot was used to help plan the imagery acquisition and site preparation, e.g., spacing of GCPs. Initial installations at each site consisted of 15-17 GCPs along a ~200-m length of shoreline. The GCPs were created by driving 2-m-long 7.5-cm-diameter aluminum core pipes into the ground to a depth of ~1 m and then affixing a red end cap for visibility. Later in the study, temporary survey flags (50-60 per site) were added to the existing control points because of GCP loss and to obtain better image rectification.

During each site visit, GCPs were surveyed using a Trimble 5800 RTK (Real-time Kinematic) -GPS system prior to image acquisition (Fig. 3). The shoreline position was also surveyed with the RTK-GPS (Fig. 3). The Aerostat system was inflated and assembled in the field and deployed to a 60-75 m elevation using a manual Hannay Reel winch. Total deployment time was between one and two hours per site. Aerostat images were acquired with varying but substantial overlap, and the center of each image tile was used for the final mosaics in order to

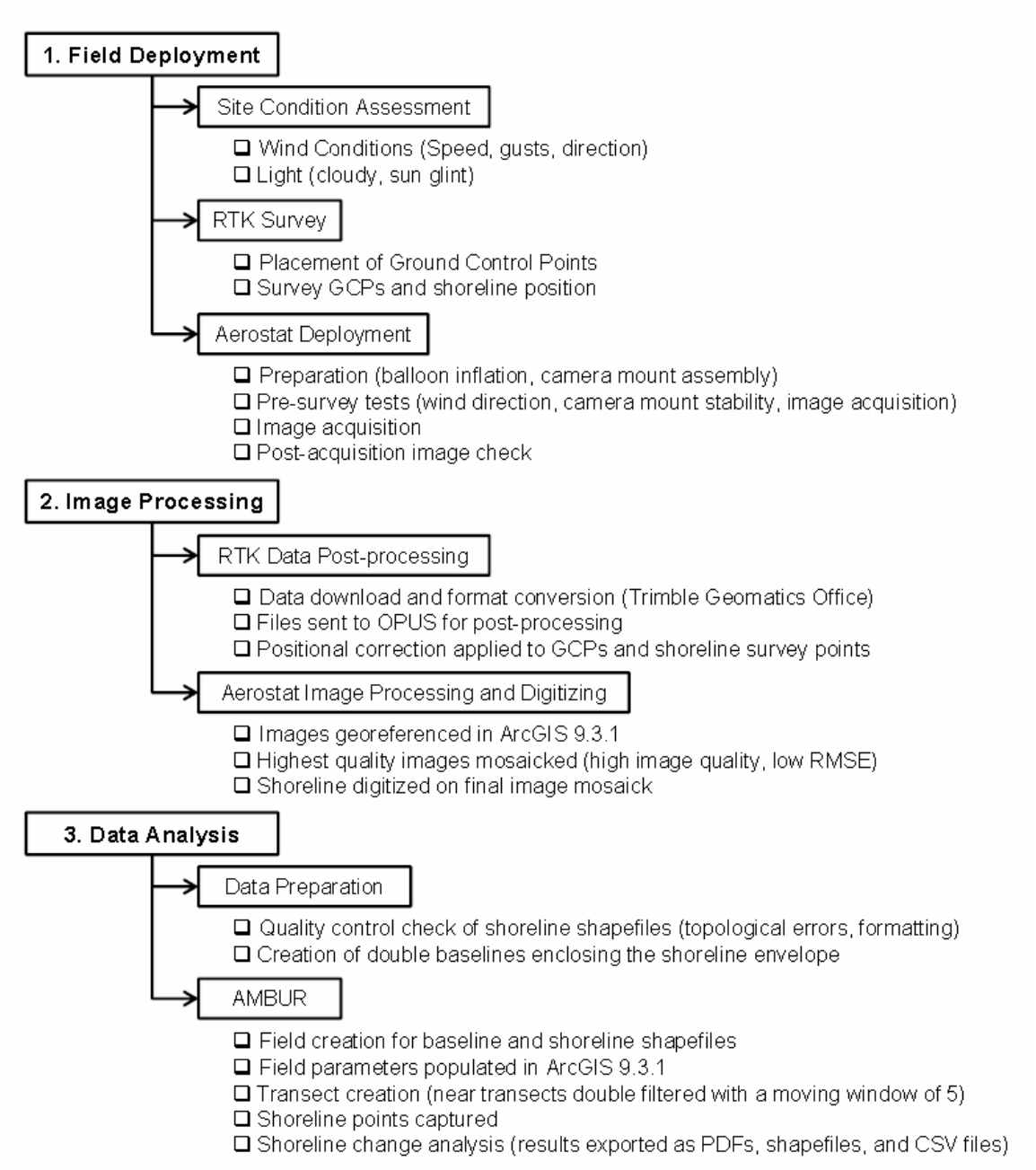

Figure 3 Work-flow diagram for obtaining Aerostat imagery, image post-processing, shoreline position acquisition, and shoreline change analysis.

reduce edge distortion. The primary limitation on Aerostat usage over the course of the study period was wind conditions. Wind direction (on-shore versus off-shore) impacted spatial coverage as well as the potential for interference with obstacles such as trees. Prior to deployment at each site wind conditions were assessed and a test flight conducted of the inflated balloon before attaching the camera platform (Fig. 3). Optimal conditions were found to be steady winds at less than 8 m/s. However, this was highly site dependent and the system was deployed in winds as high as 10-12 m/s along obstacle-free shorelines. Aerostat image collection during two surveys at the Gull Rock site (Surveys 2 and 4) was not possible because of high, gusting, winds.

Georeferencing of the images was conducted in ArcGIS 9.3. GCPs and shoreline position data were downloaded from the RTK and processed using the Trimble Geomatics Office software. The RTK base station position was adjusted using NOAA's automated processing system, OPUS (Online Positioning User Service) with the "Static" (>2 hour record) option, and then GCPs were adjusted in ArcGIS 9.3 using the appropriate OPUS-generated offset. The individual Aerostat images were imported as TIFs into ArcGIS and georeferenced using the built-in function with a second-order polynomial transformation (Fig. 3; Huges et al. 2006). Sufficient GCPs were available for individual images to allow the use of a third-order polynomial transformation or other transformations (i.e., spline or cubic), however due to the distribution of points these would result in excessive distortion and warping of the images between control points (Hughes et al. 2006). Processed images were subsequently rectified using the Nearest Neighbor function, clipped to the shorezone region, and mosaicked in ArcGIS. While not done for this project, Aerostat acquired images could be further processed and orthorectified using RTK-GPS data. In this study, RTK-GPS derived shorelines were

primarily utilized as an independent data-set to ground-truth shoreline positions obtained from Aerostat imagery. Shorelines were heads-up digitized on existing, recent orthophotos (obtained from Tyrrell and Hyde Counties via the Division of Coastal Management) and the mosaicked balloon images using the method of Geis and Bendell (2008; Fig. 4). Orthophotos of Tyrrell and Hyde used in this study had a pixel size of 0.3 m (Table 1). For visual comparison, the shorelines produced by the RTK-GPS surveys and digitized from the Aerostat imagery were plotted and initially analyzed in ArcGIS. However, the full analysis of shoreline change was completed using the AMBUR (Analyzing Moving Boundaries Using R) package developed for R (Jackson et al. 2012). The reported values for horizontal accuracy and pixel size were obtained from image metadata, published reports, or were calculated for the Aerostat using Equation 1.

As stated in the objectives, one of the problems associated with resolving changes in shoreline position over short (sub-annual) time periods is the resolution and error associated with traditional airplane- or satellite-based imagery (Table 1). To address this concern, the uncertainty (U) associated with determining shoreline position was calculated for all periods for each of the three methods (i.e., orthophotos, Aerostat images, and the RTK-GPS surveys) using the following equation (Crowell et al. 1991; Fletcher et al. 2003; Gentz et al. 2007; Cowart et al. 2010):

$$\mathbf{U}=\sqrt{\boldsymbol{E_d^2 + E_r^2 + E_g^2 + E_u^2}} \qquad \text{Equation 1}$$

where E_d is the digitization error, E_r is the rectification error, E_g is the positional error of the RTK-GPS, and E_u is the uncertainty associated with walking the shoreline (determined by calculating the mean difference in shoreline position between repeated surveys at each site). In

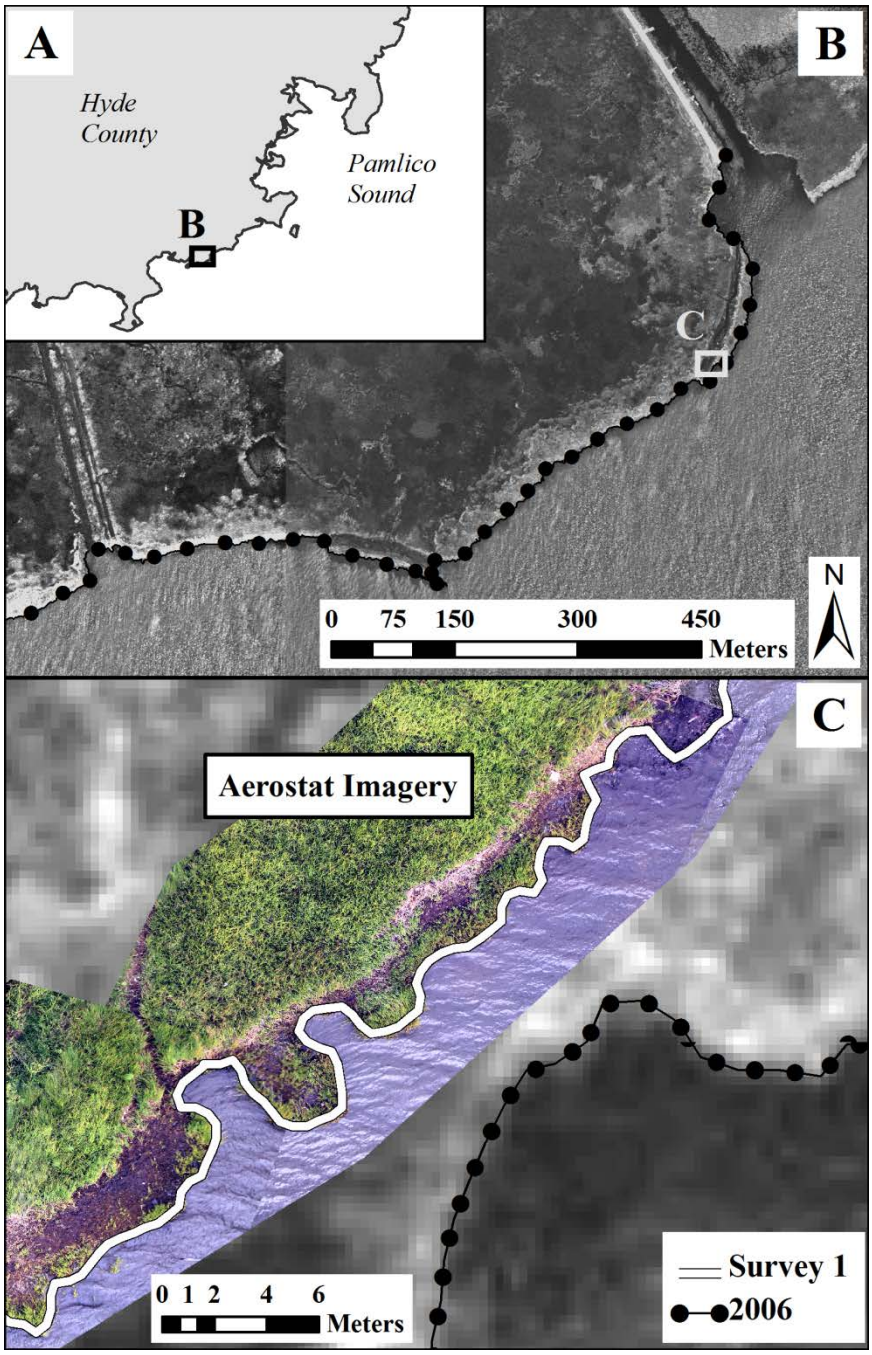

Figure 4 The GRG site as seen in 2006 Hyde County orthophotos and Aerostat imagery. A) Site location map; B) Hyde County orthophoto (2006) with the shoreline digitized, the white box denotes extent of part C; C) Aerostat image from 19 August 2010 overlain on the 2006 orthophoto with the shoreline digitized (Survey 1). Note the very high resolution of the Aerostat imagery in comparison to the underlying orthophoto.

Table 2 Shoreline-position uncertainty for each method calculated using Equation 1. For the Aerostat, the error includes image georeferencing (E_r), positional error for the GCPs (E_g), and digitizing error (E_d) based on a repeat digitization test. For the RTK-GPS, the method error includes RTK positional error and user survey error (E_u; based on repeated surveys). For the aerial imagery, image rectification error (E_r) and digitizing error (E_d) are included. Note, Aerostat error was reduced later in the study when more GCPs were utilized.

Site	Survey	Ortho (m)	RTK-GPS Survey (m)	Aerostat (m)	Mean Difference in Shoreline Position (RTK – Aerostat) (m)
PPP	20 August 2010	2.5	0.4	0.4	0.5 ± 0.4
	08 October 2010	2.5	0.4	0.3	0.3 ± 0.2
	06 January 2011	2.5	0.4	0.2	1.6 ± 1.0
	05 March 2011	2.5	0.4	0.2	0.3 ± 0.3
	06 May 2011	2.5	0.4	0.2	0.2 ± 0.2
GRG	19 August 2010	2.5	0.4	1.0	0.6 ± 1.0
	22 December 2010	2.5	0.4	0.7	0.3 ± 0.7
	06 May 2011	2.5	0.4	0.2	0.2 ± 0.1

order to minimize user error in this study, a single researcher (Eulie) conducted the RTK-GPS surveys, coordinated the Aerostat image acquisition, and digitized all the imagery.

3.0 Assessment

Out of the techniques used, the highest uncertainty was associated with using the orthophotos due to their lower horizontal accuracy (± 2.4 m; Tables 1 and 2). This was expected, as previously reported levels of error for orthophotos show a substantial range (e.g., 1.9-7.7 m from Cowart et al. 2010; Crowell et al. 1991). The uncertainties associated with shoreline position for the Aerostat and RTK-GPS were comparable. Overall, shoreline-position error from the Aerostat ranged from 0.2 m to 1.0 m, and the RTK-GPS had a 0.4 m uncertainty for all survey periods (Table 2). However, after initial georeferencing issues were solved, the Aerostat generally provided more accurate shoreline positions; the mean uncertainties for both the Aerostat and RTK-GPS methods were 0.4 m (Table 2). This could be further improved for the Aerostat through better spatial distribution of GCPs and orthorectification. For the Aerostat-based mapping, the uncertainty included the RMSE (root-mean-square-error) of image rectification (E_r), the positional error of the GCPs surveyed with the RTK-GPS (varied with survey period; E_g), and digitization error (0.2 m based on repeated digitization of the shoreline at each site; E_d). The RTK-GPS uncertainty was primarily due to user error (i.e., walking variability), which was evaluated by repeat surveys during a single visit (E_u). The error associated with GPS-position accuracy (E_g) was also included in the total RTK-GPS method error and varied with survey period but was less than 0.02 m for all surveys. Positional dilution of precision (PDOP) was controlled through the use of threshold settings programed into the RTK-GPS that prevented point collection when PDOP exceeded 6.5. Not surprisingly, for both

the Aerostat and RTK shoreline mapping methods, the "user" error (i.e., from digitizing or walking) represented the majority of the uncertainty in the shoreline position.

The mean difference (or offset) in the shoreline position as determined from the Aerostat and RTK-GPS methods at both sites was generally minimal and ranged from 0.2 to 1.6 m over the study (Table 2) with an average difference of 0.5 ± 0.5 m. At the GRG site, the difference was highest during the initial survey and decreased over time as Aerostat rectification was improved with the addition of more GCPs (Table 2). The initial installation of GCPs at each site resulted in 4-7 points per image, but by the last survey period, a total of 10-15 points per single (~ 500 m^2) image was used. At the PPP site, the difference between the Aerostat and RTK-GPS shorelines was highest during the 6 January 2011 survey, but exhibited a decreasing trend for the following survey periods (Table 2). The large offset in January 2011 is attributed to a wind shift that resulted in a water-level change and a relatively long elapsed time between the RTK-GPS survey and Aerostat image acquisition (almost 4 hours instead of the typical 1-2). The smallest difference in shoreline position (0.2 ± 0.2 m) was measured at the PPP site during the last survey period (06 May 2011; Table 2). Despite the reported differences in shoreline position for each methodology, a student T-test determined that there was no significant difference (at $p=0.05$) in the shoreline position determine by the two methods. This highlights that both approaches can be used to generate a similarly accurate shoreline. However, as the RTK-GPS is required to precisely survey the GCPs for the Aerostat method and because it has the advantage that it is not restricted by wind conditions, this technology is essential for high-resolution shoreline studies. But because the Aerostat provides an invaluable spatial perspective, it is most optimal to use both methods concurrently to acquire the best quality data and perspective on coastal changes.

The shoreline change rates (SCRs) for each site and period can be compared to the calculated uncertainty to determine if the average rates (along a stretch of shoreline) exceed the methodological error and therefore may be viewed as real rates of change. On average for the PPP site, the shoreline change was greater than the calculated uncertainty range for both the Aerostat and RTK-GPS methods (Table 3 versus Table 2). However, at the GRG site, where the calculated rates of shoreline change were less (-0.03 to -5.1 m/yr), the uncertainty was not always exceeded. Nevertheless, at both sites during most periods, substantial portions of the studied shoreline showed change well beyond the estimated error, indicating significant shoreline dynamics over short time periods.

4.0 Discussion

The data reveal how the shoreline at each site exhibited different behavior over time (Table 3), and this likely reflects a combination of the composition of the shoreline and its processes. Difference in the composition of the shoreline was reflected in the behavior of the two study sites. The PPP site was predominantly a sandy sediment bank shoreline while the GRG site is a peaty marsh platform. Less variability in shoreline position was observed at the GRG site. The smallest measured average change (-0.3 m/yr from the Aerostat) occurred at the GRG site between December 2010 and May 2011 (Table 3). The greatest variability in shoreline position over the study period was measured at the PPP site. In fact, the greatest annualized rate of change (-31.5 m/yr) for the study occurred at PPP between August and October of 2010 (Table 3; Fig. 5: Surveys 1 and 2). Yet overall, the mean SCR at the PPP site was positive (i.e., indicative of accretion), unlike the GRG area, and this was likely driven by differences in shoreline type.

Table 3 Shoreline change rates (SCR) calculated from the RTK-GPS survey method and the Aerostat method at two sites. The SCRs in bold type represent the net change over the course of the study. A positive value is net accretion, while negative values refer to net erosion.

Site	Survey Period	Mean Shoreline Change Rate (m/yr)	
		RTK	**Aerostat**
PPP	20 Aug 2010 to 08 Oct 2010	-31.3	-31.5
	08 Oct 2010 to 06 Jan 2011	27.4	21.6
	06 Jan 2011 to 05 Mar 2011	-11.9	-2.5
	06 Mar 2011 to 06 May 2011	-5.2	-4.8
	20 Aug 2010 to 06 May 2011	**0.3**	**0.2**
GRG	19 Aug 2010 to 22 Dec 2010	-3.8	-5.1
	22 Dec 2010 to 06 May 2011	0.1	-0.3
	19 Aug 2010 to 06 May 2011	**-1.6**	**-2.6**

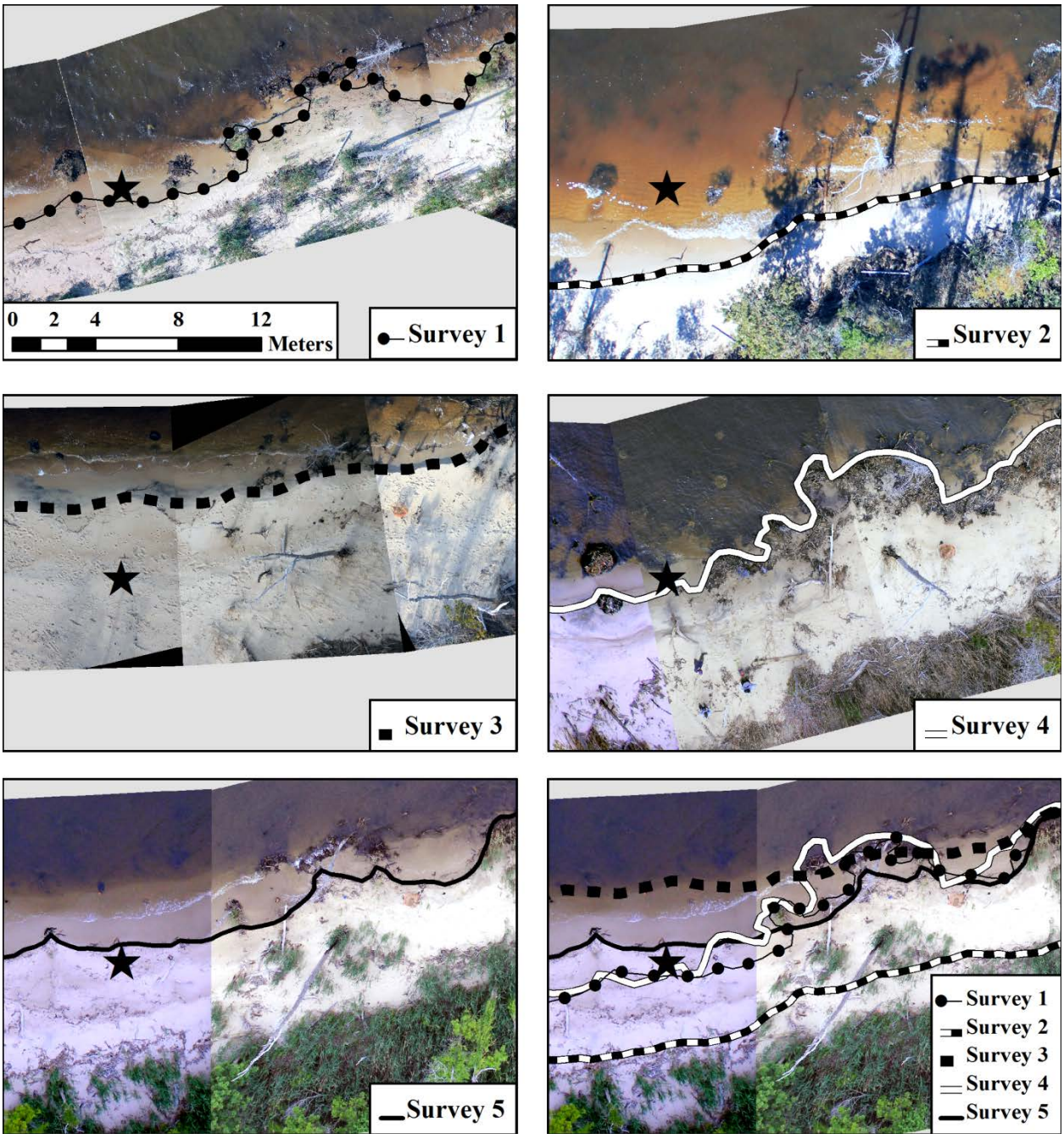

Figure 5 Aerostat images and digitized shorelines for all five surveys conducted at PPP from August 2010 to May 2011. Images are at an identical spatial scale, and the black star represents a common geographic point. The final panel shows all five shorelines on the May 2011 (Survey 5) images. The time series highlights significant variability in shoreline position due to sediment redistribution on this generally erosive coastline.

Previous research has suggested that marsh shorelines are better able to resist erosion, while unconsolidated sandy shorelines are more prone to reworking by waves (Riggs and Ames, 2003; Cowart et al., 2011). The timeseries of images for the PPP site shown in Figure 5 clearly illustrates the highly mobile nature of the sandy sediment at this location. Along with shoreline type, wave energy has also been recognized to impact SCR (Schwimmer 2001; Riggs and Ames 2003; Cowart et al. 2011). For example, in the nearby Neuse River estuary (also a part of the APES), Cowart et al. (2011) determined an empirical relationship between exposure to wave energy and shoreline change. While not directly investigated in this study, the Aerostat imagery indicate the PPP site was likely responding to wave climate variations, in a manner similar to profile changes observed on oceanfront sandy beaches (Aubrey 1979; Larson and Kraus 1994). For example, dramatic sand removal was observed between August 2010 and October 2010 (-31.5 m/yr; Table 3) at the PPP site when Hurricane Earl influenced the coast. Large waves created by this event probably moved sand off shore. Following this period of removal, massive accretion was measured (21.6 m/yr; Table 3), probably reflecting a return of these sediments. As both the PPP and GRG sites are immediately adjacent to the open waters of the Albemarle and Pamlico Sounds, it might be expected that both experience similarly high wave energy and therefore shoreline change, but different responses may be related to their orientation. However, shoreline composition is also likely to have an important influence.

Along with the ability to obtain high-frequency observations, the high resolution of Aerostat imagery provides very useful information on the environmental context. The larger pixel size of the orthophotos is unable to resolve small-scale (sub-meter) shorezone features such as the remnants of peat deposits, fallen trees, stumps, wrack, bulkheads or other natural or man-made features that can affect shoreline response. But, such features are clearly visible on the

Aerostat images (Figs. 5 and 6). To a limited extent, other contextual information such as local turbidity and nearshore bathymetry can also be discerned from the Aerostat imagery. The visibility of subaqueous features, such as submerged tree stumps and relict peat, depends on water level and water clarity on a given day.

A limitation of the RTK-GPS shoreline mapping is that the context of measured shoreline change cannot be determined, and as a result it may be difficult to discern an interpreted shoreline change because of water-level variability from actual change caused by sediment dynamics. Fortunately, shoreline features identified in balloon imagery can aid the interpretation of along-shore variations in SCR at different sites. For example, at the PPP site some of the shoreline segments that exhibited the least variation in shoreline position over the course of the study were located along areas with more stable fringing vegetation (Fig. 6A), while the least complex (i.e., most linear) and greatest variation in shore position was associated with gently sloped, un-vegetated, sandy beach (Fig. 6B). Another factor to consider is that massive redistribution of sediments along estuarine coastlines (e.g., that noted in Figs. 5 and 6B) can potentially have important effects on ecosystem processes (e.g., marsh and SAV dynamics). Consequently, an aerial perspective, such as that provided by the Aerostat, gives great insight into nature of measured changes. The system can also provide oblique imagery that would be valuable where vegetation obscures the shoreline in more traditional aerial photographs. Depending on the type of camera there is also the potential for capturing high-definition video. The camera platform can also be modified to carry additional sensors or sampling equipment provided it does not exceed the weight limit for the balloon. Possible additions (or in place of the camera) could include altimeters, near-infrared (NIR) or multispectral (MSI) cameras, video recorders, and other light instrumentation.

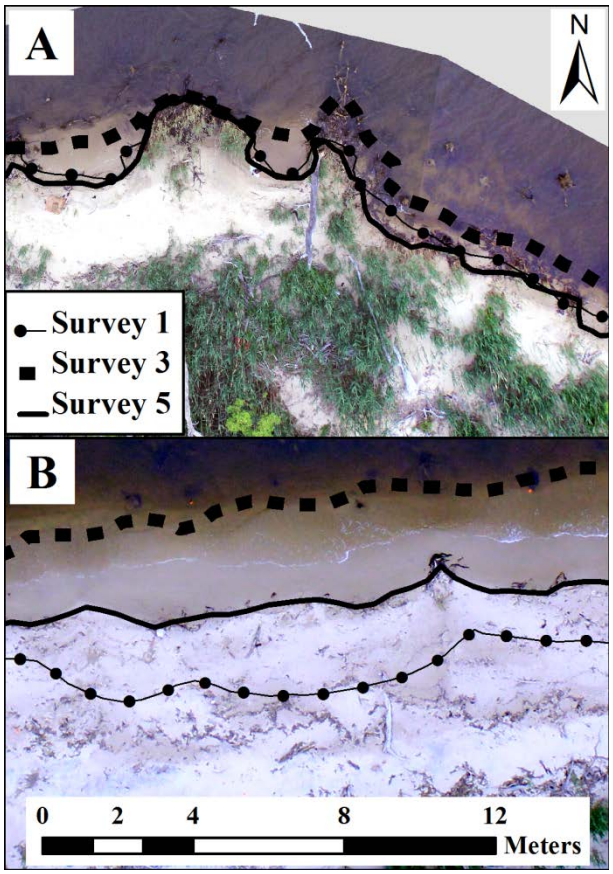

Figure 6 The PPP site with RTK-GPS survey shorelines from periods one, three, and five. A) A shoreline segment composed of fringing marsh, relict peat, and tree roots. B) A shoreline segment composed of un-vegetated, sandy sediment. Note the differing responses for the two different types of shoreline.

From this study it is evident that the shorezone context provided by balloon imagery provides invaluable information that can be used to explore the process and drivers of shoreline change in greater detail and that the shoreline of the Albemarle-Pamlico estuarine system is complex in time and space.

5.0 Summary

High-resolution aerial photography such as the Aerostat utilized in this study provides valuable imagery that, when paired with RTK-GPS measurements, can be used to examine changes in the shorezone over sub-annual timescales. The Aerostat can be used to accurately map the shoreline position and, in some cases, provides better accuracy than the RTK-GPS mapped shoreline alone. However, RTK-GPS is required to give precise GCP positions for accurate balloon image georectification. Ultimately, these two methods are best utilized together to obtain the highest possible accuracy, resolution, and insight into a coastal shoreline. The greatest value in imaging systems, such as the Aerostat, is that they provide a much needed birds-eye perspective on shoreline change and are a lower-cost, high-quality solution to obtaining high-frequency observations. The imagery creates a snapshot of the shorezone environment, including natural and man-made features, and can provide a useful environmental context for field observations. As demonstrated in the analysis here, parts of the shoreline of the Albemarle-Pamlico estuarine system are quite dynamic, and their change is likely influenced by shoreline composition and processes. In this manner and in conjunction with other measurements, this methodology can greatly aid understanding of the processes of shoreline change and presents a lower-cost, high-quality solution to obtaining high-frequency observations.

REFERENCES

Aubrey, D. G. 1979. Seasonal Patterns of Onshore/Offshore Sediment Movement. Journal of Geophysical Research 84**:** 6347-6354.

Boak, E. H., and I. L. Turner. 2005. Shoreline definition and detection: a review. Journal of Coastal Research 12**:** 688-703.

Cowart, L., D. R. Corbett, and J. P. Walsh. 2011. Shoreline Change along Sheltered Coastlines: Insights from the Neuse River Estuary, NC, USA. Remote Sensing**:** 1516-1534.

Cowart, L., J. P. Walsh, and D. R. Corbett. 2010. Analyzing Estuarine Shoreline Change: A Case Study of Cedar Island, North Carolina. Journal of Coastal Research 26**:** 817-830.

Crowell, M., S. P. Leatherman, and M. K. Buckley. 1991. Historical Shoreline Change: Error Analysis and Mapping Accuracy. Journal of Coastal Research 7**:** 839-852.

---. 1993. Shoreline Change Rate Analysis: Long Term Versus Short Term Data.

Dolan, R., B. Hayden, and J. Heywood. 1978. A New Photogrammetric Method for Determining Shoreline Erosion. Coastal Engineering 2**:** 21-39.

Fletcher, C. H., J. J. Rooney, M. Barbee, S. C. Lim, and B. M. Richmond. 2003. Mapping shorline change using digital orthophotogrammetry on Maui, Hawaii. Journal of Coastal Research SI 38**:** 106-124.

Gentz, A. S., C. H. Fletcher, R. A. Dunn, L. N. Frazer, and J. J. Rooney. 2007. The Predictive Accuracy of Shoreline Change Rate Methods and Alongshore Beach Variation on Maui, Hawaii. Journal of Coastal Research 23**:** 87-105.

Graham, D., M. Sault, and C. J. Bailey. 2003. National Ocean Service Shoreline - Past, Present, and Future. Journal of Coastal Research SI38**:** 14-32.

Hughes, M. L., P. F. Mcdowell, and W. A. Marcus. 2006. Accuracy assessment of georectified aerial photographs: Implications for measuring lateral channel movement in a GIS. Geomorphology 74**:** 1-16.

Jackson, C. W., C. R. Alexander, and D. M. Bush. 2012. Application of the AMBUR R package for spatio-temporal analysis of shoreline change: Jekyll Island, Georgia, USA. Computers and Geosciences 41**:** 199-207.

Langley, S. K., C. R. Alexander, D. M. Bush, and C. W. Jackson. 2003. Modernizing Shoreline Change Analysis in Georgia Using Topographic Survey Sheets in a GIS Environment. Journal of Coastal Research SI38**:** 168-177.

Larson, M., and N. C. Kraus. 1994. Temporal and spatial scales of beach profile change, Duck, North Carolina. Marine Geology 117**:** 75-94.

Massada, A. B., O. Gabay, A. Perevolotsky, and Y. Carmel. 2008. Quantifying the effect of grazing and shrub-clearing on small scale spatial patter of vegetation. Landscape Ecology 23**:** 327-339.

Miyamoto, M., K. Yoshino, T. Nagano, T. Ishida, and Y. Sato. 2004. Use of Balloon Aerial Photography for Classification of Kushiro Wetland Vegetation, Northeastern Japan. Wetlands 24**:** 701-710.

Riggs, S. R., and D. V. Ames. 2003. Drowning the North Carolina Coast: sea-level rise and estuarine dynamics. North Carolina Sea Grant.

Schwimmer, R. A. 2001. Rates and processes of marsh shoreline erosion in Rehoboth Bay, Delaware, USA. Journal of Coastal Research 17**:** 672.

Smith, M. J., J. Chandler, and J. Rose. 2009. High spatial resolution data acquisition for the geosciences: kite aerial photography. Earth Surface Processes and Landforms 34**:** 155-161.

Thieler, E. R., and W. W. Danforth. 1994. Historical Shoreline Mapping (I): Improving Techniques and Reducting Positioning Errors. Journal of Coastal Research 10**:** 549-563.

Wang, Y., and T. R. Allen. 2008. Estuarine Shoreline Change Detection Using Japanese ALOS PALSAR HH and JERS-1-HH SAR Data in the Albemarle-Pamlico Sounds, North Carolina, USA. International Journal of Remote Sensing 29**:** 4429-4442.

CHAPTER 3

Temporal and Spatial Dynamics of Estuarine Shoreline Change in the Albemarle-Pamlico Estuarine System, North Carolina, USA

Abstract

A majority of shoreline studies rely on historical change rates to predict shoreline position and determine set-back distances for coastal structures. They do not provide insight into finer-scale spatial variability or short-term variability in shoreline position from seasonal or episodic processes and most often focus on ocean front shorelines. In this study, shoreline change rates (SCRs) were quantified at five different sites ranging from marsh to sediment-bank shorelines around the Albemarle-Pamlico Estuarine System (APES) for a series of historical and sub-annual time periods, as well as individual storm events. Historical (fifty-year) rates of approximately -0.5 ± 0.07 m yr^{-1} were observed which is consistent with previous work along estuarine shorelines in North Carolina. Short-term (sub-annual) rates of shoreline change were highly variable, both spatially and temporally. Meteorological observations and coupled hydrodynamic-wave models using Delft3D and SWAN were utilized to examine hourly variability in the wave climate at the study sites. In the fetch-limited APES, wind direction was found to strongly influence wave climate at the study sites, and subsequently, shoreline change over short time periods. Despite the significantly higher rates of shoreline erosion from individual events like hurricanes, the mean SCR at the sites for these sub-annual eras was found to fall within the 95% confidence band when plotted in a linear regression model with historical shoreline positions. While the short-term response of these shorelines to episodic forcing should be taken into account in management plans, the long-term (historical and decadal) trends that are commonly used in ocean shoreline management can be used to determine erosion set-backs on estuarine shorelines.

1.0 Introduction

Estuarine shorelines are dynamic coastal features that are naturally shaped by a combination of hydrodynamic and biogeomorphic processes (Camfield and Morang 1996; Komar 1983; Roman and Nordstrom 1996; Phillips et al. 2006; Riggs and Ames 2004). Processes such as sea-level change, tectonic activity, tides, waves, and coastal storms can operate on varying temporal and spatial scales to influence the location of the shoreline and its morphology (Bellis et al. 1975; Camfield and Morang 1996; Esteves et al. 2006; List et al. 2006; Pajak and Leatherman 2002; Zhang et al. 2002). Changes in shoreline position over smaller spatial scales (e.g., 1 m to 10 km) and time scales ranging from hours to decades are primarily a function of hydrodynamic processes, human activities, sediment supply, and shoreline composition (Ali 2010; Bellis et al. 1975; Camfield and Morang 1996; French 2001; Jackson and Nordstrom 1993; Phillips 1986; Riggs and Ames 2003). These fluctuations in shore position occur over timescales that, while often considered historical when compared to timescales for human activity, are relatively recent in terms of geologic processes. However, they may also be rapid and operate on both temporal and spatial scales that intersect with coastal development and the functioning and use of coastal ecosystems (French 2001).

Shoreline change data is becoming more available to both the public and coastal managers and is primarily to help identify areas and structures at risk to erosion (Douglas et al. 1998; NRC 1990). Studies of oceanfront shoreline change are numerous, and historical or "long-term" rates of erosion are commonly used by managers to determine building set-back regulations in state coastal management plans (CMPs; Crowell et al. 1993; Douglas et al. 1998). Rates of estuarine shoreline change have been less studied and few states have set-back regulations that incorporate projected shoreline loss (NRC 2007). However, these complex

shorelines represent some of the most ecologically productive coastal habitats. In particular, wetlands are a critical habitat and there is concern regarding their potential loss. Studies also indicate that the rate of erosion along estuarine shorelines can exceed that of oceanfront shores (Corbett et al. 2008; Cowart et al. 2011; NRC 2007; Rosen 1967; Stevenson and Kearney 1996; Stirewalt and Ingram 1974). In North Carolina, there is about 20,000 km of estuarine shoreline compared to approximately 520 kilometers of oceanfront beaches (McVerry 2012). This includes 16,945 km of estuarine wetlands (marshes and riparian swamps; McVerry 2012). Previous studies have observed rates of change along estuarine shorelines of North Carolina from -0.5 m yr^{-1} to over -3.0 m yr^{-1} (Bellis et al. 1975; Cowart et al. 2011; Riggs and Ames 2003; Stirewalt and Ingram 1974). In the Neuse River sub-estuary, a tributary of Pamlico Sound, Cowart et al. (2011) observed a mean rate of shoreline change on the order of -0.6 m yr^{-1}.

Historical (>60 years) shoreline change rates provides an average picture of long-term coastal change, for management purposes, while minimizing the uncertainty associated with mapping methods (Crowell et al. 1993; Fletcher et al. 2003). However, these historical rates imply that the annual rate of change is constant. Set-backs or management plans based on these rates may not account for large, episodic events such as storms or seasonal variation in the shorezone position, both of which can be significant in terms of erosion (Crowell et al. 1993; Douglas et al. 1998; Douglas and Crowell 2000; List et al. 2006). These plans often also apply a mean rate of change to long stretches of coastline and commonly do not take into account fine-scale spatial variability. Differences in fetch, nearshore bathymetry, and shoreline morphology have all been shown to influence the rate of change (Cowart et al. 2011; Hardaway 1980; Phillips 1986; Rosen 1980; Schwimmer 2001; Stevenson and Kearney 1996; Wilcock et al. 1998).

The objective of this study is to examine shoreline change over a range of temporal and spatial scales to investigate: 1) controls on spatial and temporal variability in shoreline position, and 2) the contribution of episodic storm events to rates of shoreline change. This was accomplished by field surveys using Real-time kinematic (RTK) GPS and balloon-aerial photography, heads-up digitizing of historical shorelines, and a coupled hydrodynamic and wave model.

2.0 Site Description

A total of five sites around the Albemarle-Pamlico Estuarine System (APES) were chosen based on shoreline characteristics, accessibility, and location (Fig. 1). All five sites were located in estuarine locations and within the boundaries of parklands, wildlife refuges, and preserves with no nearby coastal structures that might influence shoreline changes. The sites encompass a range of shoreline types, shore morphologies, land cover, and exposure to waves. Two sites were located on back-barrier shorelines, while the other three sites were located along the mainland estuarine coast.

The first mainland site, in Goose Creek State Park (GCP), is located on the north shore of the Tar-Pamlico estuary in Beaufort County (Fig. 1). This site consists of a sandy, low-sediment bank shoreline with fringing grasses, isolated pockets of marsh, and some trees. The adjacent nearshore is shallow (<1 m) and large mobile sand shoals were present at times during the study. This site also had the most limited fetch due to estuary geometry (Fig. 1). The second mainland site, Gull Rock Gamelands (GRG), is located on Pamlico Sound in Hyde County (Fig. 1). This has a marsh shoreline characterized by a sharp subaqueous vertical scarp (generally <1 m) and an

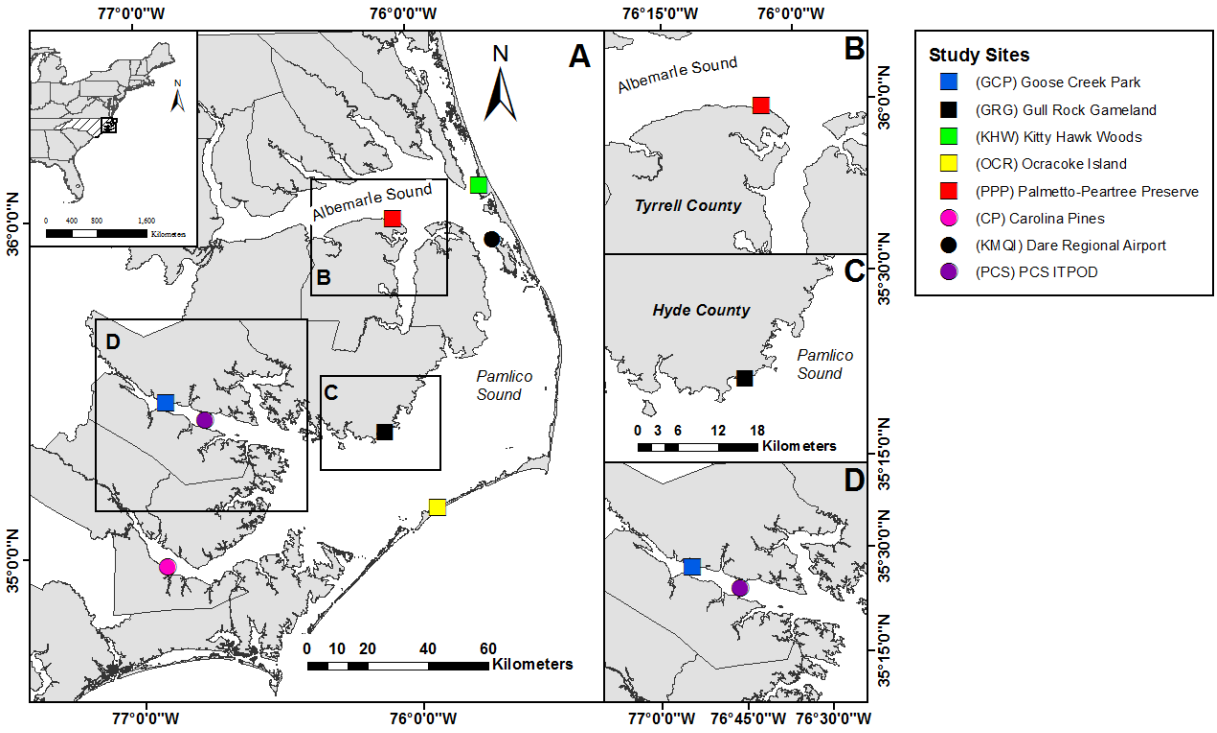

Figure 1 Map of locations utilized in this study. The full name for each site and abbreviated site initials are provided. The five shoreline sites are denoted by the squares (GCP, GRG, KHW, OCR, and PPP). The two sites used in the wave model validation are CP and PCS, and the source of wind data for the 2010-2011 period is station KMQI.

erosional morphology with extensive cleft-and-neck formations, undercutting, and pocket beaches analogous to that described by Schwimmer et al. (2001). The site is also backed by a man-made canal system. The third mainland site is the Palmetto-Peartree Preserve (PPP), which lies on Albemarle Sound in Tyrrell County (Fig. 1). This site consists of a sediment bank and swamp forest shoreline characterized by scattered woody debris, tree stumps, and some fringing grasses. Marshes are present in isolated pockets sheltered by large cypress trees and remnants of larger peat deposits. The adjacent nearshore is shallow (<1.5 m) and covered largely with sandy sediments and littered with woody debris.

The first of the two back-barrier sites is in the Kitty Hawk Woods Estuarine Research Reserve (KHW), located just south of the Wright Memorial Bridge connecting the Northern Outer Banks to Currituck County, NC (Fig. 1). The shoreline consists of alternating marsh platforms and pocket beaches that lie along a wooded coast. The marsh platforms stand 0.25 - 0.5 m higher in elevation than the adjacent beaches and are bounded at the water's edge by a vertical scarp. Locally, patches of marsh grass and peat are seen just offshore surrounded by shallow, sandy shoals. The second back-barrier site is on Ocracoke Island (OCR), just north of Ocracoke Village (Fig. 1). The site consists of two distinct sections, one dominated by sandy sediments and a gentle slope with less dense stands of marsh grasses. The other section is salt marsh with a subaqueous scarp of 20–30 cm and bisected by wide (5 to 10 meters across), shallow, tidal creeks with a sandy bottom.

This research will focus in more detail on the GCP, GRG, and PPP sites. These sites were chosen for their contrasting morphology, fetch limitation, and shoreline type. The GRG and PPP sites have opposite shoreline orientations (southeast-facing and north-facing, respectively), and represent the two most common shoreline types within the APES, marsh and

sediment bank. These sites are also exposed to some of the greatest fetches. The GCP site, in contrast, is the most fetch-limited of all the study sites and represents a mix of shoreline types.

3.0 Methods

3.1 Shoreline Mapping

Shoreline position was mapped at the five study sites over historical and sub-annual time periods. Table 1 lists the dates and properties of shoreline position data for each time period, hereafter referred to as 'eras'. Historical (fifty-year and decadal) eras are designated by an 'H', intermediate eras (less than 5 years) are designated by an 'I', and sub-annual eras by an 'S' (Table 1). The historical shoreline eras were digitized from aerial photos and the sub-annual eras were obtained from a series of in-situ surveys that were conducted every two months from June 2010 to May 2011. Due to technical and logistical difficulties, the timing and duration of the sub-annual S1 and S2 eras at the OCR site do not match the rest of the study site eras.

At each site approximately five kilometers of shoreline from historical aerial photos were digitized using the method of Geis and Bendell (2008). Aerial photos from the 1950s and 1982 were obtained from a U.S. Department of Agriculture (USDA) repository and the U.S. Geological Survey (USGS) online portal. Digital Orthophoto Quarter Quadrangle (DOQQs) Images for 1993 and 1998 were obtained from the North Carolina Department of Transportation (NCDOT) GIS portal. The most recent shoreline (digitized using aerial images) used 2006 or 2007 county photos, depending-on availability, and was completed as part of a larger shoreline mapping project for the North Carolina Division of Coastal Management (NCDCM). The 1950s and 1982 tagged-image-formatted (tif) images were imported into ArcGIS 9.3.1 and georeferenced with ground-control-points (a minimum of 9) from the 1998 DOQQ and

Table 1 Shoreline measurement dates and properties. Historical shoreline periods are designated by an 'H', an intermediate time period with 'I', and the bi-monthly surveys with an 'S' to indicate sub-annual.

	Eras	Shoreline Dates	Mean Total Era Uncertainty (m/yr)
Historical Eras (H)	50yr	1950's – 2006/2007	0.1
	H1	1950's – 1982	0.2
	H2	1982 – 1993	0.8
	H3	1993 – 1998	2.2
	H4	1998 – 2006/2007	0.9
Intermediate Era (I)	I	2006/2007 – June 2010	0.7
Sub-annual Eras (S)	S	June 2010 – May 2011	0.6
	S1	June 2010 – Aug 2010	3.6
	S2	Aug 2010 – Oct 2010	3.1
	S3	Oct 2010 – Jan 2011	2.5
	S4	Jan 2011 – Mar 2011	2.9
	S5	Mar 2011 – May 2011	3.1

2006/2006 county images using a second-order polynomial transformation. The average root-mean-square-error (RMSE) for all of the georeferenced images (averaged across all image tiles) was 1.7 m.

In-situ measurements of shoreline position at the study sites were collected every two months from June 2010 to May 2011. During each site visit the shoreline position was surveyed using a Trimble 5800 RTK-GPS system along a one-kilometer stretch of shoreline. The location of the shoreline was determined by the same criteria used in digitizing the historical shoreline positions, using the wet/dry line, the edge of the marsh platform, or the line of stable vegetation depending on the character of the shore (Geis and Bendell 2008). The RTK-GPS base station position was post-processed using the National Oceanic and Atmospheric Administration's (NOAA) automated processing system, OPUS (Online Positioning User Service). The data was processed with the 'Static' (>2 hour record) option and then shoreline points were re-projected using the OPUS-generated base station coordinates. The final shoreline position points were used for the calculation of shoreline change rates.

3.2 Shoreline Change Rate and Uncertainty

Calculations of shoreline change obtained from the different methods were completed using the AMBUR (Analyzing Moving Boundaries Using R) package (Jackson et al. 2012). Within this software the end-point method was used to measure change in the shoreline position over the eras of this study. A double-baseline method is used by AMBUR to create transects for calculating change across the shoreline envelope (Jackson et al. 2012). These were created in ArcGIS 9.3.1 by buffering the inner- and outer-most shorelines (buffer distances based on geometry and width of the shoreline envelope for each set of historical and sub-annual eras.

Shoreline transects were placed at 1-meter-intervals along the double-baseline at each site. While testing at two of the sites indicated coarser transect spacing of 5, 10, 25, and 50 meters would result in mean site SCRs that were not significantly different, the fine-scale of 1 meter transect spacing was deemed more appropriate for examining intra-site variability.

The uncertainty (U_t) associated with the annualized SCR for each era was calculated for each of the three methods (i.e., orthophotos, Aerostat images, and the RTK-GPS surveys) using the following equations (Cowart et al. 2010; Crowell et al. 1993; Eulie et al. 2013; Fletcher et al. 2003; Gentz et al. 2007):

$$\mathbf{U}=\sqrt{\boldsymbol{E_d^2}+\boldsymbol{E_r^2}+\boldsymbol{E_g^2}+\boldsymbol{E_u^2}} \qquad \text{Equation 1}$$

where E_d is the digitizing error, E_r is the image rectification error, E_g is the RTK-GPS instrument measurement error, and E_u is the uncertainty associated with surveying the shoreline (as determined by calculating the mean difference in shoreline position from repeated surveys at each site). The error for each individual shoreline survey (U_{ti}) where i represents a particular era was used to determine the annualized uncertainty (U_t) for each era by:

$$\mathbf{U_t}=\frac{\sqrt{\mathbf{U_{t1}^2}+\mathbf{U_{t2}^2}}}{\boldsymbol{T}} \qquad \text{Equation 2}$$

where T is the total length of time included in the era (Anders and Byrnes 1991; Crowell et al. 1993; Fletcher et al. 2003). The mean U_t for each era is reported in Table 2. Individual U_t values will be provided for each shoreline change rate. Calculating the total uncertainty associated with reported shoreline change rates provides a measure of confidence for the data (Crowell et al. 1993; Moore 2000). This mean U_t is foremost dependent on the error associated

Table 2 Calculated (using Eq.1) values for total uncertainty (U_t) for each type of aerial image or method utilized in this study.

Method	Horizontal Uncertainty (m)
1950's images	+/- 3.0
1982 images	+/- 2.9
1 m 1993 and 1998 DOQQs	+/- 7.7
0.3 m 2006/2007 orthophotos	+/- 2.4
Aerostat images	+/- 0.4
RTK-GPS	+/- 0.4

with each set of imagery and the length of time over which it is annualized (Crowell et al. 1993). As is seen in shoreline change time-series data, the longer the time frames of the data, the lower the annualized error or uncertainty typically (Crowell et al. 1993; Fletcher et al. 2003). For comparison, a U_t determined by Cowart et al. (2010) for a forty-year-era of shoreline change at Cedar Island, North Carolina, was found to be very close to the fifty-year-era U_t for this study (0.05 m yr^{-1} and 0.07 m yr^{-1}, respectively). The difference between these specific U_t values was due to the image rectification error (E_r), for the oldest photographs.

3.3 Balloon-based Aerial Imagery

A balloon-photography system (hereafter referred to as the Aerostat) was used to acquire high-resolution, high-frequency imagery. The imagery provided additional environmental observations to be used with the shoreline surveys. The Aerostat system consists of a polyurethane helium balloon designed to carry a remote-controlled gimbal mount that holds a digital SLR camera. The camera used in this study was a Canon Rebel T2i 18 megapixel with an EF-S 18-55 mm lens. A series of ground control points (GCPs) were installed and surveyed by RTK-GPS for accurate georeferencing. Initially, a total of 15-17 GCPs were installed at each of the study sites. To improve georeferencing, temporary survey flags (50-60 per site) were added to the existing control points. Georeferencing of the Aerostat images was conducted in ArcGIS 9.3.1. Additional details on this method can be obtained from Eulie et al. (2013).

3.4 Meteorological Observations

Observations of wind speed and direction were obtained for the sub-annual eras from the State Climate Office of North Carolina, at North Carolina State University, using their data

request service. Hourly observations for the 2010-2011 sub-annual eras were obtained from station KMQI (Manteo, NC; Fig. 1). Wind records for wave model validation were also obtained from the Cherry Point Marine Corps Air Station (MCAS) and station KHSE (Cape Hatteras; Fig. 1). All wind speed observations are reported in m s^{-1} and wind direction in the nautical convention (from direction) as degrees from geographic North. The wind record from station KMQI was filtered to remove hours where no data was available. Table 3 summarizes the percent of time there is no hourly wind data per sub-annual era for the GRG and PPP sites, with the greatest amount of missing data in late December 2010 to early January 2011. During this period entire days of the wind record were unavailable. This time period occurred during the S3 and S4 sub-annual eras (Table 2).

3.5 Wave Modeling

The numerical model Delft3D (Lesser et al. 2004) was used to simulate water level elevations in the APES for specific wind events during the sub-annual shoreline change eras. The model consists of a series of modules that can be utilized individually or coupled to simulate current flow, waves, sediment transport, and other parameters in shallow coastal or inland waters (Deltares 2011; Lesser et al. 2004). This study utilized the coupled Delft3D FLOW model for hydrodynamics and the SWAN (Simulating WAves Nearshore) WAVE model to simulate the surface waves (Booij et al. 1999; Ris et al. 1999). SWAN is a third-generation, spectral wave model based on the action balance equation. The model has been applied to the APES system by Mulligan et al. (2014) for simulating the waves and hydrodynamics of Hurricane Irene that impacted the study sites in August 2011, and used a computational grid in spherical coordinates that was developed for the study.

Table 3 The percent of time (hourly) per era that there is no wind data available for the GRG and PPP sites. Percentages calculated using the number of hours of available wind data and the total number of hours in each era. The majority of hours where wind data was unavailable occurred between December 2010 and January 2011.

Eras	Percent Time No Wind Data	
	GRG	PPP
S1	6.0 %	5.6 %
S2	10.7 %	11.4 %
S3	11.5 %	17.0 %
S4	22.4 %	19.0 %
S5	5.3 %	5.5%

The grid had a horizontal resolution of 250 m and was based on bathymetric data from NOAA. The model was initially set-up using hydrodynamic constants (e.g., bottom roughness, eddy viscosity) and wave parameters (e.g., bottom friction, whitecapping, wave breaking,) determined from previous testing by Mulligan et al. (2014) in the APES system. Sensitivity tests for bottom roughness, bottom friction, and spectral resolution were completed and the model results were calibrated to best match wave observations at Carolina Pines (CP) in the Neuse River Sub-estuary and at site PCS in the Tar-Pamlico sub-estuary (locations in Fig. 1). Wave observations were collected at the CP site using a Nortek Aquadopp that sampled at a frequency of 2 Hz in September, 2005, and at the PCS site using a Nortek Vector that sampled at a frequency of 8 Hz in August 2011. All simulations were run using a 1 minute time step with wave computations and FLOW-WAVE module coupling every 60 minutes. A spatially uniform wind-field produced with observations from the nearby Cherry Point MCAS station was used to force the model. The model validation at CP and PCS are shown in Fig. 2, indicating good agreement with spectral estimates of the significant wave height (H_s) and peak period (T_p) during the storm events.

After model validation was completed a series of simulations were run for three meteorological events during a period of high shoreline erosion (S2 era) in order to gain an understanding of the wave energy at the mainland study sites (GCP, GRG, PPP) during this era of high erosion. The first event was the passage of Hurricane Earl offshore of the NC coast in early September (Sept. 2-3, 2010) with wind speeds of up to 17 m s^{-1} measured at the KMQI station. Event 1 and Event 2 were frontal storms with wind speeds of >6.0 m s^{-1} that occurred during Sept. 16-17, 2010 and Sept. 27 - Oct. 4, 2010. Wind speeds of <6.0 m s^{-1} have been

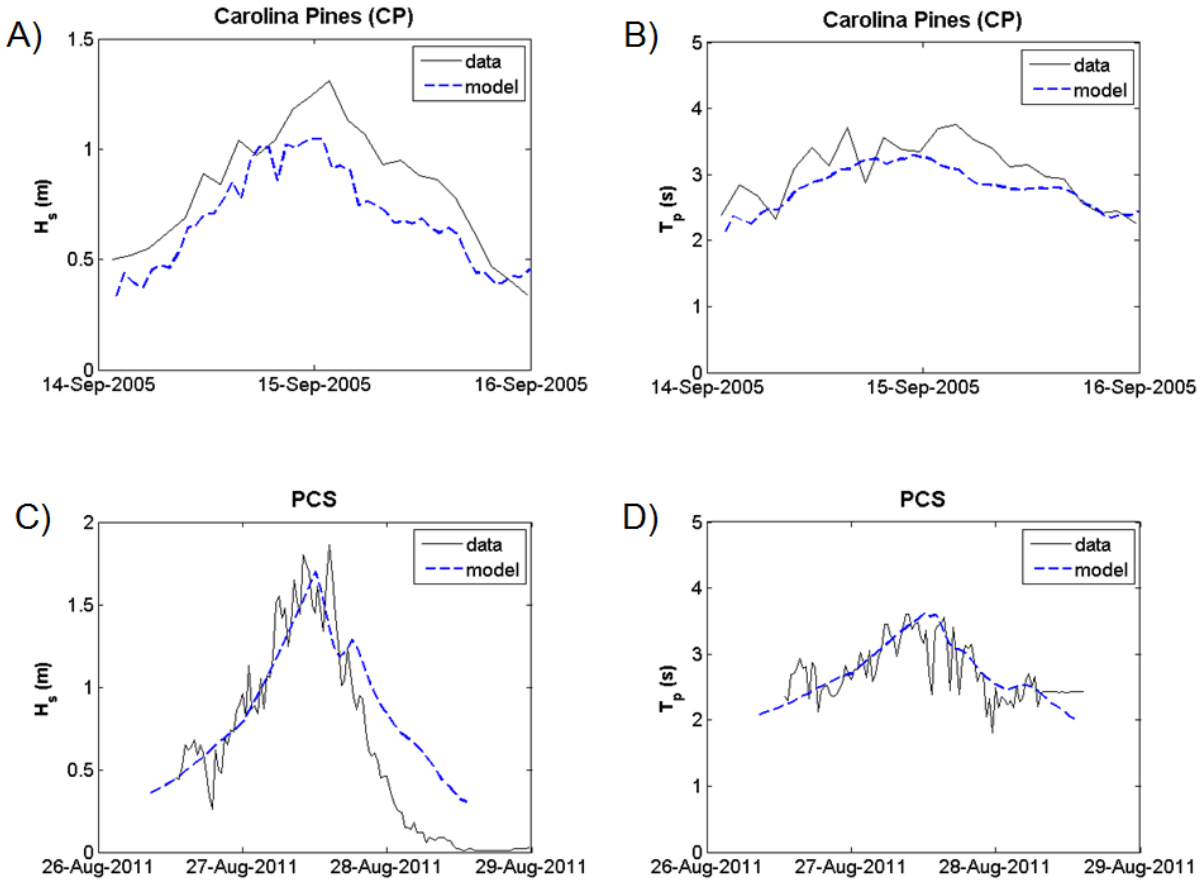

Figure 2 Comparison of wave observations and model results. At the CP site for Hurricane Ophelia, Sept. 14-16, 2005; A) significant wave height; B) peak wave period. At the PCS site for Hurricane Irene, Aug. 26-28, 2011; C) significant wave height; D) peak wave period.

shown in other fetch-limited systems to result in relatively low wave conditions (< 0.2 m)and were not included in these simulations (Jackson et al. 2002; Pierce 2004).

A fourth simulation was run to examine the distribution of wave energy at the sites for all of the sub-annual eras. This was accomplished by creating a wind record that used wind speeds in bins of 2 m s^{-1} ranging from 6 m s^{-1} to 30 m s^{-1} for each of the eight cardinal and ordinal compass directions (e.g., North, North Northeast, Northeast). This simulation will hereafter be referred to as the 'wind ramp'. The results for this simulation were then matched to the actual 335-day long wind record for the entire sub-annual period (June 2010-May 2011).

3.6 Statistical Analysis

Descriptive statistics and tests were calculated using the MINITAB software package. Analysis of variance (ANOVA) tests were conducted at a 95% confidence interval and a significance level of $p \leq 0.05$. Post-hoc testing used Tukey's Honestly-Significant-Difference (HSD) test to determine significant differences between sites and eras.

4.0 Results

4.1 Historical Shoreline Change

Over the fifty-year era, all of the study sites exhibited erosion and at a rate that exceeded the calculated mean uncertainty of ± 0.1 m yr^{-1} (Table 1 and Fig. 3). Four of the sites, GCP, GRG, OCR, and PPP had rates of change of approximately -0.5 m yr^{-1} (-0.5 ± 0.3, -0.5 ± 0.5, -0.6 ± 1.2, and -0.5 ± 0.5 m yr^{-1}, respectively). In contrast, the KHW site showed significantly less erosion with an SCR of only -0.3 ± 0.3 m yr^{-1} for the fifty-year-era. In pairwise comparisons

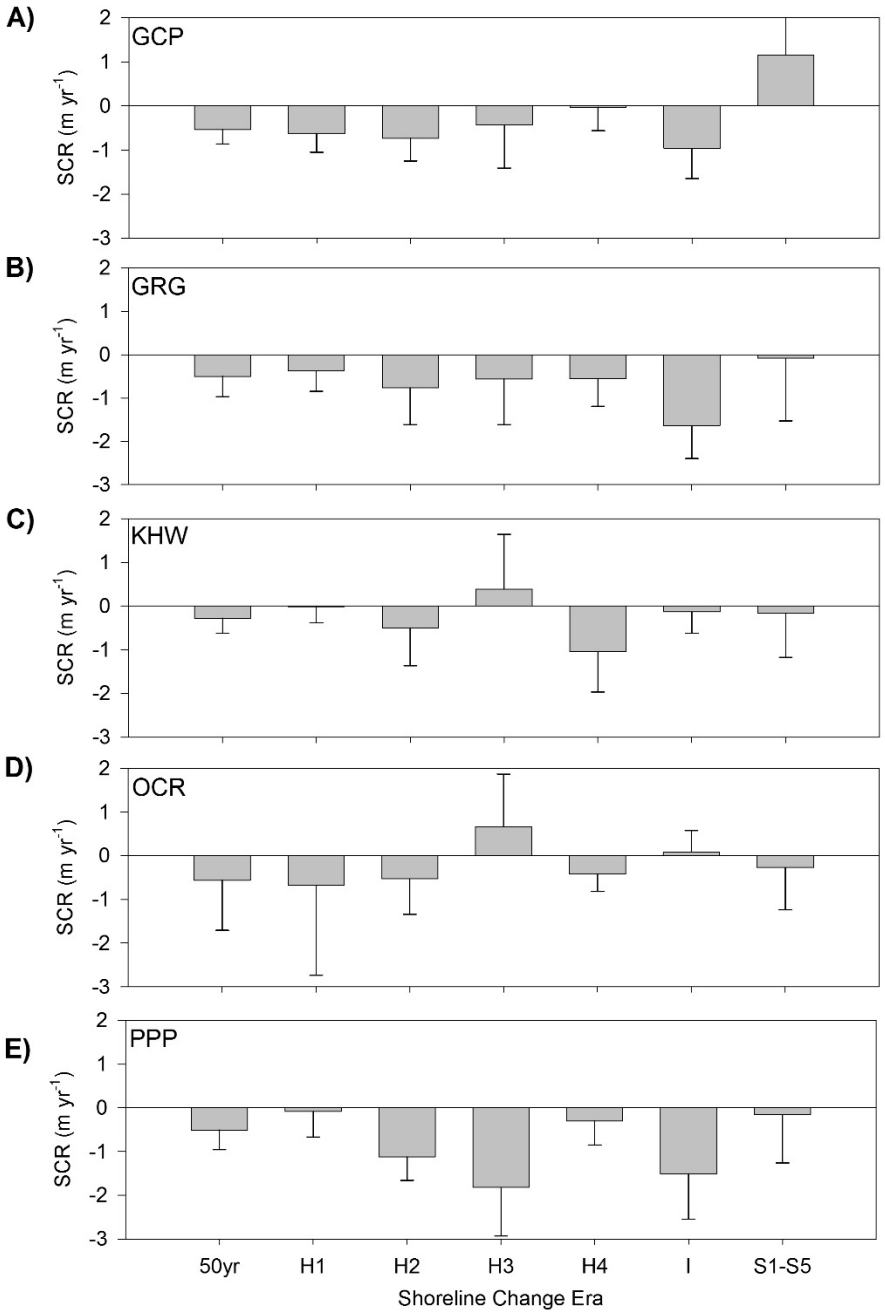

Figure 3 Mean historical shoreline change rates (SCRs) for all of the study sites, for all historical time intervals (eras; see Table 1), with error bars representing one standard deviation. Negative SCRs are indicative of erosion and positive SCRs indicate accretion.

the OCR site had a significantly greater rate of erosion than all but the GCP site, but it also had the greatest variability with a standard deviation of ±1.2 (Fig. 3).

Rates of shoreline change were also examined over the following individual eras within the fifty-year period; a multi-decadal era of approximately thirty-years (H1), two individual decades (H2 and H4), and a five-year era (H3). The dates for each of these eras and their calculated uncertainty (U_t) are reported in Table 1. Overall, SCRs for the H1-H4 eras were highly variable, by era and site. There were no clear trends of either accelerated erosion or accretion at the individual sites over the eras (Fig. 3). Rates of change were most consistent at the GRG site over all of the eras and only ranged from -0.4 ± 0.5 to -0.8 ± 0.8 m yr^{-1} (Fig. 3B). In contrast, the PPP site exhibited some of the greatest variability (-0.1 ± 0.6 to -1.8 ± 1.1 m yr^{-1}) and the OCR site had the greatest era (H3) of accretion (0.7 ± 1.2 m yr^{-1}; Figs. 3D and 3E).

During the H1 era (1950's to 1982), all of the sites exhibited erosion, however rates were highly variable and all were significantly different (Fig. 3). The GCP, GRG, and OCR sites had rates of change that exceeded the uncertainty of ±0.2 m yr^{-1}, -0.6 ± 0.4, -0.4 ± 0.5, and -0.7 ± 2.0 m yr^{-1}, respectively. However, the KHW and PPP sites had minimal erosion that was well within the error, indicating little average change at either location (Fig. 3C and 3D). For the H2 era, all of the sites exhibited rates of change that exceeded the long-term (fifty-year) average SCR, but were within the U_t for this era (H2), with the exception of the PPP site; the PPP site which had an SCR of -1.1 ± 0.5 m yr^{-1}.

During the H3 era (1993-1998) rates of shoreline change were variable and included the only positive SCRs during the fifty-year period. SCRs of approximately -0.5 m yr^{-1} were again observed at the GCP and GRG sites (-0.4 ± 1.0 and -0.6 ± 1.1 m yr^{-1}, respectively). However, the SCR at site PPP was significantly higher than the fifty-year average and represented the

greatest erosion rate observed during all of the historical eras of -1.8 ± 1.1 m yr^{-1} (Fig. 3E). In contrast, the two back-barrier sites, KHW and OCR, both exhibited mean accretion. However, the U_t for this period is the greatest of all the historical eras due to the short time span and high error associated with the aerial imagery. Therefore, it is likely that only the high rate at the PPP site reflects a stastically measurable average change. The most recent historical era of approximately a decade (1998-2006/2007, H4) was also highly variable by site, but all sites exhibited erosion and were significantly different, ranging from -0.03 ± 0.5 to -1.0 ± 0.9 m yr^{-1} (Fig. 3). As with the H3 era, only the SCR at one site, this time KHW (-1.0 ± 0.9 m yr^{-1}) appeared to be measurable change beyond the annualized error.

4.2 Intermediate Shoreline Change

Modern shoreline position since the last (H4) historical era (measured using RTK-GPS) is used to determine the intermediate era (I) and for net sub-annual change (S; Table 1). During the intermediate era (I), SCRs were variable between sites and displayed a similar trend to the H3 era (Fig. 3). The GCP, GRG, and PPP sites had higher rates of erosion that exceeded the error of ± 0.7 m yr^{-1}, while sites KHW and OCR exhibited minimal change that was well within error (Fig. 3). Over the five sub-annual eras (June 2010 to May 2011), net shoreline change was erosional at the GRG, KHW, PPP, and OCR sites and accretionary at the GCP site (S1-S5; Fig. 3). However, only the 1.2 ± 1.4 m yr^{-1} change at the GCP site exceeded the ± 0.6 m yr^{-1} uncertainty for the era (Table 1; Fig. 3). However, there was significant variability between sites and eras over the approximately one-year period.

4.3 Sub-annual Shoreline Change

The S1 era was similar to the net change over the year (S); exhibiting moderate erosion at the GRG, KHW, and PPP sites and accretion at the GCP site. There is no sub-annual data for the OCR site until the S3 period due to logistical constraints. The next several eras illustrate a trend of alternating erosion and accretion at the different sites. During the S2 era there was significant change at the GRG and PPP sites of -8.6 ± 9.8 and -19.3 ± 11.5 m yr^{-1}, respectively, that exceed the error of ± 3.1 m y^{-1}. There was comparatively little change at the GCP and KHW sites, all within error (Table 1). After this era of high erosion, the S3 period was characterized by accretion at all of the sites (Fig. 4). However, the accretion was only statistically significant at the two sediment bank sites, GCP and PPP (10.3 ± 11.7 to 15.8 ± 7.5 m yr^{-1}; Figs. 4A and 4E). At the GCP site, this was due to significant accretion along a segment of the shoreline. This accretion widened a small section of the shoreline by over 10 m. At the PPP site, the greatest accretion was also localized to a small segment of the shoreline (Fig. 5). For both the GCP and PPP sites, this period of accretion was followed by another era (S4) of significant erosion, with SCRs of -9.7 ± 8.8 and -5.6 ± 8.4 m yr^{-1}, respectively (Figs. 4A and 4E). During the final sub-annual era (S5), the PPP site exhibited a similar rate of erosion to the S4 era with an SCR of 5.4 ± 6.1 m yr^{-1} (Fig. 4E). Figure 5 exhibits the overall erosion-accretion cycle observed at the PPP site using the Aerostat imagery. Moderate shoreline change rates were observed at the other four sites during the S5 era and all were within the range of uncertainty (Fig. 4A).

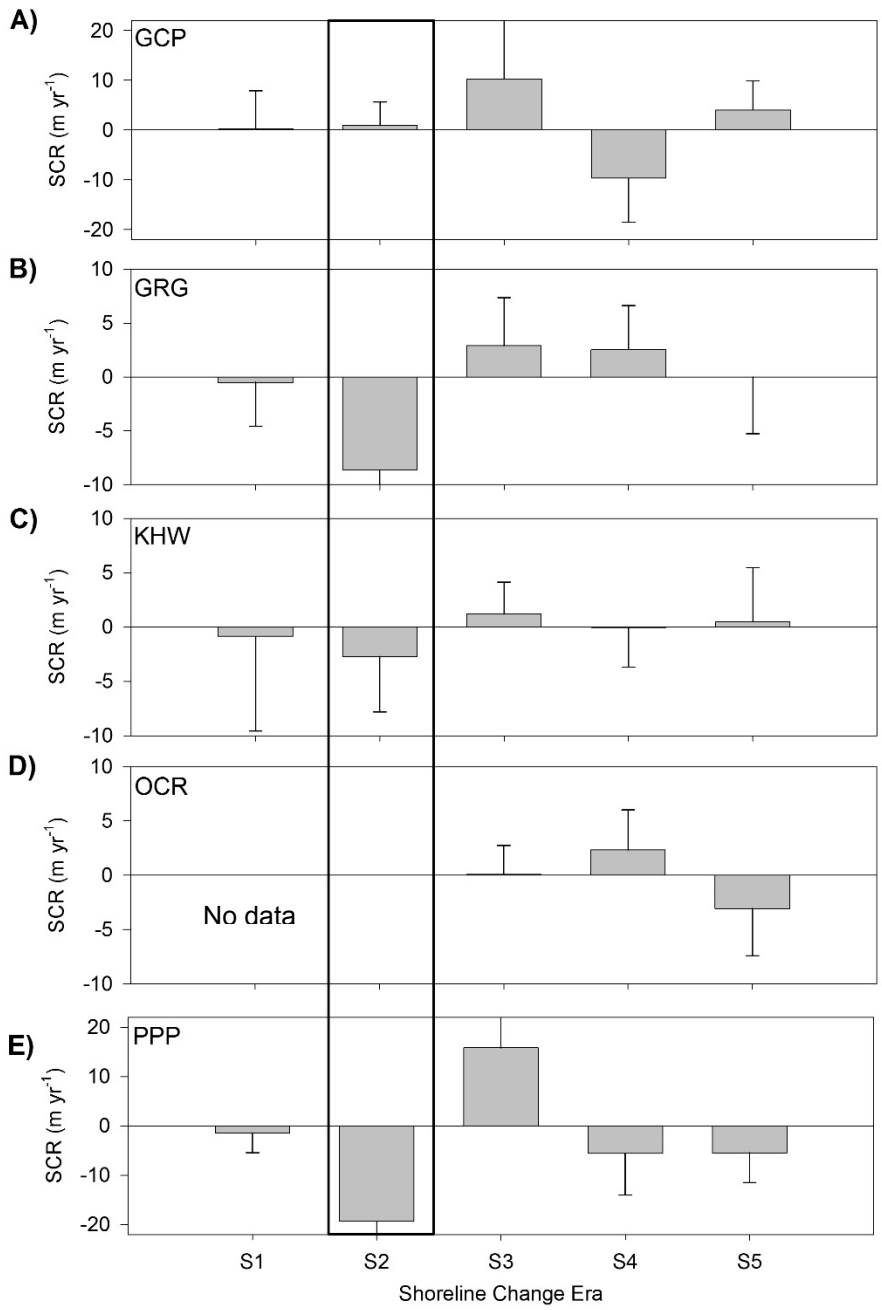

Figure 4 Mean sub-annual (see Table 1) shoreline change rates (SCRs) for all of the study sites. Error bars represent one standard deviation. Negative SCRs are indicative of erosion and positive SCRs indicate accretion. The box indicates era in which Hurricane Earl occurred.

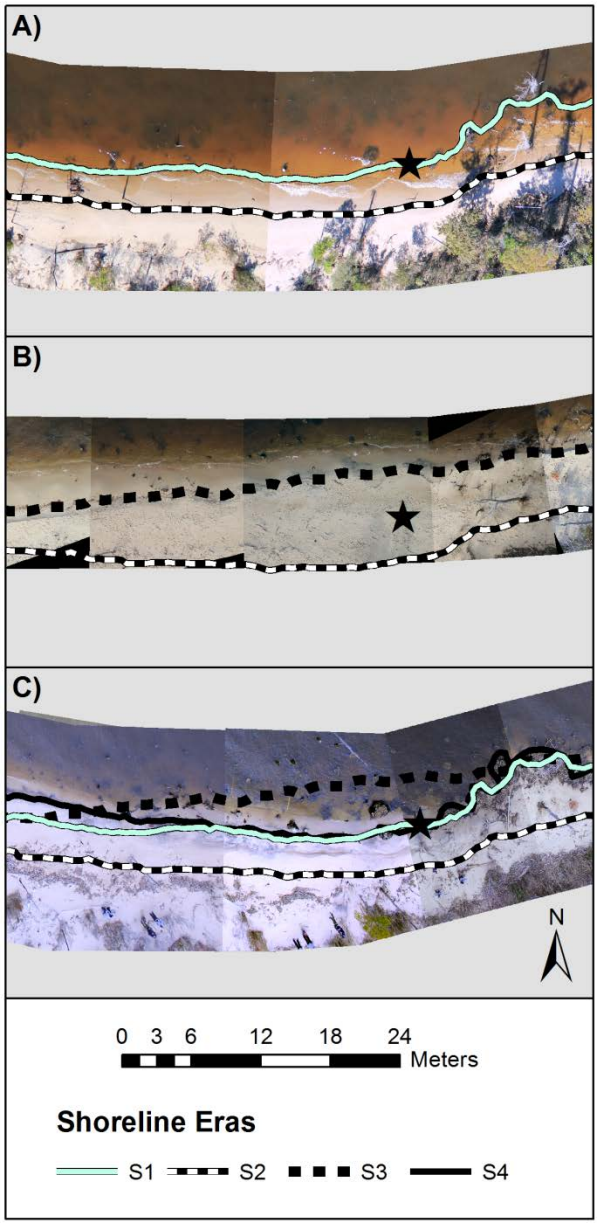

Figure 5 Aerostat imagery at the PPP site over three sub-annual eras; A) S2, B) S3, C) S4. The black star indicates the same geographic location in all three images.

4.4 Spatial Variability in Shoreline Change

Within each study site there was significant along-shore variability in the rates of shoreline change. Over the historical eras alongshore trends in shoreline change were relatively consistent at individual sites and exhibited distinct trends. For example, at the PPP site the highest (50-year) rates of shoreline erosion (greater than 1.0 m yr^{-1}) were consistently observed across transects ~3500-5000 (Fig 6A). Distinct patterns of shoreline change were also noted between transects 1 and 2500, where the shoreline forms a series of point features. Rates of erosion greater than 1.0 m yr^{-1} dominate the western side of each point feature, while the eastern shoreline of each is characterized by either minor changes in shoreline position, or no observable change (Fig. 6A). The GCP and GRG sites also exhibited distinct 50-year patterns of shoreline change (Figs 7 and 8). These sites have more complex shorezone morphologies of marsh and sediment bank, dissected by the presence of canals and creek systems. The highest historical rates of erosion were along the most exposed (to open water and longer fetches) segments and minor accretion or little change was observed locally in protected embayments and along creeks. The mouth of canals and creeks were also seen to have higher rates of erosion then surrounding shoreline segments. At the GRG site, the highest erosion occurred along a section of shoreline between transects 3800 and 4000 (Fig. 7A). This segment of shoreline was backed by a shore-parallel canal first in 1972 imagery, but not present in the 1956 imagery. Over the subsequent decades a high rate of erosion removed the fronting section of marsh platform, exposing the canal and its shoreline to Pamlico Sound. This is especially prominent following periods of high water and greater wave energy. At the GCP site, some of the greatest 50-year change in shoreline position was associated with a small cove and the entrance to a small creek at the western end of the site (Fig. 8A).

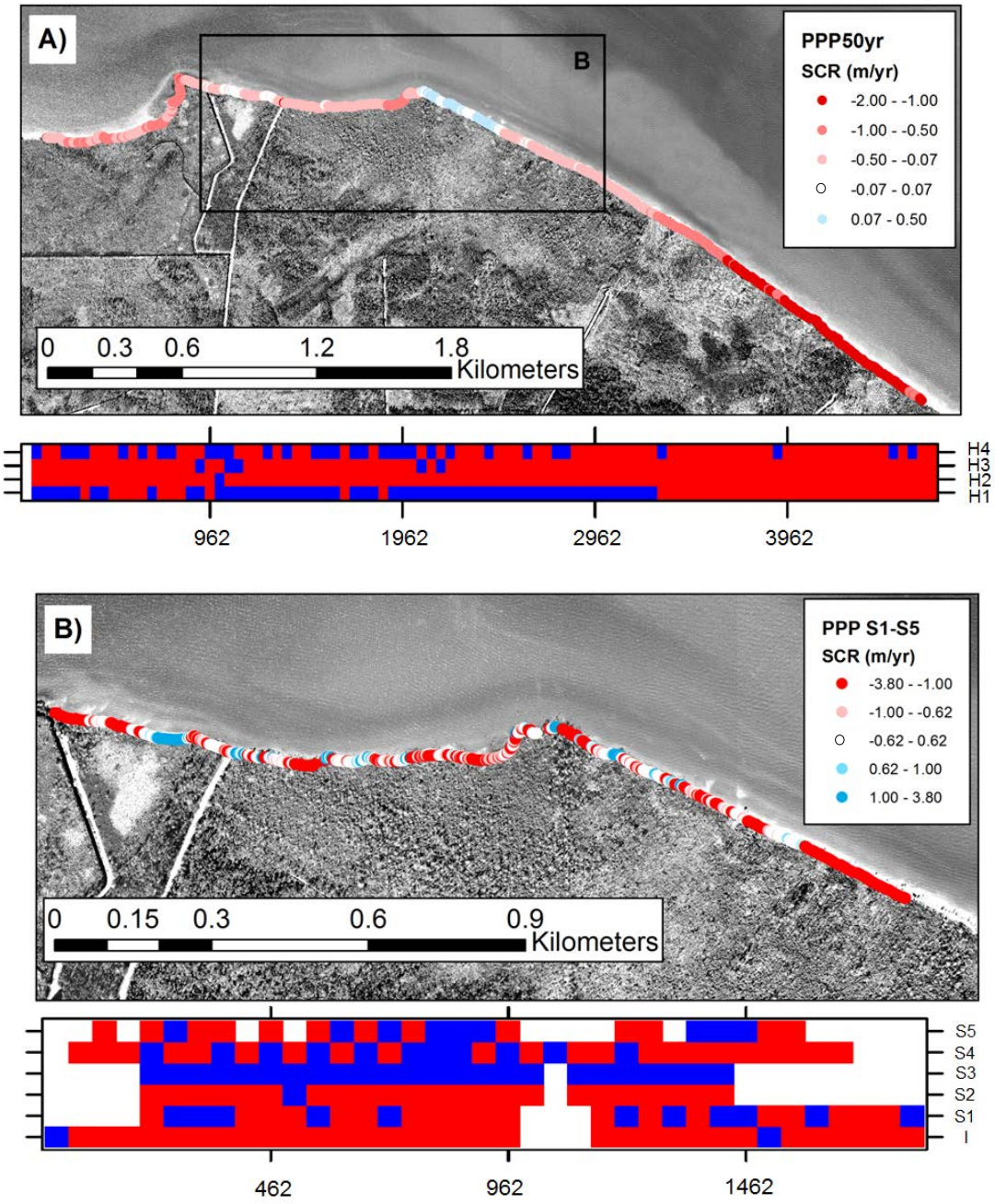

Figure 6 Shoreline change at the PPP site; A) Shoreline change over the 50yr era, B) Shoreline change over the modern (S1-S5) era. Spatial extent of 6B is indicated by the black rectangle in 6A. The plots located below each map indicate erosion (red blocks) or accretion (blue blocks) averaged over 50 m along the shoreline. The plots show era along the y-axis and along-shore transect number along the x-axis.

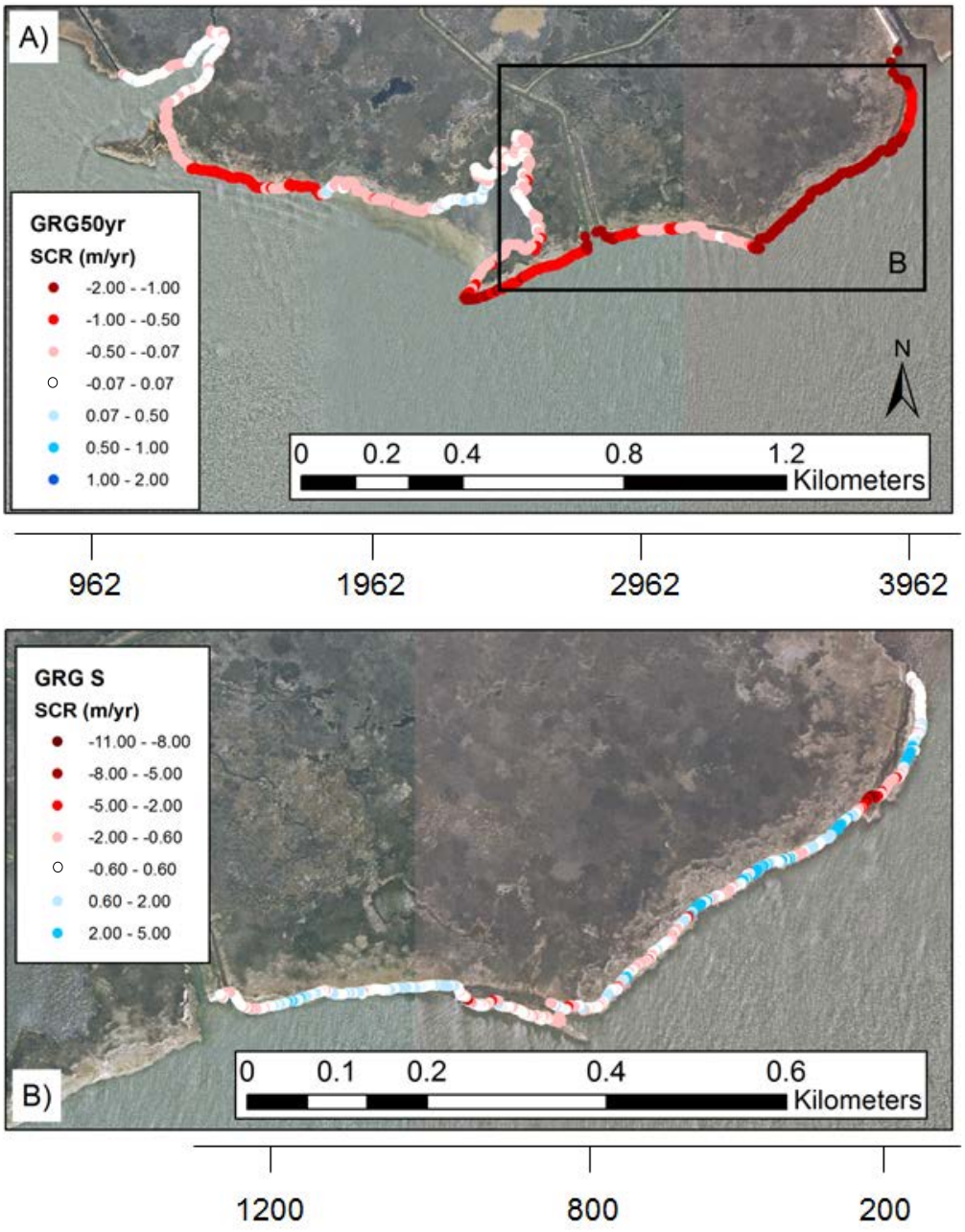

Figure 7 Shoreline change at the GRG site; A) Shoreline change over the 50yr era, B) Shoreline change over the modern (S1-S5) era. Spatial extent of 7B is indicated by the black rectangle in 7A. The bars below 7A and 7B indicate along-shore transect number.

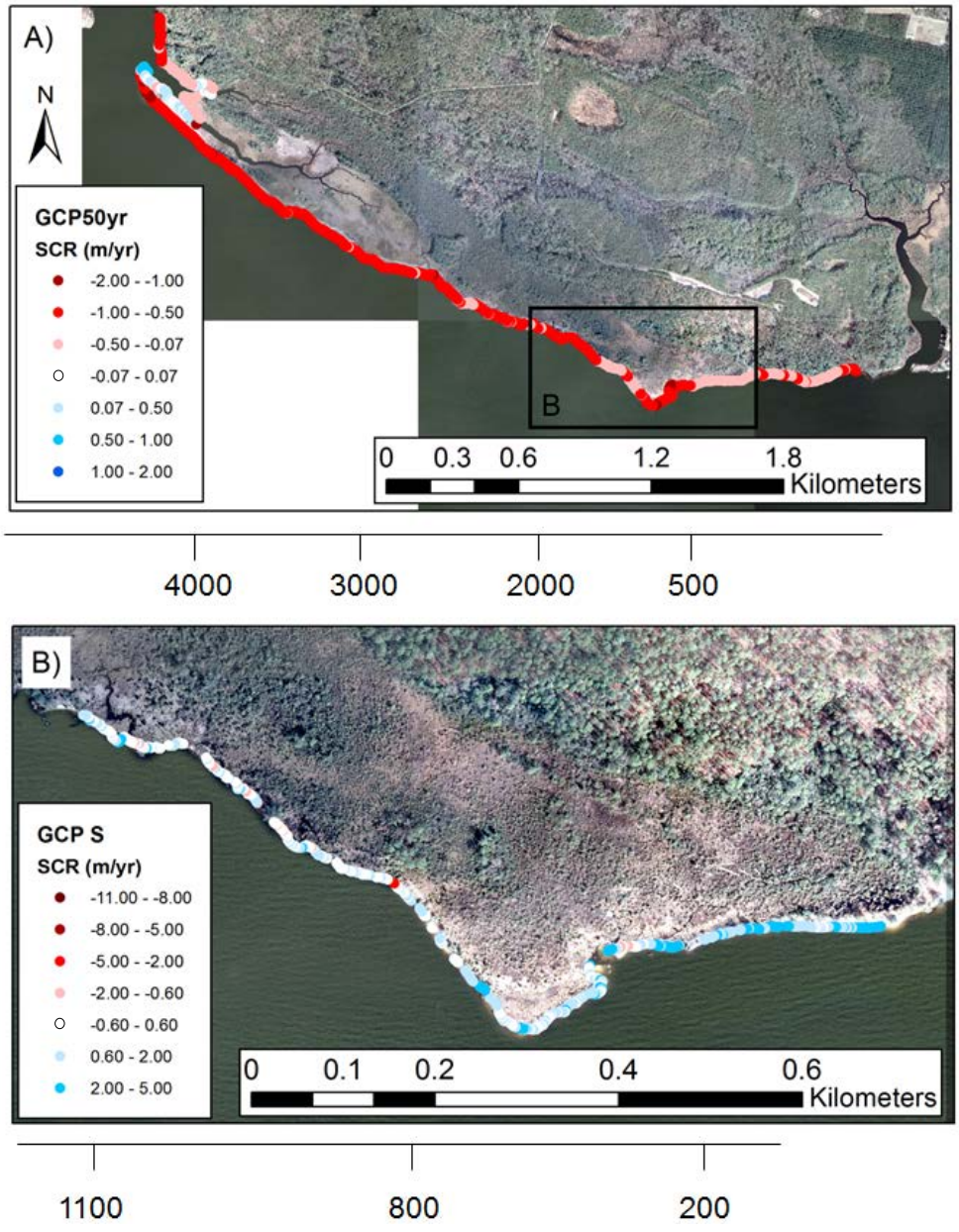

Figure 8 Shoreline change at the GCP site; A) Shoreline change over the 50yr era, B) Shoreline change over the modern (S1-S5) era. Spatial extent of 8B is indicated by the black rectangle in 8A. The bars below 8A and 8B indicate along-shore transect number.

Over the modern eras (I and sub-annual periods), spatial trends were less clearly defined at some of the sites due in part to the higher uncertainty values and greater temporal variability. Segments of shoreline that were clearly defined as consistently eroding over the fifty-year era were observed to erode, accrete, or have no change depending on the sub-annual era. For example, at the GRG site between transects ~3800 and 5000, the historical eras exhibit consistently high rates of shoreline erosion (Figs. 7A and 7B). Whereas, during the sub-annual eras, the same shoreline is characterized by alternating segments of erosional and of no observable change, or even minor accretion (Figs. 7A and 7B). At some locations (eg. Fig. 6B, transects 400-500; Fig. 8B, transects 100-200) there was a large degree of along-shore variability within a relatively small (<100 meter) shoreline segment. At the GCP site, there was less along-shore variability in shoreline position over the study (Fig. 7). The exception was a small segment of the shoreline characterized by an ephemeral, transient, sand accumulation.

4.5 Wind and Waves

Prior to running simulations for three wind events during the S2 sub-annual era, the model was calibrated using the Hurricane Ophelia and Hurricane Irene storm events. In general, model results at the Carolina Pines (CP; Fig. 1) site were found to be in good agreement with observations of the Hurricane Ophelia storm event that occurred Sept. 14-15, 2005 (Figs. 2A and 2B). The model was found to slightly under-estimate significant wave height (H_s) and peak wave period (T_p; Figs. 2A and 2B). The maximum predicted (model) H_s was 1.1 m (observed H_s = 1.3 m) and predicted T_p = 3.3 s (observed T_p = 3.7 s). Model validation carried-out for the Hurricane Irene event using model grids and set-up modified from Mulligan et al. (2014) and parameters determined by sensitivity testing for this study also found good agreement between

the predicted and observed values (Figs. 2C and 2D). Predicted maximum H_s = 1.7 m (observed H_s = 1.8 m) and predicted T_p = 3.6 s (observed T_p = 3.6 s; Figs. 2C and 2D).

The wave model was run for three meteorological events that occurred during the S2 period of high erosion. The results from these models are illustrated in Figures 9 and 10. The overall greatest significant wave heights occurred at the PPP site from the passage of Hurricane Earl in early September (Fig. 9A-D; Table 4). As the storm passed offshore, the dominant wind direction was from the North at speeds of 16-17 m s^{-1} (Fig. 9A). These conditions resulted in an H_s of 1.2 m at the site (Fig. 9B; Table 4). Whereas at the GCP and GRG sites, significant wave height peaked at only 0.6 m (Fig. 9B; Table 4). This difference was due to the wind direction (from the North) that resulted in the greatest wave heights occurring on the southern shorelines of the Albemarle and Pamlico sounds (Fig. 11A). The GCP and GRG sites, located along northern shorelines of the Tar-Pamlico and Pamlico Sound, were exposed to smaller waves (less than 1.0 m; Fig. 11A). The wind direction also resulted in a lowering of water-level by 0.25 m at the GCP site, which contributed to limiting wave growth at the site (Fig. 9D; Table 4). Peak periods at the three sites ranged from 2.2 s (GCP and GRG) to 3.8 s (PPP; Fig. 9C; Table 4).

The second event modeled during the S2 era was for a typical frontal system that moved over the study area Sept. 16-18, 2010 and resulted in wind speeds of 7-9 m s^{-1} from the South during the peak of the storm (Fig. 9E; Table 4). While wind speed was much lower than the Hurricane Earl event, the model calculated significant wave heights of over 0.5 m and wave peak periods of almost 3 s for the GRG site (Figs. 9F and 9G; Table 4). Model results for the PPP and GCP site indicated H_s of only 0.4 m and T_p close to 2 s for this same storm (Figs. 9E and 9F; Table 4). Change in water-level was less than 0.1 m for the duration of the event (Fig. 9H). The distribution of significant wave heights for peak wind speed during this event is illustrated in

Table 4 Wave characteristics for the GCP, GRG, and PPP sites at the time of peak wind speeds for each model run. Characteristics include significant wave height (H_s), water-level (η), and peak period (T_p).

Model	Wind	Site	H_s (m)	η (m)	T_p (s)
Hurricane Earl	N (350°) 17 m s^{-1}	GCP	0.6	-0.25	2.2
		GRG	0.6	0.07	2.2
		PPP	1.2	-0.12	3.8
Event 1	S (190°) 9.3 m s^{-1}	GCP	0.4	0.01	2.0
		GRG	0.6	-0.02	2.9
		PPP	0.4	0.05	2.2
Event 2a	SSE (150°) 13.4 m s^{-1}	GCP	0.7	0.26	2.7
		GRG	0.8	-0.02	3.1
		PPP	0.8	0.15	2.9
Event 2b	NE (40°) 7.7 m s^{-1}	GCP	0.3	0.07	1.8
		GRG	0.4	0.03	2.2
		PPP	0.6	-0.01	2.8

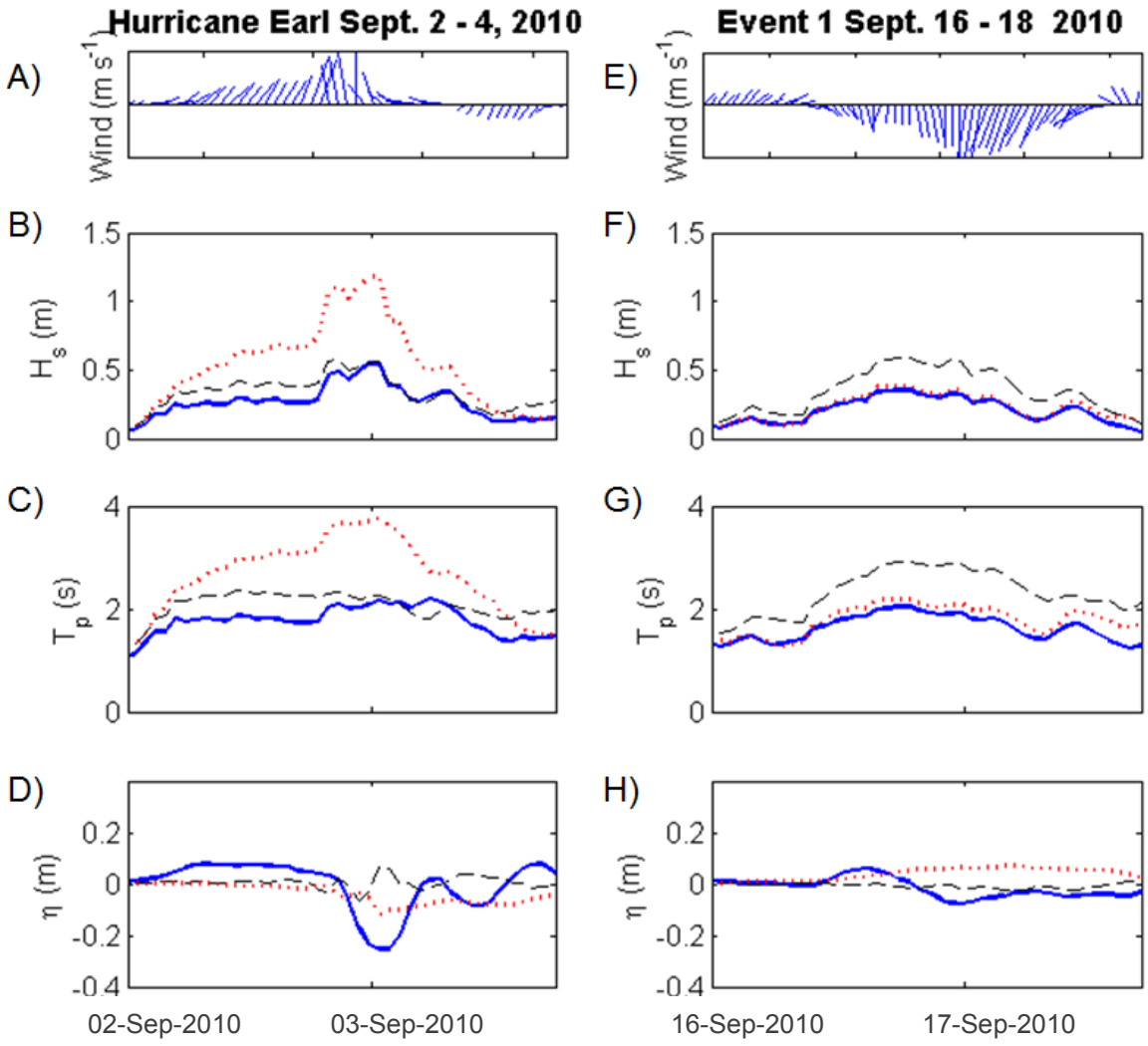

Figure 9 Model results for the Hurricane Earl and Event 1 wind events during the S2 era, at the GCP (blue), GRG (dashed black), and PPP (dashed red) sites. A) and E) Wind stick vectors indicating speed and direction , B) and F) Significant wave height (H_s), C) and G) Peak period (T_p), and D) and H)Water-level (η).

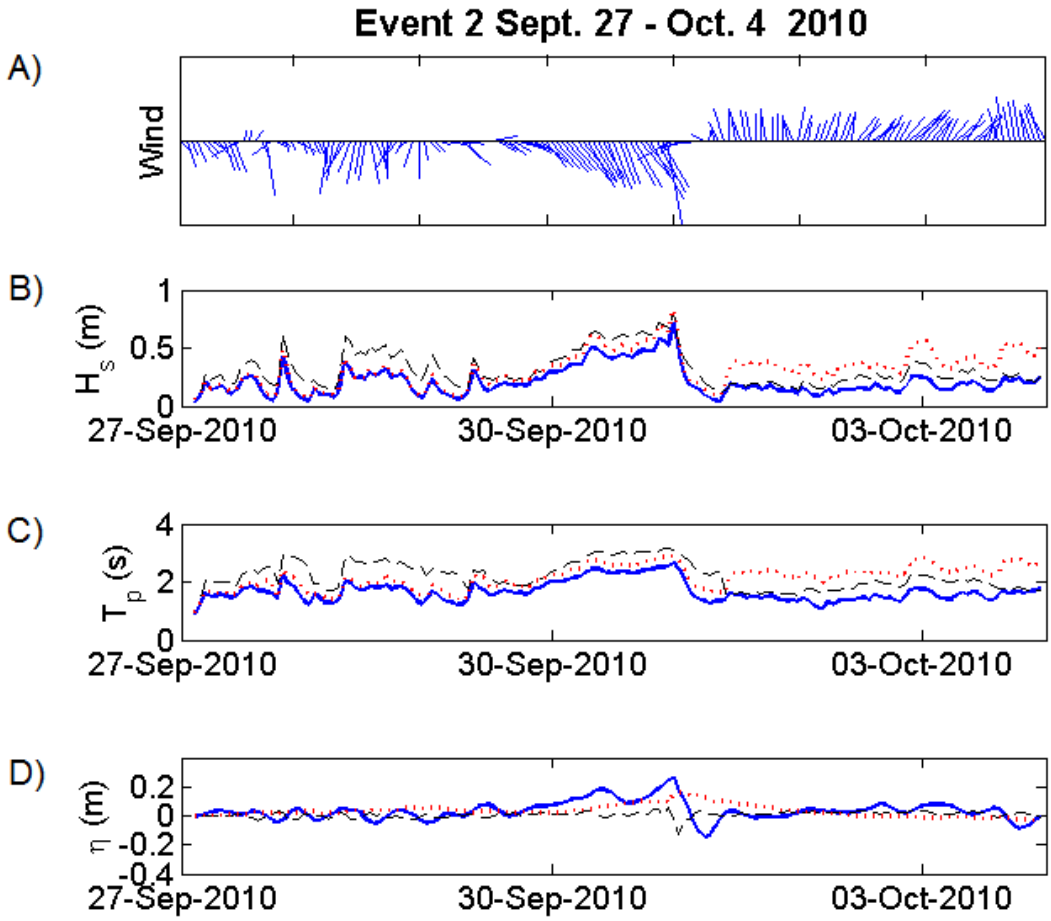

Figure 10 Model results for Event 2 during the S2 era, at the GCP (blue), GRG (dashed black), and PPP (dashed red) sites. A) Wind stick vectors indicating speed and direction, B) Significant wave height (H_s), C) Peak period (T_p), and D) Water-level (η).

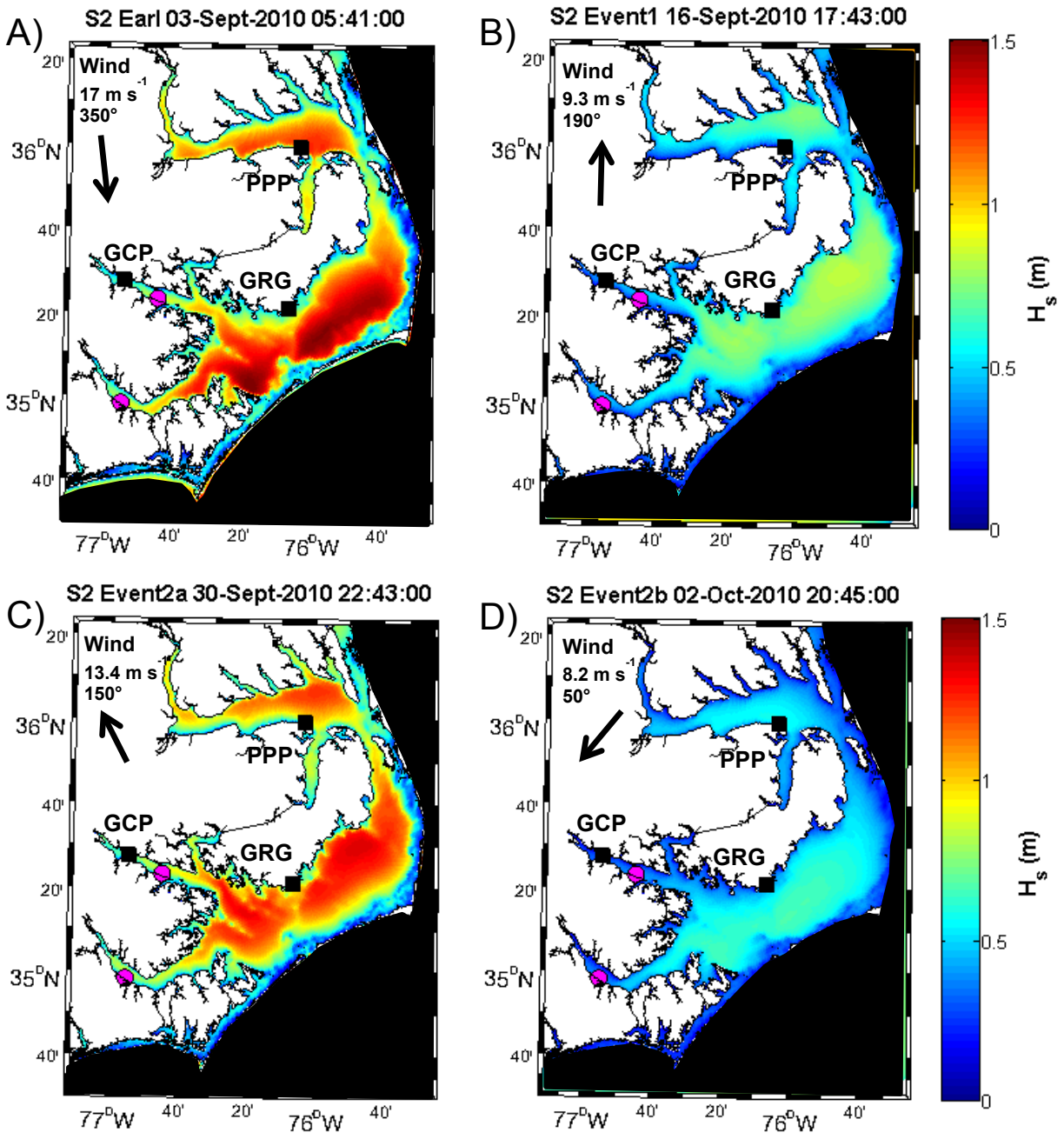

Figure 11 Model results across the APES for significant wave height (H_s) at the GCP, GRG, and PPP sites for peak wind speed during S2 era; A) Hurricane Earl, B) Event 1, C) Event 2a, and D) Event 2b. The arrows indicate wind direction at each time in degrees from true North; wind speed is indicated in m s^{-1}.

Figure 11B and indicates highest H_s values occurred along the northern shore of Albemarle Sound, and along the northern and western Pamlico Sound, near site GRG.

The final event modeled for the S2 era was a week-long (Sept. 27-Oct. 4, 2010) frontal system that contributed several inches of precipitation to the area and had multiple periods of winds >6 m s^{-1}. The precipitation and water-level increases observed across the APES contributed to extensive coastal flooding in several counties and at the three study sites. The greatest recorded wind speeds of 13.4 m s^{-1} (from the South-southeast; 150°) occurred early on Sept. 1, 2010 (Fig. 10A). This was preceded by 12-hours of consistent Southeast winds over 8 m s^{-1} (Fig. 10A). Due to this 12-hour set-up, water-level was predicted by the model to have increased by 0.26 m and 0.15 m at the GCP and PPP sites, respectively (Fig. 10D; Table 4). Significant wave height was greatest for all three sites at this time and ranged from 0.7-0.8 m (Fig. 10B; Table 4). As with event 1, significant wave heights were greatest during this period along the northern Albemarle and Pamlico Sounds (Fig. 11C). After Oct. 1, 2010 the wind direction shifted to the North and wind speed dropped to 5-8 m s^{-1} but was sustained for the next two days (Fig. 10A). While this resulted in overall lower wave heights across the APES, H_s at the PPP site was much higher than those calculated at the GCP and GRG sites (almost double the significant wave heights at GCP; Fig. 10B; Table 4). Greater wave heights were again along the southern shorelines of the APES, as was observed for the Hurricane Earl event (Fig. 11D). It is clear that wind direction over this six-day-period played a significant role in determining wave height at the different sites.

To further investigate the role of wind direction and speed on the distribution of wave energy, the wind ramp simulation was run for the GRG and PPP sites using the same coupled hydrodynamic-wave model utilized for the S2 event simulations. The wind ramp was not

examined at the GCP site due to its similar orientation to the GRG site shoreline (both are most exposed to southerly wind directions), and the GCP site is located at the upper reach of the Tar-Pamlico tributary where fetch is more limiting (Fig. 1). The results from the wind ramp for the GRG and PPP sites are shown in Figure 12 for all of the 8 main compass directions and the individual results for North, East, South, and West shown in Figure 13. The GRG site was found in the simulation to have overall lower wave heights than the PPP site with a maximum of 1.1 m when the wind was from the Southeast (135º) at 30 m s^{-1} (Figs. 12A and 13). The largest wave heights simulated at the GRG site occurred when the wind direction ranged from East to Southwest (90º-225º), which also represent the greatest fetches for the site (31-54 km; Figs. 12A and 13B-C). The PPP site exhibited the greatest significant wave height of 1.7 m when the wind was from the North (0º; fetch 18 km) at 30 m s^{-1} (Figs. 12B and 13A). Overall, the largest wave heights were simulated at the PPP site when the wind direction was from the West, South, or East (270º-90º) with fetches of 18 to 33 km (Figs. 12B, 13A-B, and D).

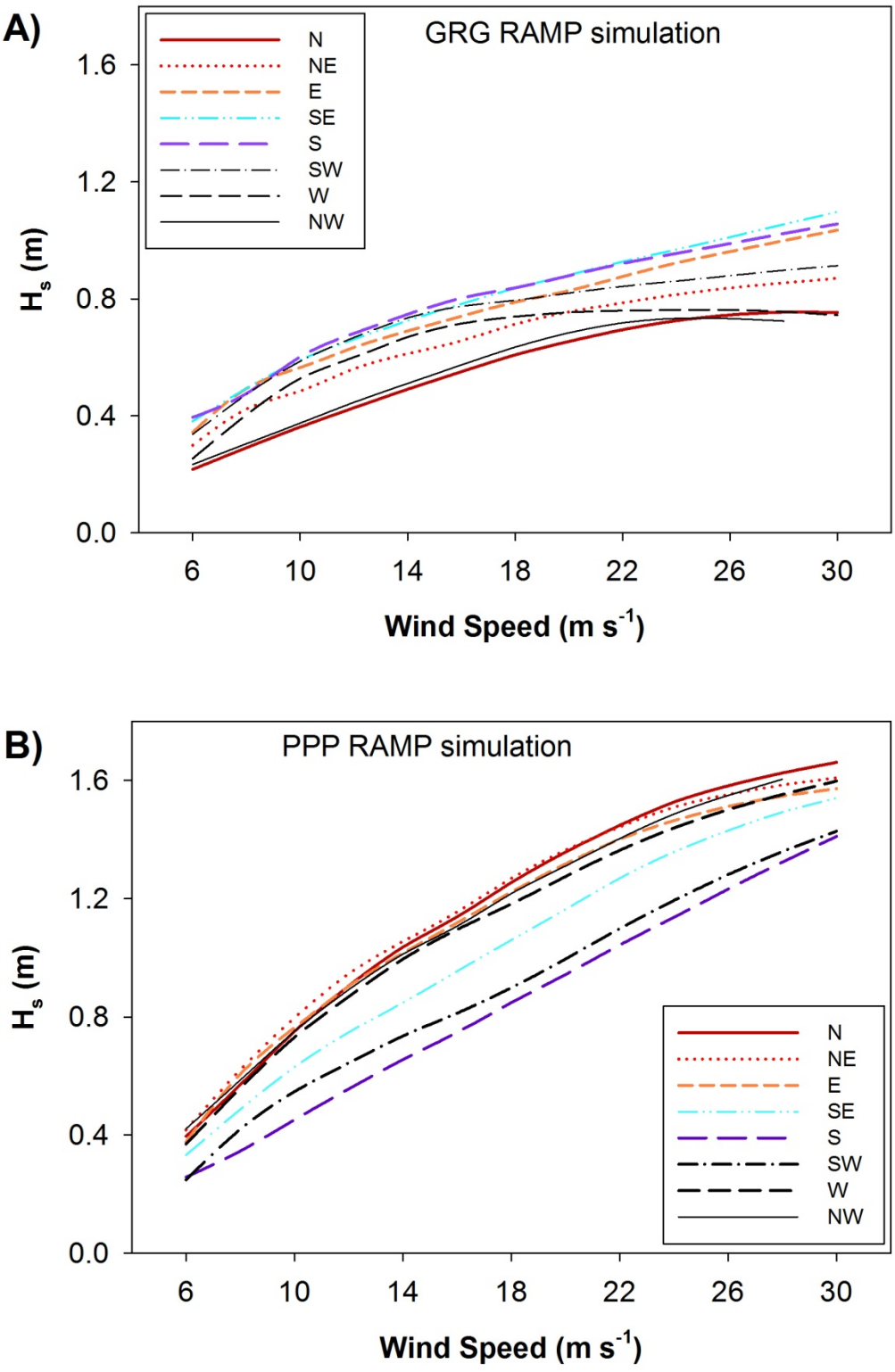

Figure 12 Significant wave height (H_s) for each wind speed and direction in the wind ramp simulation (wind speeds 6-30 m s^{-1}, 8 cardinal and ordinal compass directions) at; A) the GRG site, and B) the PPP site.

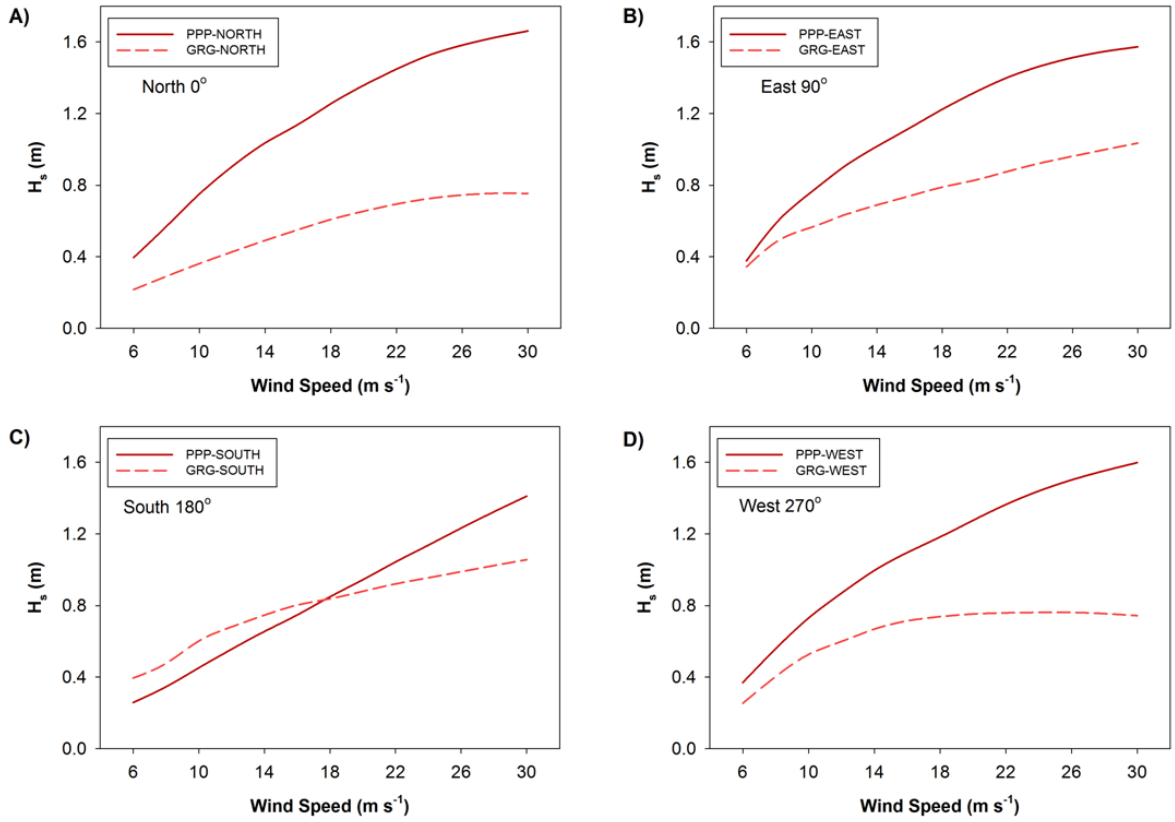

Figure 13 Significant wave height (H_s) for wind speeds of 6-30 m s^{-1} at both the GRG and PPP sites for varying wind direction: A) North (0°), B) East (90°), C) South (180°), and D) West (270°).

5.0 Discussion

5.1 Historical versus Sub-annual SCRs

Annualized rates of shoreline change were found to be significantly different for sub-annual eras in comparison to historical eras ($P<0.01$). To determine if the high annualized SCR values for the sub-annual eras were anomalous with the long-term, historical rate, the values were plotted in a linear regression model for the GCP, GRG, and PPP sites (Fig. 14). The spatial average shoreline position (SASP) for each historical and intermediate era was plotted and linear regression analysis performed at a 95% confidence interval. Position is plotted as mean distance in meters between each historical shoreline (i.e., 1983, 1993, 1998, and 2006/2007) and the initial shoreline of 1956. The SASP for each sub-annual era was then plotted to determine if they fell within the 95% confidence interval band for each site (Fig. 14). A shoreline change rate for the historical eras was also calculated from the linear regression for comparison with the end-point-rate determined by the AMBUR software. The linear regression models were observed to fit the historical data well, as evidenced by a high r^2 value for all three sites; 0.95, 0.95, and 0.85 at the GCP, GRG, and PPP sites, respectively (Fig. 14). The linear regression SCRs (-0.6 m yr^{-1} for all three sites) were found to agree well with those calculated by the end-point method. Previous comparisons of the linear regression and end-point methods for calculating shoreline change by Dolan et al. (1991) also found good agreement between the two methodologies.

All of the sub-annual era SASPs were found to fall within the 95% confidence interval band at all three sites. So, while annualized sub-annual SCR rates are significantly higher than those of the 50yr, H1-H4, or I eras, the spatially averaged net change in position falls within the long-term trend (Fig. 14). This indicates that the sub-annuals cycles of erosion and accretion,

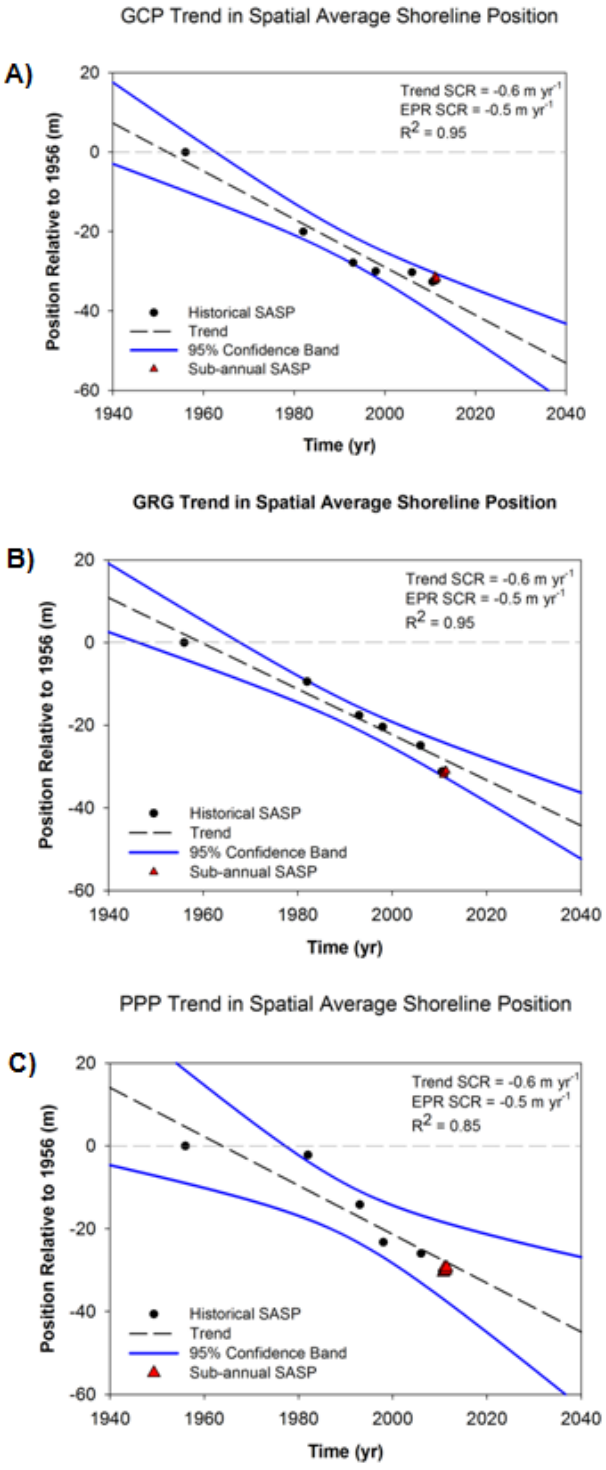

Figure 14 Trend in spatial average shoreline position (SASP) for all study eras; A) the GCP site, B) the GRG site, C) the PPP site. The trend value is the SCR (m yr^{-1}) calculated from the linear regression. The EPR (end-point-rate) value is the H50yr (1956-2007) SCR (m yr^{-1}) calculated using AMBUR.

as well as the storm-influenced shorelines, are likely a part of the long-term cycle of shoreline change observed at these sites. Therefore, these sub-annual changes in shoreline position are accounted for in the more commonly used long-term calculations of SCRs.

5.2 Wave Climate and Sub-annual Shoreline Change

Shoreline change is thought to be controlled by the complex interaction of processes and shoreline characteristics that can be highly location-specific. Significant differences in the rates of shoreline change were observed both between and within individual sites. Wave energy has previously been recognized to influence the rate of shoreline change (Riggs and Ames, 2003; Schwimmer, 2001; Cowart et al., 2011). For example, in the nearby Neuse River estuary (also a part of the APES), Cowart et al. (2011) determined an empirical relationship between exposure to wave energy and the rate of erosion. In the current study, results from the coupled hydrodynamic-wave model also indicate a relationship between wave energy and the rate of shoreline change. As no hydrodynamic observations were available for the sub-annual period, the wind ramp simulation results were utilized to hind-cast the wave climate at the GRG and PPP sites. The hourly wind record from station KMQI was filtered and then each hour matched with the analogous simulation result for that wind speed bin and compass direction.

At the GRG and PPP sites, 84-90% of the time during the sub-annual period (S1-S5) was simulated to have significant wave heights of <0.4 m (Fig. 15). This demonstrates that most of time during the study the shorelines were exposed to a climate of shorter-period (<2 s), smaller waves, and likely were experiencing no transport. The two sites were found to have H_s >0.4 m 10-16% of the time during the sub-annual period (Fig. 15). During that time, the shoreline at each site was exposed to approximately 46-60% of the total wave energy calculated for the entire

sub-annual period (Fig. 15). At the GRG site, much energy was associated with H_s <0.8 m during S5 was actually a time when no shoreline change occurred (Figs. 16A and 17A). A study by Cowart et al. (2010; 2011) indicated the importance of shoreline characteristics such as scarp height, substrate cohesion, and vegetation type that may modify the erosion potential of marsh shorelines. At the GRG site these factors may reduce the potential for erosion. However, during the S2 era when wave heights exceeded 0.8 m there was significant erosion recorded at the site, suggesting that wave energy likely exceeded the threshold necessary to induce sediment erosion (Fig. 17A).

At the PPP site, the 16% of simulated wave heights >0.4 m occurred during the S2, S4, and S5 eras when rates of erosion exceeded 5 m yr^{-1} (Fig. 17B). The greatest H_s (0.1% of the time) and approximately 4% of total wave energy (S1-S5) occurred during the S2 era when the rate of erosion was almost 20 m yr^{-1} due to the influence of Hurricane Earl (Figs. 16B and 17B). In contrast, during the S3 era, the shoreline returned to its pre-Earl position through the accumulation of material. Wave heights were predominantly 0.2-0.6 m with the greatest energy from the 0.4-0.6 m bin (Figs. 16B and 17B). During the S3 and S4 eras, most wave energy was observed in the 0.6-0.8 and 0.8-1.0 H_s bins (Fig. 16B), and this was accompanied by some of the highest rates of erosion observed in the study at the PPP site (5.6 and 5.4 m yr^{-1}, respectively). Again, this suggests that during periods of smaller waves, sand can move onshore, but during periods with larger waves the critical erosion stress of marsh substrates can be surpassed, resulting in erosion.

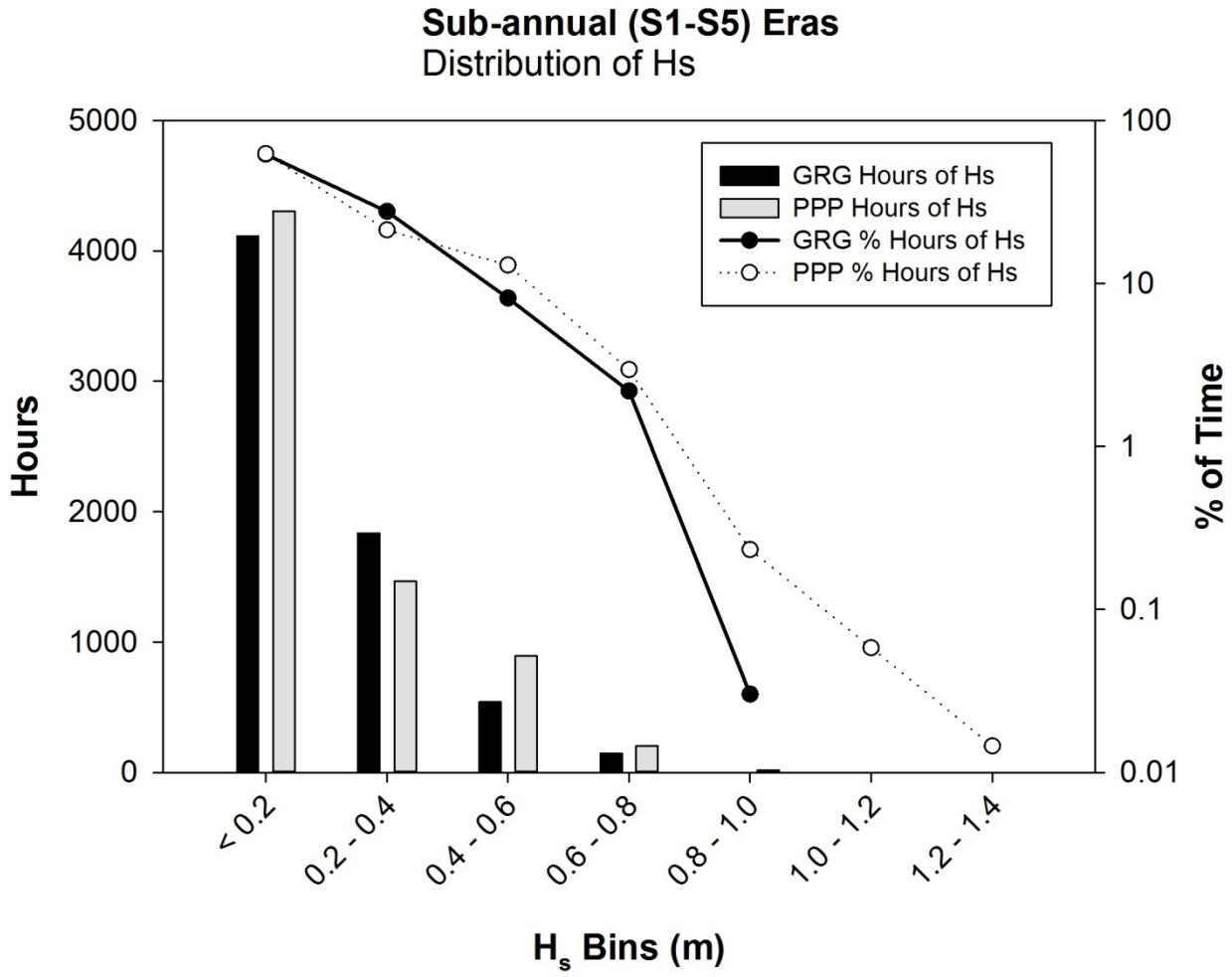

Figure 15 Probability density distribution of hours of significant wave heights over all of the sub-annual era (S1-S5) at the GRG and PPP sites. Significant wave height divided into height bins of 0.2 m (x-axis) and time reported in hours (left y-axis) and percent (%; right y-axis) of time. The bars denote hours of significant wave height for both sites, per bin. The lines denoted percent of time for both sites, per bin.

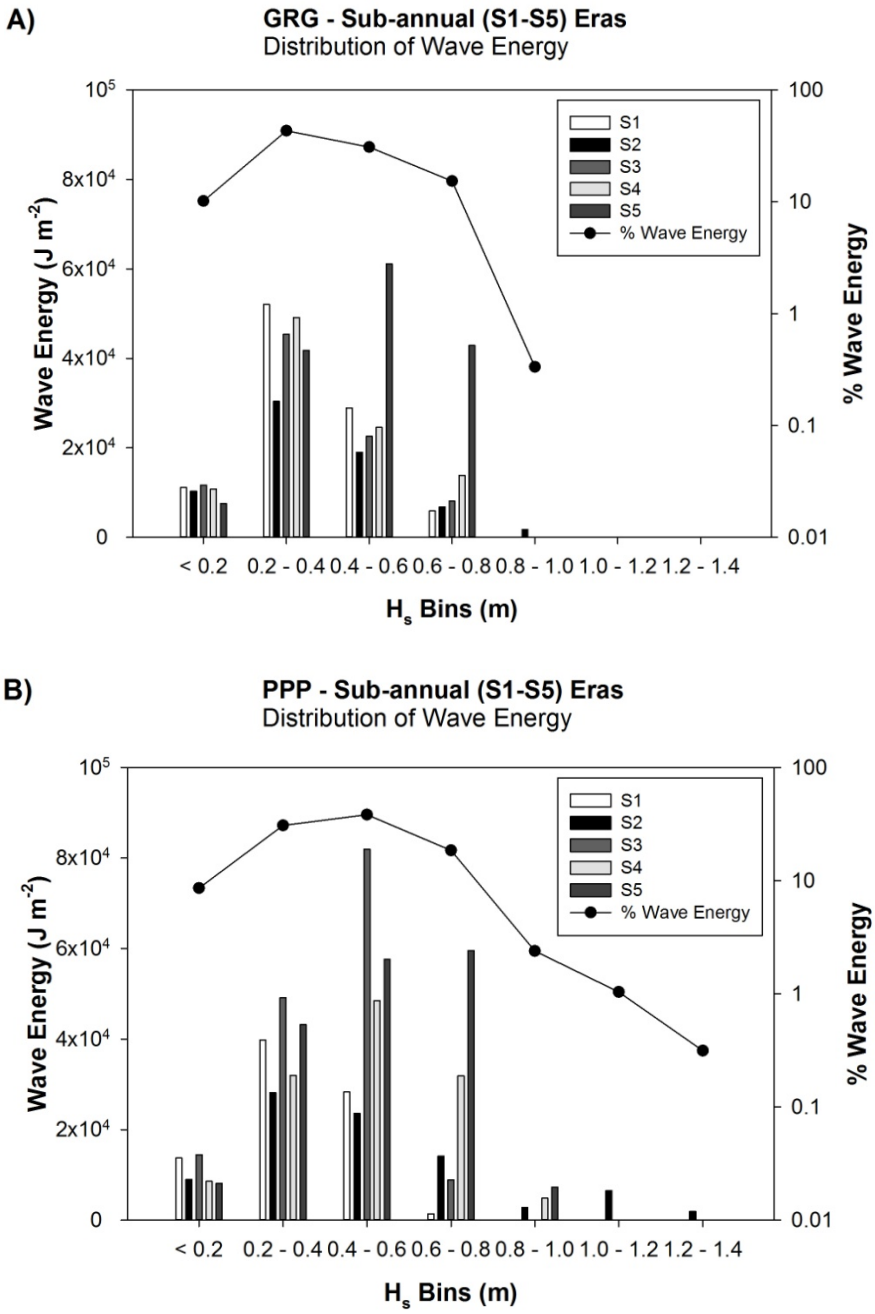

Figure 16 Probability density distribution of wave energy (J m-2) for all of the sub-annual eras at; A) the GRG sites, B) the PPP site. Wave energy was calculated from the wind ramp results for significant wave height (H_s). The black line denotes the total percentage of wave energy per wave height bin for the entire sub-annual period (S1-S5).

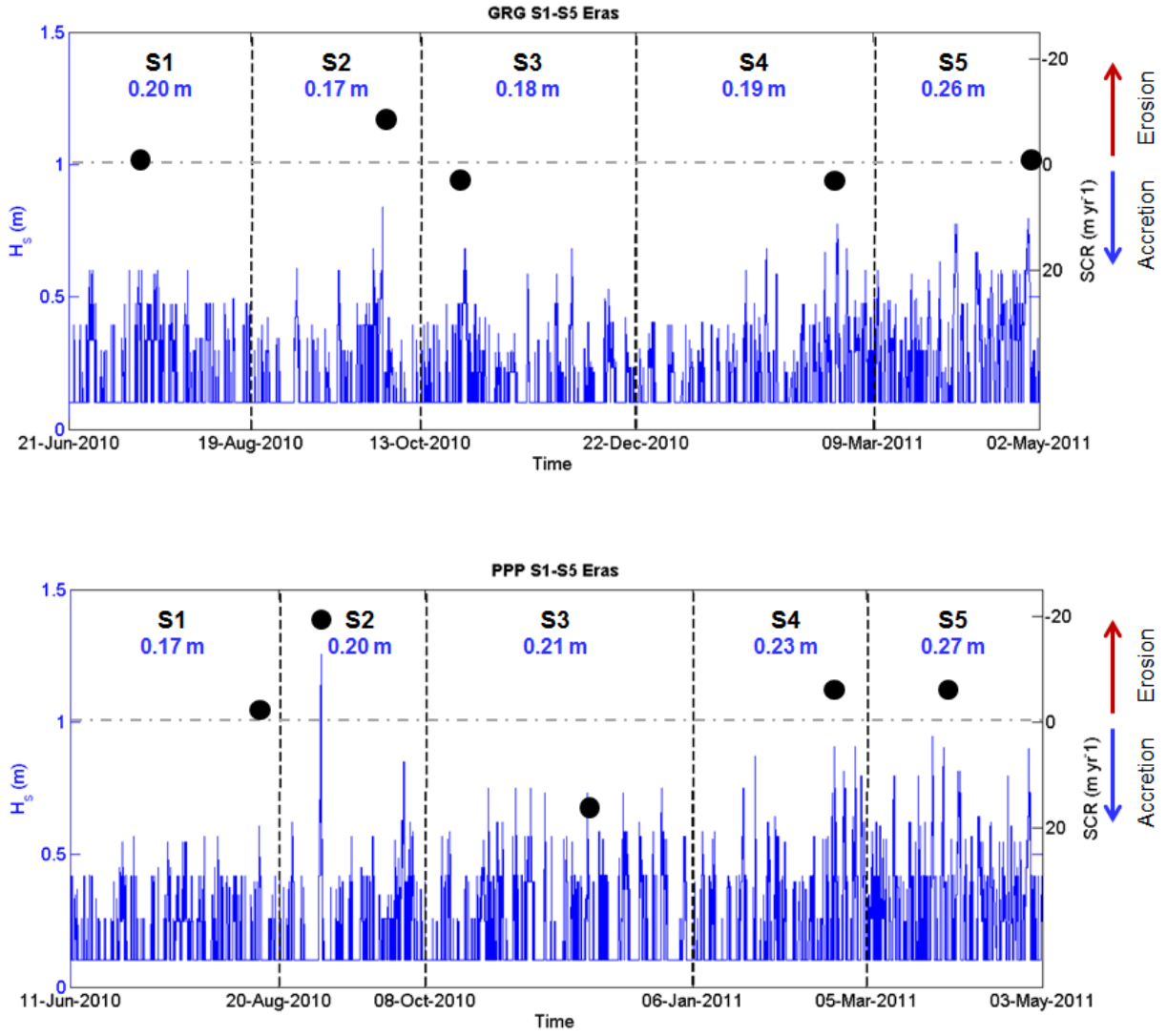

Figure 17 Time-series of wave heights using the wind ramp simulation results at the GRG and PPP sites, and the annualized shoreline change rate (SCR, m yr^{-1}) for all of the sub-annual eras (S1-S5). Individual eras are denoted by the dashed lines. The blue line represents hourly significant wave height (H_s) as determined from the coupled hydrodynamic-wave model. Due to constraints of the model when simulation waves under low wind conditions (<6 m s^{-1}), the minimum wave height is 0.1 m. Mean H_s (blue text) for each era listed in meters. The black circles denote the mean annualized SCR for each era. The red arrow indicates negative SCR values (erosion) and the blue arrow indicates positive SCR values (accretion).

There is also a seasonal component to the observed trends in wave climate and shoreline change. At both the GRG and PPP sites, the summer months (June-August) were characterized by consistently smaller wave heights and an absence of any significant change in shoreline position (Fig. 17). Historically, and during this study, winds are from the southwest at this time of the year, and few fronts occur (Cowart et al. 2010; Wells and Kim 1989). At the PPP site, this wind direction limits wave development along the southern shorelines of the Albemarle Sound. At the GRG site, while the fetch for wind from the southwest is large, much wave energy is likely reduced by the extensive shoals seaward of the site (Fig. 18A). During the months of September and October the passage of tropical and extra-tropical storms can result in high-energy events (with large wave heights), but these relatively short periods can significantly erode these estuarine shorelines (Fig. 17). During the winter and early spring months (December-March) the wind is predominantly from the north and northeast, directions that were found in simulations to produce the greatest wave heights at the PPP site, and were characterized by >5 m yr^{-1} of erosion (Cowart et al. 2010; Wells and Kim 1989).

As alluded to above, water depth is another factor that controls wave climate. In Figure 13, wave height was almost always greater at the PPP site. However, the GRG site has greater fetches of 31-54 km, in contrast to fetches of 18-33 km at the PPP site. These results from the model are likely a function of the bathymetry at the sites (Fig. 18). At the GRG site, where wave heights were simulated to be lower, the water depth is only 2.2 m, and the bathymetry shows extensive shallows with little slope (Fig. 18). Water depths also remain shallow (<5 m) along the entire south (180º) fetch direction due to a shoal that divides Pamlico Sound (from Gull Rock to Ocracoke Inlet). At the PPP site where wave height was simulated by the model,

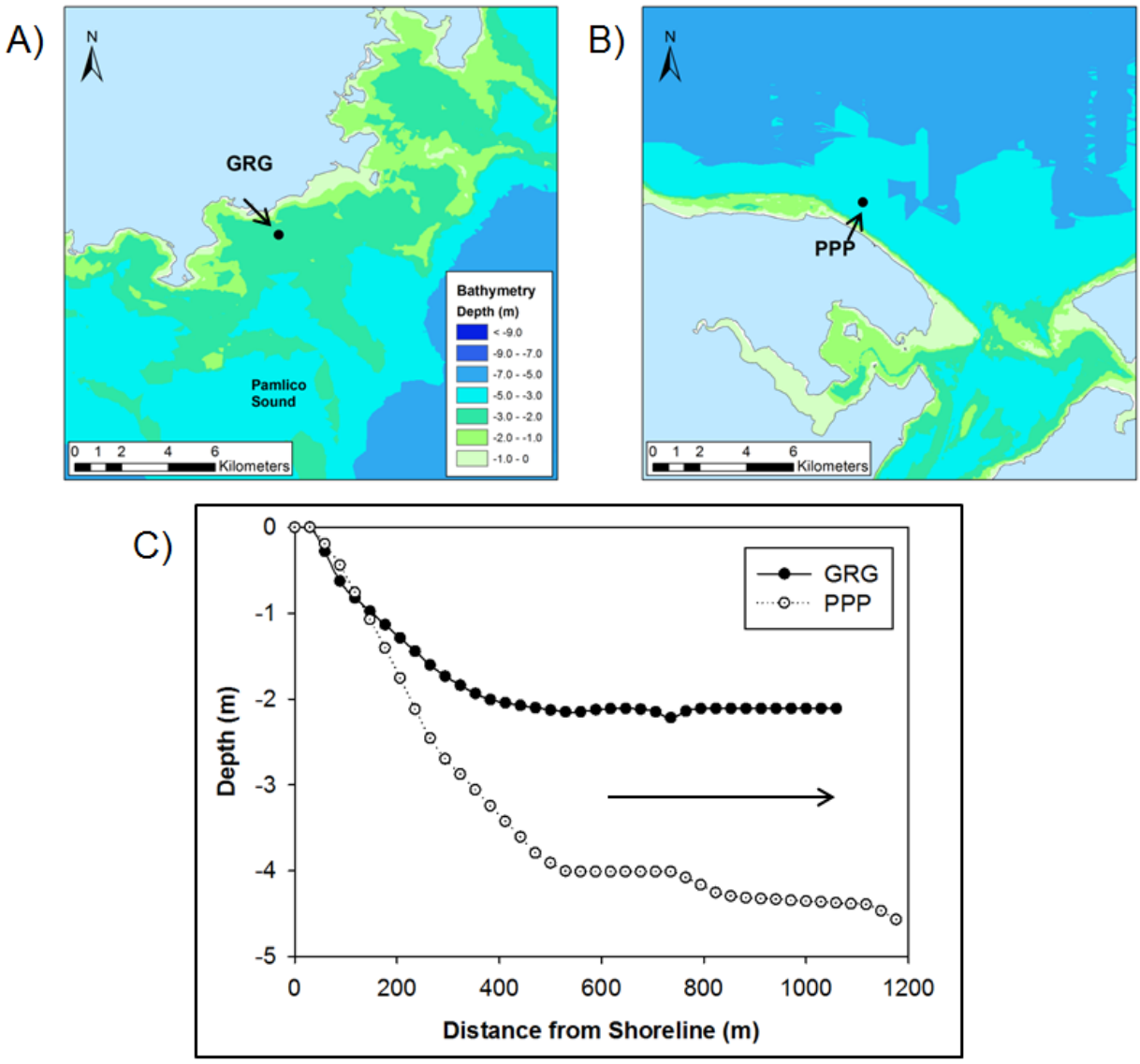

Figure 18 Bathymetry; A) the GRG site, B) the PPP site, and C) depth profiles at both sites. In A and B, black circles denote the location adjacent to each site used in the coupled hydrodynamic-wave model. Black arrows indicate the location of bathymetry profiles displayed.

water depth was 4.4 m (Fig. 18B). The bathymetry shows steeper slopes less than 500 m from shore, and water depths of 4 m ~1 km from shore (Fig. 18). The shallower water depths and extensive shoals around the GRG site would limit wave growth in the model simulations, despite greater fetches at the site, resulting in the overall lower wave heights.

5.3 Storm Events

Coastal storms are commonly indicated as drivers behind episodic, but significant erosion of shorelines (Camfield and Morang, 1996; Dolan et al., 1978; List et al., 2006; Phillips, 1999). Studies on oceanfront coasts highlight the ability of storms to remove significant volumes of sediment from beaches and also indicate the potential for the subsequent recovery of those sediments during the quiescent period following a storm event (Dolan et al. 1978; Dolan et al. 1988; Douglas and Crowell 2000; List et al. 2006; Phillips 1999). List et al. (2005) noted the existence of storm driven "erosion hotspots". These hotspots represent segments of shoreline that are characterized by a significantly higher rate of short-term erosion then surrounding segments of the same type and morphology (List et al. 2006). These processes were observed at sites after the passage of two different storm events; Hurricane Earl that passed within 50 nautical miles of North Carolina on September 2, 2010 and Hurricane Irene that crossed directly over eastern North Carolina on August 27, 2011. The peak wind speed of the Hurricane Earl event was 17 m s^{-1} and from the North (0°); resulting in the highest significant wave heights (> 1 m) and greatest peak period (T_p; 3.8 s) along the southern shorelines of Albemarle and Pamlico sounds, including at the PPP site (Fig. 11A; Table 4). During Hurricane Irene, H_s of over 1.5 m was observed at the PPP site as the storm passed over the site and winds of >30 m s^{-1} shifted from the Southeast to the Northwest. For the GRG site, wave heights between 0.6 and 1.2 m

were observed for Hurricanes Earl and Irene, respectively. A greater rate of change (-9.7 m yr^{-1}) was measured post-Irene than post-Earl at the site (-8.6 m yr^{-1}). As discussed previously, the wind direction, bathymetry, and resulting wave climate play a critical role in the amount and location of shoreline erosion. These short-duration, high energy events can lead to significant erosion even along more resistant shoreline types such as marsh (GRG). While significant erosion also occurs along sediment bank shores (i.e., PPP), there is a potential for recovery post-storm. In contrast, along a marsh shoreline (i.e., GRG), the post-storm position defines a new marsh-edge-shoreline. This suggests that storm-driven erosion represents a more significant contribution to the long-term rate of change along marsh shorelines then sediment bank shorelines. However, the SCRs for these events still fall within the 95% CI of the longer-term trend in SASP.

5.4 Coastal Management Implications

There are currently no set-back requirements on the estuarine shoreline in North Carolina that are comparable to the oceanfront setbacks determined by the long-term erosion rate. There are, however, designated areas of environmental concern (AECs) that require permits for structures located within a certain distance from the shoreline and based on shoreline classification (CAMA, 1974). Set-backs for structures based on rates of estuarine shoreline change could be incorporated within the existing permitting structure and would provide coastal managers with a way to manage estuarine shoreline development in the face of environmental changes such as erosion and sea-level rise. In the long-term, such policies could increase the resilience of estuarine communities and provide a regulatory mechanism for addressing shoreline retreat that does not rely on hardening the estuarine shore. However, because of the vast size of

the APES, many critical locations (e.g., wetlands) are at risk, so some type of ecosystem friendly shoreline modification may be required.

6.0 Conclusions

A combination of field surveys (RTK-GPS and Aerostat), digitizing from historical aerial photos, and a coupled hydrodynamic-wave model were used to examine rates and processes driving shoreline change at varying spatial and temporal resolutions at several sites across a large estuarine system (e.g., APES). These sites encompassed a range of shoreline types (e.g., marsh, sediment bank), shoreline orientations, and wave exposure directions. Historical (50yr) rates of shoreline change ranged from -0.3 ± 0.3 to -0.6 ± 1.2 m yr^{-1}. Rates for individual historical (H1-H4) and intermediate (I) eras were variable by site and era. The most variability in SCR was observed during the sub-annual eras (S1-S5), and specifically, at the sediment bank PPP site. Storm events such as Hurricane Earl were found to contribute to this short-term variability along sediment bank shorelines.

In the micro-tidal APES system, waves have previously been identified as an important mechanism for shoreline change. Shoreline orientation and wind direction were found to be important in determining wave energy at a given site with the greatest wave heights simulated when wind direction and shoreline orientation resulted in the most exposure (greater fetch). The greatest wave heights simulated by the model occurred at the sites during the era (S2) of greatest erosion.

The high variability observed at both fine temporal and spatial scales in comparison to the long-term historical SCRs illustrates the importance of examining shoreline change at multiple timescales and spatial resolutions. Historical rates of change provide a view of the net

movement of the shoreline over decades with low methodological error. However, as observed by Douglas et al. (1998) for oceanfront shorelines, these historical rates and the set-backs that are based on them, do not account for episodic or highly variable sub-annual changes in shoreline position. While these short-term rates, when annualized, can far exceed the historical SCR, they were found in linear regression models to be within the range of predicted shoreline positions. Over these sub-annuals periods it is suggested that wave energy at the sites is a major driving force behind changes in shoreline position. The contribution of large storm events to shoreline erosion can be significant in the short-term at any shoreline, but may be most important at marsh sites in the longer-term as there is little potential for post-storm recovery of eroded material.

REFERENCES

Anders, F.J., Byrnes, M.R., 1991. Accuracy of Shoreline Change Rates as Determined from Maps and Aerial Photographs. Shore and Beach 59, 17-26.

Aubrey, D.G., 1979. Seasonal Patterns of Onshore/Offshore Sediment Movement. Journal of Geophysical Research 84, 6347-6354.

Boak, E.H., Turner, I.L., 2005. Shoreline definition and detection: a review. Journal of Coastal Research 12, 688-703.

Booij, N., Ris, R. Aagaard, T., 1999. A third-generation wave model for coastal regions: 1. Model description and validation. Journal of Geophysical Research 104(4), 7649-7666.

Charlier, R.H., De Meyer, C.P., 1998. Coastal Erosion: Response and Management. Springer, New York.

Corbett, D.R., Walsh, J.P., Cowart, L., Riggs, S.R., Ames, D.V., Culver, S.J., 2008. Shoreline change within the Albemarle-Pamlico Estuarine System, North Carolina. East Carolina University.

Cowart, L., Walsh, J.P., Corbett, D.R., 2010. Analyzing Estuarine Shoreline Change: A Case Study of Cedar Island, North Carolina. Journal of Coastal Research 26, 817-830.

Cowart, L., Corbett, D.R., Walsh, J.P., 2011. Shoreline Change along Sheltered Coastlines: Insights from the Neuse River Estuary, NC, USA. Journal of Remote Sensing 3, 1516-1534.

Crowell, M., Leatherman, S.P., Buckley, M.K., 1991. Historical Shoreline Change: Error Analysis and Mapping Accuracy. Journal of Coastal Research 7, 839-852.

Crowell, M., Leatherman, S.P., Buckley, M.K., April 1993. Shoreline Change Rate Analysis: Long Term Versus Short Term Data. Shore and Beach, 13-20.

Deltares, 2011. DELFT3D User Manual.

Dolan, R., Hayden, B., Heywood, J., 1978. A New Photogrammetric Method for Determining Shoreline Erosion. Coastal Engineering 2, 21-39.

Douglas, B.C., Crowell, M., Leatherman, S.P., 1998. Considerations for Shoreline Position Prediction. Journal of Coastal Research 14, 1026-1033.

Douglas, B.C., Crowell, M., 2000. Long-term Shoreline Position Prediction and Error Propagation. Journal of Coastal Research 16, 145-152.

Eulie, D.O., Walsh, J.P., Corbett, D.R., 2013. High-resolution Analysis of Shoreline Change and Application of Balloon-based Aerial Photography, Albemarle-Pamlico Estuarine System, North Carolina, USA. Limnology and Oceanography: Methods 11, 151-160.

Fenster, M.S., Dolan, R., Morton, R.A., 2001. Coastal Storms and Shoreline Change: Signal or Noise? Journal of Coastal Research 17, 714-720.

Fletcher, C.H., Rooney, J.J., Barbee, M., Lim, S.C., Richmond, B.M., 2003. Mapping shorline change using digital orthophotogrammetry on Maui, Hawaii. Journal of Coastal Research SI 38, 106-124.

Geis, S., Bendell, B., 2010. Charting the Estuarine Environment: A methodology spatially delineating a contiguous, estuarine shoreline of North Carolina. Division of Coastal Mangement, Raleigh, NC.

Gentz, A.S., Fletcher, C.H., Dunn, R.A., Frazer, L.N., Rooney, J.J., 2007. The Predictive Accuracy of Shoreline Change Rate Methods and Alongshore Beach Variation on Maui, Hawaii. Journal of Coastal Research 23, 87-105.

Jackson, C. W., C. R. Alexander, and D. M. Bush. 2012. Application of the AMBUR R package for spatio-temporal analysis of shoreline change: Jekyll Island, Georgia, USA. Computers and Geosciences 41**:** 199-207.

Larson, M., Kraus, N.C., 1994. Temporal and spatial scales of beach profile change, Duck, North Carolina. Marine Geology 117, 75-94.

Lesser, G.R., Roelvink, J.A., van Kester, J.A.T.M., Stelling, G.S., 2004. Development and validation of a three-dimensional morphological model. Coastal Engineering 51, 883-915.

List, J.H., Farris, A.S., Sullivan, C., 2006. Reversing Storm Hotspots on Sandy Beaches: Spatial and Temporal Characteristics. Marine Geology 226, 261-279.

Moore, L.J., 200. Shoreline Mapping Techniques. Journal of Coastal Research 16, 111-124.

Mulligan, R., Walsh, J.P., Wadman, H.M., (2014). Storm surge and surface waves in a shallow lagoonal estuary during the crossing of a hurricane Journal of Waterway, Port, Coastal, and Ocean Engineering.

Pilkey, O., Hume, T.M., 2001. The shoreline erosion problem: Lessons from the past. Water and Atmosphere 9, 22-23.

Ris, R.C., Holthuijsen, L.H., and N. Booij, 1999. A third-generation wave model for coastal regions: 2. Verification. Journal of Geophysical Research 104(4), 7667-7681.

Schwimmer, R.A., 2001. Rates and Processes of Marsh Shoreline Erosion in Rehoboth Bay, Delaware, U.S.A. Journal of Coastal Research 17, 672-683.

Stevenson, J.C., Kearney, M.S., 1996. Shoreline Dynamics on the Windward and Leeward Shores of a Large Temperate Estuary, in: Nordstrom, K.J., Roman, C.T., (Ed.), Estuarine Shores: Evolution, Environments and Human Alterations. John Wiley & Sons Ltd.

Thieler, E.R., Danforth, W.W., 1994. Historical Shoreline Mapping (I): Improving Techniques and Reducing Positioning Errors. Journal of Coastal Research 10, 549-563.

Wells, J.T., and Kim, S., 1989. Sedimentation in the Albemarle-Pamlico Lagoonal System: Synthesis and Hypotheses. Marine Geology 88, 263-284.

CHAPTER 4

Decadal Sediment Accumulation and the Role of Shoreline Erosion in the Tar-Pamlico Estuary

Abstract

Understanding the source of sediment and its storage is important for examining the impact of human activities and natural processes such as sea-level rise on the functioning of estuarine systems. Specifically, as more estuarine shoreline erodes or becomes modified with hard structures, there is the potential for significantly altering the availability of sediment within the estuarine system. This study quantified rates of sediment accumulation using the radionuclide tracers ^{210}Pb and ^{137}Cs at 11 sites in the Tar-Pamlico sub-estuary, a tributary of the larger Albemarle-Pamlico Estuarine System (APES). Shoreline erosion was also quantified for the 1998-2007 decade. A preliminary budget for fine sediments (grain-size <63 μm) was then calculated. Radionuclide activities and sediment accumulation rates identified several regions as depositional centers, specifically the mid-estuary site PRE-6. Linear accumulation rates ranged from 0.1 ± 0.02 to 0.38 ± 0.02 g cm^{-2} yr^{-1} and total storage of fine sediment in the system was 1.6 x 10^5 t yr^{-1}. The average end-point shoreline change rate (SCR) was -0.5 ± 0.9 m yr^{-1} for the Tar-Pamlico, contributing 0.6 x 10^5 tons of fine sediment to the system annually, or 39.6% of the total sediment supply to the sub-estuary. Almost all (98.0%) of the fine sediment entering the system was accumulated and stored, while 2.0% was exported to Pamlico Sound.

1.0 Introduction

1.1 Estuarine Systems

Estuaries are vital coastal ecosystems that provide habitat, facilitate the cycling of biogeochemical constituents, and are utilized for recreation and commercial activities. These functions are influenced by the dynamic physical processes that control the morphology and behavior of these ecosystems, the storage of sediments and other materials (e.g. carbon, nutrients, and pollutants), and have impacts on coastal development. For example, shoreline change can erode important habitat and damage or destroy human infrastructure (Riggs and Ames 2003). Seabed resuspension alters the environment by disturbance of the benthos and affecting water quality (Arfi and Bouvy 1995; Cloern 1987; Giffin and Corbett 2003; Soetaert and Middelburg 2009), and wetland processes influence sediment and carbon storage as well as shoreline erosion and flooding. The temporal and spatial variability of these and other processes must be better understood to determine estuarine functioning and evolution.

Estuarine ecosystems are found at the boundary between terrestrial and marine environments. Evidence from estuarine deposits show that these systems have existed in a wide range of geographic locations over geologic time (Dyer 1997). However, their origin reflects the transient nature of these ecosystems. At the end of last glacial period (~18,000 years ago) sea-level was 120 m below present (Masselink and Hughes 2003). Modern estuaries are the result of the subsequent sea-level transgression that has occurred since that time (Dyer 1997; Perillo 1995). A period of rapid melting and sea-level rise with rates on the order of 1 cm/yr transpired until approximately 7000-5000 years ago when the rate slowed to 2-3 mm yr^{-1} (Dyer 1997; Horton et al. 2009; Mallinson et al. 2010; Perillo 1995; Pethick 1984). The resulting inundation of the paleotopography formed estuarine systems (Dyer 1997; Mallinson et al. 2005; Mallinson et al. 2010; Perillo 1995; Pethick 1984). As the rate of sea-level rise stabilized to near current

rates, estuaries began to fill with sediments. Their modern structure and function results from the complex interaction of antecedent morphology, hydrology, and sediment accumulation (Hibma et al. 2004; Pethick 1984).

1.2 Sediment Budgets

The sources and storage of sediment in an estuary are important to understand as they give insight into the functioning of the system and how alterations from natural or anthropogenic activities may impact the larger coastal environment. Understanding the storage of sediment will also be of increasing interest as rates of sea-level rise (SLR) are predicted to continue accelerating for North Carolina (Horton et al., 2009; Kemp et al. 2009). During periods of relatively stable sea-level a balance of accumulating and eroding processes may be reached that is expected to maintain a constant water depth and basin geometry in a system (Meade 1969; Meade 1972; Nichols and Poor 1967; Nichols 1989; Nichols et al. 1991; Pritchard 1967; Rusnak 1967). The system can continue to infill depending on rates of sediment accumulation and the available accommodation space (Jaeger et al. 2009; Meade 1969; Nichols and Poor 1967; Nichols 1989; Pethick 1984; Pritchard 1967; Rusnak 1967).

One way to examine the response of an estuarine system to natural or anthropogenic forcing factors is to construct a sediment budget. A sediment budget provides a quantitative measure of sediment sources and the estimated storage or export from the system (Jaeger et al. 2009; Patchneelam et al. 1999; Phillips 1997; Phillips and Slattery 2006; Rosati 2005; Yarbro et al. 1983). In large, complex estuarine systems such as the Albemarle-Pamlico Estuarine System (APES), material is supplied by river discharge, shoreline erosion, reworked shelf sediment, and in-situ production of biogenic material (Phillips 1989; Wells and Kim 1989). The majority of the

supplied sediment is stored in the drowned-river tributaries, such as the South or Susquehanna Rivers in the Chesapeake Bay, with only a fraction exported to the larger estuary (Donoghue et al. 1989; Marcus and Kearney 1991; Phillips and Slattery 2006; Schubel and Carter 1970; Wells and Kim 1991). Estimates of storage in estuarine tributaries range from 80% to 100% of supplied material, with an average of approximately 6% exported to nearby bays or sounds (Donoghue et al. 1989; Marcus and Kearney 1991; Phillips 1987; Phillips 1989; Phillips 1991; Phillips and Slattery 2006; Schubel and Carter 1970).

Early sediment budgets in estuarine systems, however, did not include shoreline erosion as a source of sediment. Recent studies in the Chesapeake Bay, and regions of the APES, indicate that shoreline erosion can be a significant source of material (Marciniak, 2008; Marcus and Kearny 1991; Pachineelam et al. 1999; Yarbro et al. 1983). Marcus and Kearney (1991) estimated that over 80% of material in a tributary of Chesapeake Bay came from shoreline erosion. A study in two tributary creeks of the Neuse River, NC, observed a similar fraction of sediment (85-98%) is supplied by shoreline erosion (Marciniak 2008). In the main trunk of the Neuse River Estuary, it was estimated that 6×10^5 tons of material, or approximately 75% of the annual sediment supply, is from shoreline erosion (Benninger and Wells 1993). Other studies indicate that as river discharge decreases due to human activities, shoreline erosion will become an increasingly significant source of sediment and nutrients to coastal systems (Marcus and Kearny 1991; Phillips and Slattery 2006).

1.3 Radionuclide Tracers

The radionuclides ^{210}Pb and ^{137}Cs are commonly used as tracers to determine sediment accumulation in estuarine systems. Their half-lives, 22.3 and 30.1 years, respectively, make

these tracers useful over modern timescales (approximately 100 years) to characterize sedimentation rates (Kirshnaswamy et al. 1971; Oldfield and Appleby 1984; Robbins and Edgington 1975). The radionuclide ^{210}Pb is naturally occurring as part of the ^{238}U decay series (Kirshnaswamy et al. 1971; Oldfield and Appleby 1984). The parent isotope, ^{226}Ra has a much longer half-life (1602 years), and is present in most rock or sediment. The ^{226}Ra isotope produces an intermediate daughter isotope, the inert gas ^{222}Rn, that rapidly decays to ^{210}Pb. This ^{210}Pb quickly adsorbs to particles and is removed from the atmosphere by wet or dry deposition, typically within a few days (Appleby and Oldfield 1992; Kirshnaswamy et al. 1971). It is the disequilibrium that results from the production of ^{210}Pb through in-situ decay of ^{226}Ra (supported) and the excess ^{210}Pb that is adsorbed to particles that allows the radionuclide to be useful as a tracer (Appleby and Oldfield 1992; Kirshnaswamy et al. 1971).

The man-made radionuclide, ^{137}Cs, is also used to determine sediment accumulation and commonly used to corroborate sedimentation rates from ^{210}Pb geochronologies (Appleby and Smith 1993; Ritchie and McHenry 1990; Robbins and Edgington 1975). It was introduced into the atmosphere as a result of nuclear testing (DeLaune et al. 1978; Ritchie and McHenry 1990). The activity of ^{137}Cs marks human activity, namely the first creation of the nuclide in 1954 and the peak of nuclear testing in 1963 (DeLaune et al. 1978). These variations in ^{137}Cs activity in down-core profiles (when present) can be used to calculate sedimentation rates.

The objectives of this study were to characterize sedimentation within the Tar-Pamlico sub-estuary, quantify changes in shoreline position and type, and calculate a sediment budget for the system, including the potential supply of fine sediments from shoreline erosion. These are addressed using a combination of sedimentological measures, radionuclide tracers, and GIS tools.

2.0 Study Area

The Tar-Pamlico River estuary is a part of the larger Albemarle-Pamlico Estuarine System (APES; Fig 1). The system is a product of multiple glacial and inter-glacial cycles and accompanying fluctuations in sea-level that have shaped the coastal plain region (Curray 1965; Mallinson et al. 2005; Mallinson et al. 2010; Riggs et al. 1995; Riggs and Ames 2003). The APES is classified as a compound estuary that includes two large, shallow lagoons, the Albemarle and Pamlico sounds that are enclosed by the Outer Banks barrier islands, and a series of drowned-river tributaries that supply water and sediment (Geise et al. 1979; Hobbie 1970; Riggs and Ames 2003; Wells and Kim 1989). The Tar-Pamlico River estuary (hereafter referred to as the PRE) encompasses an area of approximately 583 km^2 and reaches from the town of Washington, NC to where it connects to the open Pamlico Sound approximately 56 km to the southeast (Fig. 1). The head (western) region of the PRE meets the freshwater Tar River that drains both the piedmont and coastal plain of North Carolina and discharges into the Pamlico River at Washington with an average annual discharge of approximately 70.8 $m^3 s^{-1}$ from 1998 to 2011 at the U.S. Geological Survey (USGS) Greenville gauging station (historical discharge 69 $m^3 s^{-1}$; Amein and Airan 1976; Geise et al. 1979). The lower PRE is primarily fed by several estuarine tributaries and joins with the Pungo River at its mouth of the estuary where it discharges into Pamlico Sound (Fig. 1; Geise et al. 1979). Average discharge from the PRE to Pamlico Sound is approximately 150 $m^3 s^{-1}$ (Geise et al. 1979). The PRE thought to be an important source of freshwater, sediment, and nutrients to Pamlico Sound (Geise et al. 1979).

Like the Neuse River, the PRE has spatially and temporally varying salinity, and its hydrography is primarily influenced by river discharge, wind-driven waves, and tides (Benninger and Wells 1993; Geise et al. 1979; Hobbie 1970; Leuttich et al. 2002; Wells and Kim 1989). While typically well-mixed vertically with regards to salinity, the PRE can become stratified

during periods of low discharge (e.g., drought conditions), or during hot, low-wind conditions as seen in the Neuse River (Geise et al. 1979; Hobbie 1970; Leuttich et al. 2002). Lower surface salinities along the southern bank of the estuary also indicate the presence of weak estuarine circulation, such as observed in the Neuse River (Geise et al. 1979; Hobbie 1970; Leuttich et al. 2002).

Overall, the coast of North Carolina is subject to semi-diurnal, microtidal conditions; however, the astronomical tide in the APES is generally less than 10 cm (Geise et al. 1979; Wells and Kim 1989). In the PRE, due to the geometry of the estuary, a funneling effect is observed, and the tide range increases to almost 30 cm near the mouth of the Tar River at Washington (Geise et al. 1979). The estuary has an average depth of 3.35 m and a maximum depth of 6.9 m (Geise et al. 1979). Sediment load at the Tar River, Tarboro station was estimated to be 1.89×10^5 t yr^{-1} (Geise et al. 1979). The sediment load discharged into the PRE at Washington is thought to be reduced to 1.0×10^5 t yr^{-1} because of floodplain trapping (Quafisi 2010). Sediments in the main channels of the PRE have been described as fine-grained, muddy sediments derived from terrestrial weathering (Allen 1964; Duane 1962; Park 1971; Geise et al. 1979; Wells and Kim 1989). Along the shallow near-shore margin, sediments are medium to coarse sands (Bellis et al. 1975; Duane 1964; Wells and Kim 1989).

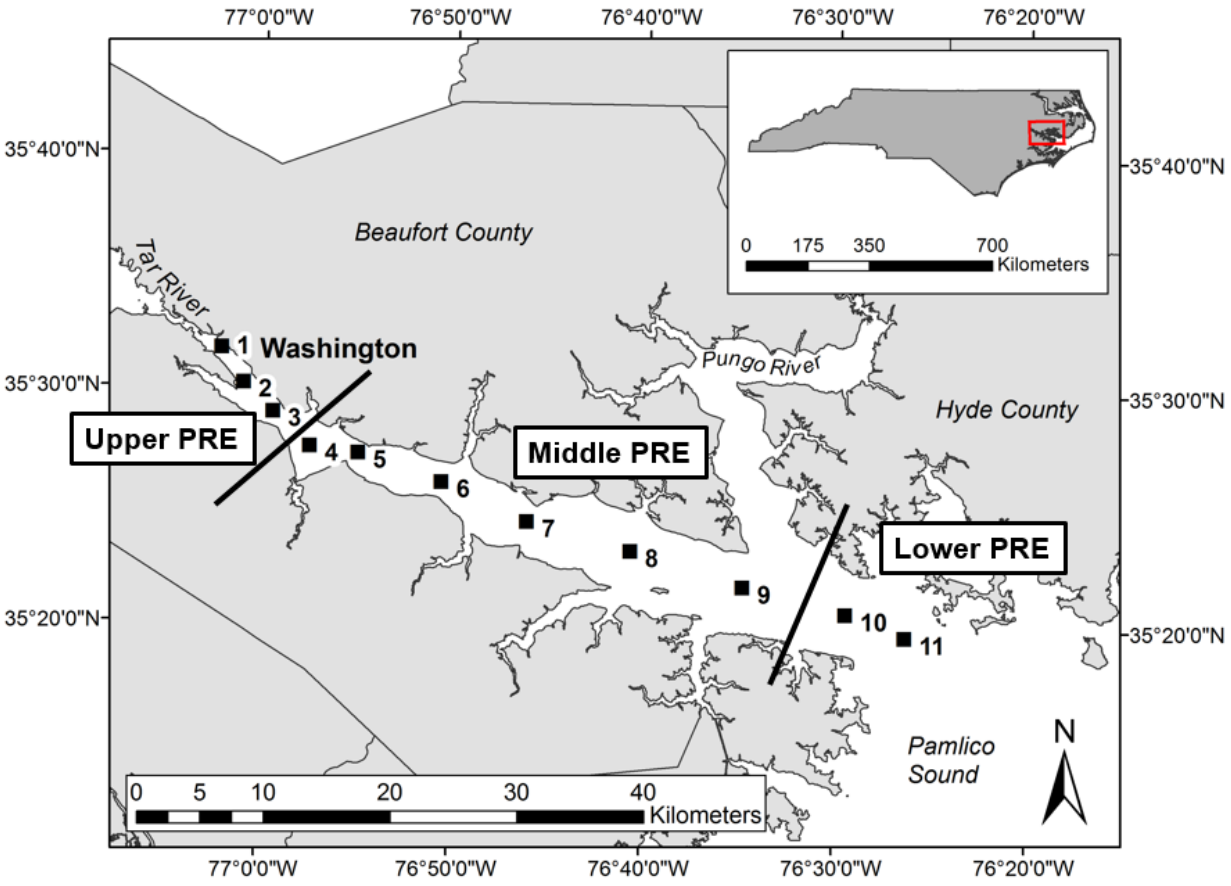

Fig. 1 Map of the PRE study area. Coring sites are denoted by the square symbols. A rate of accumulation was not calculated for the PRE-5 site. Rates of accumulation were calculated from the other sites.

3.0 Methods

3.1 Sampling

A total of 11 sites within the PRE were sampled from a small boat by push-core during the summers of 2010 and 2011 (Fig. 1). The push-core utilized for sample collection consisted of a PVC pipe that had been fitted with a one-way check valve and a 10.2 cm diameter plexiglass core tube (Giffin and Corbett 2003). A total of two cores were collected at each site for analysis. One core was sub-sampled using a ~10 x 10 cm square acrylic tube and imaged using X-radiography. The second core was extruded and sectioned at 2-centimeter-intervals, and samples were stored for subsequent sedimentological and radioisotope analysis.

3.2 Sedimentological Analysis

Sub-samples of wet sediment from each interval were placed in pre-weighed containers and dried at 60° C to determine the water content. The salt-corrected dry bulk density (DBD) of the sediment was then calculated for each 2-centimeter-interval:

$$DBD = (1 - \varphi_s)\rho_s \qquad \text{Equation 1}$$

where φ_s is the salt-corrected porosity, and assuming an average particle density (ρ_s) of 2.4 g (Benninger and Wells 1993; Corbett et al. 2006; Giffin and Corbett 2003).

The particle size distribution for each 2-cm-interval was determined using a 5100 Micromeretics SediGraph. The instrument measures X-ray absorption and applies Stokes Law to describe the mass distribution of particle sizes for a sample (Coakley and Syvitski 1991). A sub-sample of 5-15 g of wet sediment for each interval was placed in glass containers with dispersing solution. Samples were left to sit for at least 24 hours before they were wet-sieved using a 63 μm sieve to remove the sand fraction, which was dried in an oven at 90° C. The mud fraction (<63 μm) of the sample was left for another 24 hours to settle before decanting excess liquid.

The sample was then shaken and placed in a sonic bath for 1 minute prior to analysis to ensure the sediment particles were disaggregated. Instrument error and sample contamination was minimized through monthly calibration to a garnet standard, daily baseline measures, and triplicate rinses between every set of sample runs. After analysis, the sample was captured in a pre-weighed container and dried to determine the total fraction of sample finer than 63 μm. The percent of sand, silt, and clay was then calculated for each interval, and the study sites were classified based on the scheme of Folk (1954).

3.3 Sediment Accumulation

Rates of sediment accumulation (linear and mass accumulation) were determined by measuring the activity of the radionuclides ^{210}Pb and ^{137}Cs using gamma spectroscopy. Approximately 3 g (vial) or 20 g (petri dish) of dry sample was ground, homogenized, packed into containers, and sealed for radionuclide analysis. Samples were counted on one of four low-background, high-efficiency, high-purity Germanium detectors (Coaxial-, BEGe-, LEGe-, and Well-type) for at least 24 hours. After sealing, the samples were stored for at least 20 days to allow for the in-growth of the ^{226}Ra daughter isotopes (i.e., ^{214}Bi, ^{214}Pb, and ^{214}Po) before counting to determine excess ^{210}Pb and ^{137}Cs. Total ^{210}Pb was measured by direct gamma counting at the 46.5 keV energy peak. Supported ^{210}Pb was determined from the activity of ^{226}Ra as measured via the daughter isotopes ^{214}Bi and ^{214}Pb, at the 609 and 295 & 351 keV energy peaks, respectively. Excess (unsupported) ^{210}Pb was calculated by subtracting the supported ^{210}Pb from the total measured ^{210}Pb (Appleby and Oldfield 1978; Appleby and Oldfield 1992; Nittrouer et al. 1979). The activity of ^{137}Cs was measured by direct gamma counting at the 661.7 keV energy peak (Ritchie and McHenry 1973). The detectors were

calibrated at regions of interest using a series of natural matrix standards, and all activities were corrected for self-absorption (Cable et al. 2001; Cutshell et al. 1983).

The constant flux-constant supply (CF-CS), or simple model, was used to calculate rates of sediment accumulation from the excess down-core ^{210}Pb activity profiles (Appleby and Oldfield 1992; Corbett and Walsh *in-press*; Corbett et al. 2007; Oldfield and Appleby 1984). The model assumes that both the flux of unsupported ^{210}Pb and the rate of accumulation are constant (Appleby 1993; Appleby and Oldfield 1992; Corbett and Walsh *in-press*; Kirshnaswamy et al. 1971; Oldfield and Appleby 1984). Therefore, activities of excess ^{210}Pb should decrease exponentially with depth, as modeled by:

$$A_z = A_o e^{-\lambda(\frac{z}{S})} \qquad \text{Equation 2}$$

where A_o is the initial activity (dpm g^{-1}); activity at depth ($A\ z$), and λ is the ^{210}Pb decay constant (0.03114 y^{-1}). The linear sediment accumulation rate (S; cm yr^{-1}) is then calculated by fitting a linear regression to the natural log of excess ^{210}Pb activity (Appleby and Oldfield 1992; Corbett and Walsh *in-press;* Oldfield and Appleby 1984; Robbins 1978):

$$S = \frac{\lambda}{b} \qquad \text{Equation 3}$$

where the decay constant (λ) is divided by the slope of the linear regression (b).

The 1963 peak in ^{137}Cs activity was also used to determine a rate of accumulation for comparison with the CF-CS model rates (DeLaune et al. 1978; Kirshnaswamy et al. 1971; Robbins and Edgington 1975); the following equation was employed:

$$S = \frac{z}{t} \qquad \text{Equation 4}$$

where the rate of accumulation (S; cm yr^{-1}) is determined by dividing the down-core depth (z; cm) to the 1963 peak of in ^{137}Cs activity by the time (t; years from 1963 to core collection). The mass accumulation rate (MAR; g cm^{-2} y^{-1}) of the fine (muddy) sediment fraction for each site is calculated by:

$$MAR = S \times \overline{DBD} \times d \qquad \text{Equation 5}$$

where S is the linear sedimentation rate (Eq. 3); $\overline{DBD}$ is the mean dry bulk density (Eq. 1) for each site, and d is the down-core average of fine material (Corbett et al. 2006; Corbett et al. 2007). The inventory (I) of excess ^{210}Pb and ^{137}Cs was also calculated by:

$$I = \sum[(A_i) \times (\Delta X_i \times DBD_i)] \qquad \text{Equation 6}$$

where DBD_i is the dry bulk density (g cm^{-3}) of the sample interval; ΔX_i is the sample interval size (here 2 cm), and A_i is the activity of a given radionuclide (excess ^{210}Pb, total ^{137}Cs; dpm g^{-1}). The inventory for each interval is computed then summed down-core (Eq. 5).

3.4 Shoreline Change

The 1998 and 2007 shorelines of the PRE were mapped, and a rate of calculated in-order to examine the contribution of fine sediment from shoreline erosion to the study area. Shorelines were heads-up-digitized on aerial photos and attributed by shoreline type according to the method of Geis and Bendell (2008). The 1998 shoreline was digitized using Digital Orthophoto Quarter Quadrangle (DOQQs) images obtained from the North Carolina Department of Transportation. The 2007 shoreline was obtained from a larger estuarine shoreline mapping project conducted by Division of Coastal Management (DCM; ESMP 2012). Only the shoreline along the main trunk of the PRE was digitized as previous studies have shown that little sediment

is exported from creeks and tributaries along the adjacent Neuse River sub-estuary (Marciniak 2008; Phillips and Slattery 2006). Therefore, the contribution to the trunk region from shoreline erosion occurring in the tributaries of the PRE was assumed to be negligible.

The rate of shoreline change (SCR) was calculated using the AMBUR (Analyzing Moving Boundaries Using R) package (Jackson et al. 2012). Shoreline change was computed along transects at a 50-meter-interval using the end-point method. Changes in shoreline type and amount of shoreline modified by structures over the time period were also determined using the AMBUR package. An SCR was initially calculated for all shoreline transects, however only rates associated with natural shoreline types (un-modified) were used to determine the average rate of change for the PRE; shoreline transects designated as modified (with structures) in either time-step were not included in the calculation. Uncertainty in shoreline position for each time-step was computed using Equations 7 and 8:

$$\mathbf{U}=\sqrt{\boldsymbol{E_d^2}+\boldsymbol{E_r^2}} \qquad \text{Equation 7}$$

$$\mathbf{U_t}=\frac{\sqrt{\mathbf{U_{t1}^2}+\mathbf{U_{t2}^2}}}{\boldsymbol{T}} \qquad \text{Equation 8}$$

where the total uncertainty (U) for each shoreline position (e.g., 1998) is calculated from the digitizing error (E_d) and the imagery (E_r) with Equation 7. The total uncertainty for each shoreline (Ut_{t1} and Ut_{t2}, for 1998 and 2007, respectively) is then combined and divided by the time (T) over which shoreline change was calculated (Equation 8) to determine the annualized uncertainty (U_t; Anders and Byrnes 1991; Crowell et al. 1993; Fletcher et al. 2003).

4.0 Results

4.1 Characteristics of PRE Sediments

Based on location and sedimentological data, the study sites were divided into three regions within the PRE sub-estuary; Upper, Middle, and Lower (Fig. 1). Cores from the Upper region (PRE-1, PRE-2, and PRE-3) had grain-size distributions that were more variable with depth, and had a greater sand fraction (Table 1). Sites PRE-1 and PRE-3 were classified as sandy mud and sandy clay, and had a weight percent sand of 13.0 and 16.3%, respectively (Table 1; Folk 1954). The sites exhibited average dry bulk densities (DBDs) of 0.46 ± 0.13 and 0.44 ± 0.17 g cm^{-3}. The most sandy was PRE-2, with a down-core averaged weight percent of 81.3%, and a dry bulk density of 0.93 g cm^{-3} (Table 1). This site was also where the shortest core (20 cm) was collected due to a resistant layer of sand and shell material at depth.

The Middle region (including PRE-4, PRE-6, PRE-7, PRE-8, and PRE-9) was characterized by an overall greater, and more uniform, down-core weight percent of fine sediments and lower average DBDs (Table 1). The average weight percent of sand was <5 %, and all of the sites were classified as clay (Table 1). Average DBD ranged from 0.29 ± 0.7 to 0.41± 0.12 g cm^{-3} and decreased moving down the sub-estuary from site PRE-4 to site PRE-9.

Cores from the Lower region (PRE-10 and PRE-11) also exhibited a fairly uniform down-core weight percent of sand and the most uniform down-core DBDs (Table 1). The PRE-10 and PRE-11 sites were both classified as clay (C) with weight percent sand of 1.8 and 1.3%, respectively (Table 1). For both sites the average DBD was 0.35± 0.05 g cm^{-3}.

Table 1 Grain-size distributions at each study site by down-core averaged weight percent and sediment texture type. Weight percent of sand, silt, and clay determined from grain-size analyses. Sediment texture type after the classification system of Folk (1954). Site PRE-5 was not included as it was not utilized in the calculation of the fine (muddy) sediment budget. Sites are also classified by region within the Tar-Pamlico (division between regions denoted by the dashed lines).

Site	Region	Weight Percent			Texture Class (after Folk 1954)
		Sand	Silt	Clay	
PRE-1	Upper	13.0 %	36.4 %	53.0 %	Sandy Mud (sM)
PRE-2	Upper	81.3 %	2.9 %	15.8 %	Clayey Sand (cS)
PRE-3	Upper	16.3 %	13.8 %	70.0 %	Sandy Clay (sC)
PRE-4	Middle	4.3 %	2.7 %	93.0 %	Clay (C)
PRE-6	Middle	0.7 %	5.6 %	93.8 %	Clay (C)
PRE-7	Middle	1.4 %	3.2 %	95.3 %	Clay (C)
PRE-8	Middle	1.4 %	5.5 %	93.1 %	Clay (C)
PRE-9	Middle	3.1 %	14.7	82.2 %	Clay (C)
PRE-10	Lower	1.8 %	1.9 %	96.4 %	Clay (C)
PRE-11	Lower	1.3 %	2.8 %	95.9 %	Clay (C)

4.2 Radionuclide Tracers and Sediment Accumulation

Surface activities of excess ^{210}Pb and inventories for all of the study sites are presented in Table 2. Excess ^{210}Pb surface activities at the sites ranged from 6.40 ± 1.13 to 15.28 ± 0.38 dpm g^{-1} (PRE-1 and PRE-2, respectively; Table 2). Both of these sites are located in the Upper region of the sub-estuary (Fig. 1). The Middle sites exhibited surface activities ranging from 10.88 ± 1.07 to 14.28 ± 2.72 dpm g^{-1}; with the highest activities at PRE-7 (Table 2). The Lower region sites, PRE-10 and PRE-11, were characterized by similar, low, surface activities of excess ^{210}Pb (7.39 ± 1.31 and 7.77 ± 0.87 dpm g^{-1}; Table 2).

Inventories of excess ^{210}Pb at several sites (PRE-3 to PRE-9, and PRE-11; Table 2) were found to be greater than predicted for the system (Benninger and Wells 1993; Corbett et al. 2007). Predicted inventories of excess ^{210}Pb and ^{137}Cs based on atmospheric sources are 26.5 and 18.0 dpm cm^{-2}, respectively (Benninger and Wells 1993). Seven of the study sites were found to be at or above the predicted inventory for excess ^{210}Pb. Whereas only two sites were found to be near atmospheric deposited inventory for ^{137}Cs, PRE-1 (16.33 ± 2.37 dpm cm^{-2}) and site PRE-6 (18.44 ± 0.22 dpm cm^{-2}). All other sites exhibited inventories of ^{137}Cs that were <8 dpm cm^{-2} (Table 2). The greatest inventory of excess ^{210}Pb (62.15 ± 2.12 dpm g^{-1}) was observed at the PRE-6 site, centrally located within the sub-estuary (Fig. 1; Table 2). The PRE-6 site also had the greatest weight percent of mud (99.3%). The smallest inventory of excess ^{210}Pb (17.06 ± 2.37 dpm cm^{-2}) was observed at PRE-1 (Upper region); it is located in the channel of the Tar River just north of where it enters the Tar-Pamlico sub-estuary (Fig. 1). In general, excess ^{210}Pb inventories increased down the estuary from site PRE-1 to PRE-6 (Table 2). Sites PRE-7 and PRE-8 were found to have statistically similar, intermediate inventories of 33.73 ± 1.87 and 33.58 ± 1.83 dpm cm^{-2} (Table 2).

Table 2 Radionuclide surface activities, inventories, and the depth of peak ^{137}Cs for all of the study sites. Sites are classified by region within the PRE (division between regions denoted by the dashed lines). Surface activities and inventories are excess ^{210}Pb (total ^{210}Pb not reported).

Site	Region	^{210}Pb excess		^{137}Cs	
		Surface activity (dpm g^{-1})	Inventory (dpm cm^{-2})	Depth to Peak (cm)	Inventory (dpm cm^{-2})
PRE-1	Upper	6.40 ± 1.13	17.06 ± 2.37	13	16.33 ± 0.25
PRE-2	Upper	15.28 ± 0.38	21.47 ± 2.99	5	4.31 ± 0.24
PRE-3	Upper	8.39 ± 1.63	32.26 ± 2.87	10	4.17 ± 0.13
PRE-4	Upper	14.28 ± 2.72	41.11 ± 2.51	15	6.74 ± 0.22
PRE-5[a]	Middle	13.60 ± 1.57	25.95 ± 2.22	---	1.93 ± 0.33
PRE-6	Middle	10.88 ± 1.07	62.15 ± 2.12	21	18.44 ± 0.22
PRE-7	Middle	14.10 ± 1.36	33.73 ± 1.87	13	7.66 ± 0.19
PRE-8	Middle	12.49 ± 1.19	33.58 ± 1.83	13	6.34 ± 0.18
PRE-9	Middle	13.38 ± 1.30	44.76 ± 1.72	15	5.97 ± 0.19
PRE-10	Lower	7.39 ± 1.31	23.13 ± 1.34	5	3.58 ± 0.13
PRE-11[b]	Lower	7.77 ± 0.87	40.70 ± 1.92	13	4.14 ± 0.16

[a] *no ^{137}Cs peak;* [b] *^{137}Cs peak not well defined*

Linear and mass accumulation rates were calculated using Equations 3 and 4 for all of the sites, except PRE-5 due to the lack of a distinguishable peak in the ^{137}Cs activity profile. A 2-sample T-test ($P < 0.05$, 95% CI) found no statistical difference between average sediment accumulation rates derived from the two radionuclides. Down-core activities for excess ^{210}Pb and ^{137}Cs, as well as the weight percent of mud (< 63 μm fraction) are plotted for all of the study sites in Figures 2-4. In the Upper region, the greater sand fraction and down-core variability in grain-size may have influenced radionuclide activities. In all three cores, there is a high sand percent that coincides with the depth to which ^{137}Cs is detectable or the base of the core where it was observed in the field to be a deposit of coarse sand mixed with shells and woody debris (Fig. 2). However, the ^{137}Cs activity peak is well-defined at the sites, and there is good agreement in accumulation rates with the two radionuclides at sites PRE-2 and PRE-3 (Table 3).

The five Middle sites have detectable activities to greater depths, higher rates of sediment accumulation, and consistent down-core grain-size distributions (Tables 2 and 3). The depth of peak ^{137}Cs activity was 13-21 cm (Table 2), and both radionuclides had detectable activities to at least 25 cm (Fig. 4). Detectable activities of excess ^{210}Pb and ^{137}Cs at over 40 cm depth and high accumulation rates at the PRE-6 site indicate the presence of a depositional center (Fig. 4). The site exhibits the highest linear and mass accumulation rates of 0.38 ± 0.02 cm yr^{-1} and 0.12 ± 0.04 g cm^{-2} yr^{-1}. The PRE-4 site, located in a small embayment north of PRE-6, also exhibited a slightly higher rate of mass accumulation (0.11 ± 0.03 g cm^{-2} yr^{-1}) in comparison to sites PRE-7, PRE-8, and PRE-9 (Table 3). The PRE-7 and PRE-8 sites exhibited near identical sedimentation rates, grain-size distributions, and depths of peak ^{137}Cs activity. Water depth and estuary morphology are similar at the sites.

Table 3 Linear and mass sediment accumulation rates.

Site	Region	^{137}Cs Accumulation	^{210}Pb excess Accumulation	
		(cm y^{-1})	(cm y^{-1})	(g cm^{-2} y^{-1})
PRE-1	Upper	0.27 ± 0.02	0.33 ± 0.04	0.13 ± 0.04
PRE-2	Upper	0.10 ± 0.02	0.10 ± 0.14	0.02 ± 0.02
PRE-3	Upper	0.19 ± 0.02	0.14 ± 0.02	0.05 ± 0.02
PRE-4	Upper	0.31 ± 0.02	0.27 ± 0.02	0.11 ± 0.03
PRE-6	Middle	0.45 ± 0.02	0.38 ± 0.02	0.12 ± 0.04
PRE-7	Middle	0.28 ± 0.02	0.25 ± 0.02	0.08 ± 0.02
PRE-8	Middle	0.27 ± 0.02	0.24 ± 0.03	0.07 ± 0.02
PRE-9	Middle	0.31 ± 0.02	0.30 ± 0.02	0.08 ± 0.02
PRE-10	Lower	0.10 ± 0.02	0.16 ± 0.04	0.05 ± 0.02
PRE-11	Lower	0.27 ± 0.02	0.36 ± 0.02	0.12 ± 0.02

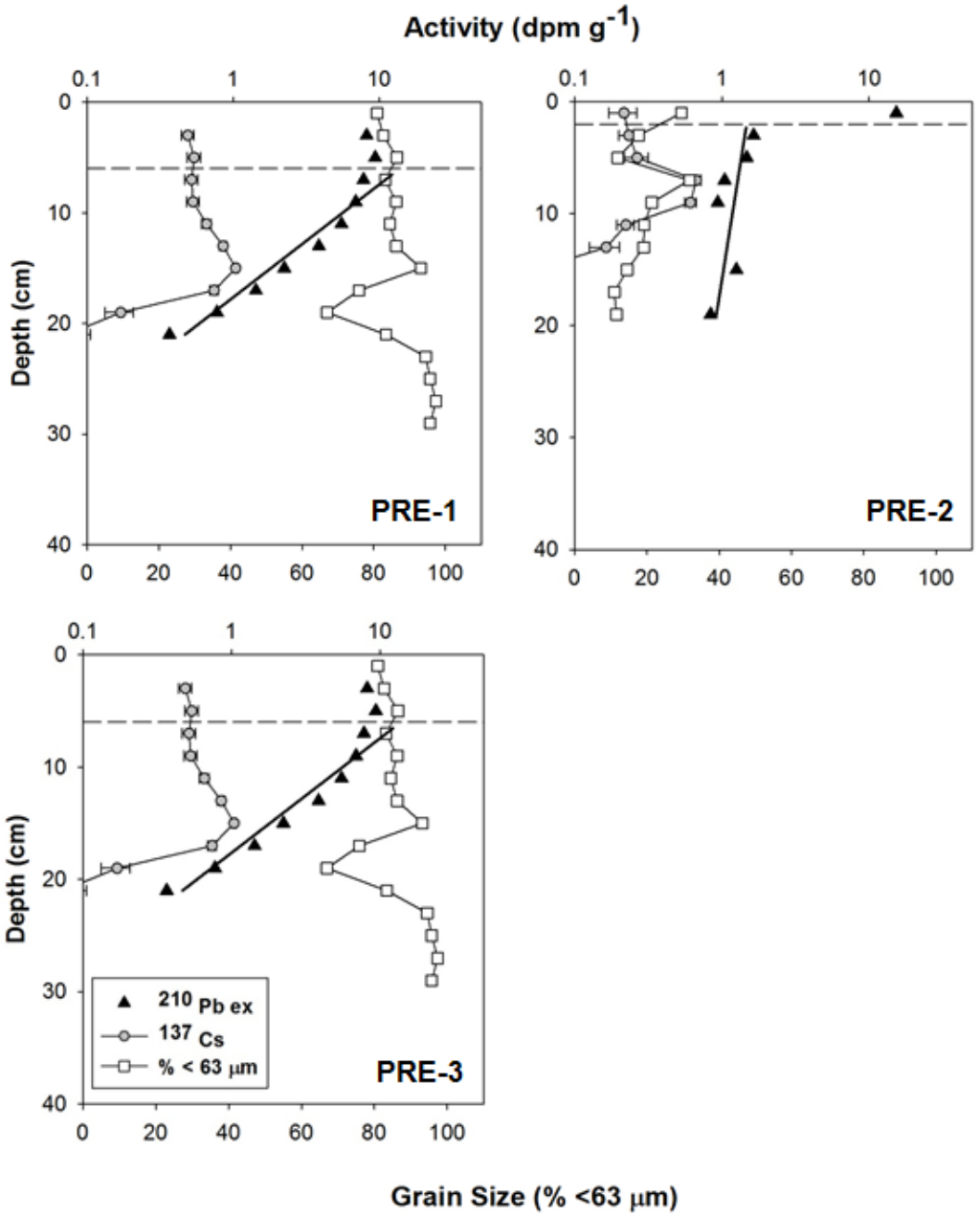

Fig. 3 Plots of radioisotope activity (excess ^{210}Pb and ^{137}Cs) and grain-size at upper Tar-Pamlico sites (PRE-1, PRE-2, and PRE-3). The dashed line on each plot denotes the depth of a surface mixed layer (when present).

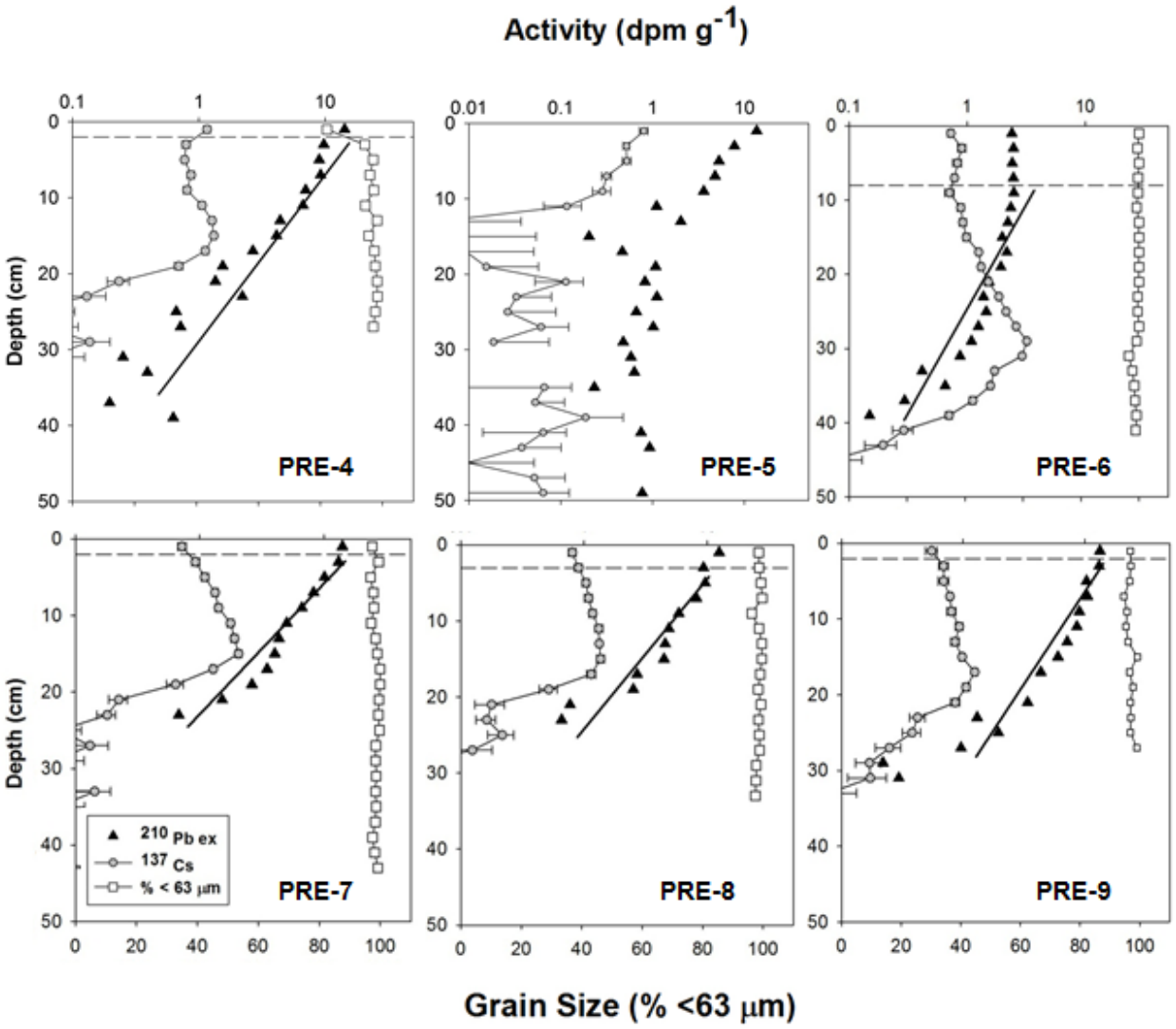

Fig. 4 Plots of radioisotope activity (excess ^{210}Pb and ^{137}Cs) and grain-size at PRE Middle sites (PRE-4, PRE-5, PRE-6, PRE-7, PRE-8, and PRE-9). The dashed line on each plot denotes the depth of a surface mixed layer (when present). The PRE-5 site was not used to calculate an accumulation rate due to the lack of a distinct ^{137}Cs peak and the down-core variability in excess ^{210}Pb.

The Lower region sites, PRE-10 and PRE-11, are located at the mouth of the PRE, at the transition from the estuary to the larger Pamlico Sound (Fig. 1). While surface activities of excess ^{210}Pb and ^{137}Cs inventories are similar, they exhibit different rates of accumulation (Tables 2 and 3). The PRE-10 site is the most southern site still within the sub-estuary. The site exhibits lower sedimentation rates and radionuclide inventories in comparison to PRE-9 (0.16 ± 0.04 cm yr^{-1}, 0.05 ± 0.02 g cm^{-2} yr^{-1}, and 23.13 ± 1.34 dpm cm^{-2}, respectively). Sedimentation rates at the PRE-11 site, in contrast, were higher (0.36 ± 0.02 cm yr^{-1}, 0.12 ± 0.02 g cm^{-2} yr^{-1}), with the greatest mass accumulation rate aside from the PRE-6 site (Table 3). The ^{137}Cs profiles were also different between the sites; the PRE-11 site had a poorly defined peak at 13 cm, in contrast to the defined peak at 5 cm for PRE-10 (Table 2, Fig. 5). Both sites had consistent grain-size distributions, with ~98% mud.

4.3 Shoreline Change

Shoreline change was characterized for the Tar-Pamlico estuary over an era of approximately one decade. While modified shorelines were included in the initial shoreline change rate (SCR) calculation, the average rate reported here is for all un-modified shoreline transects. The mean SCR for the main trunk of the PRE was determined to be -0.5 ± 0.9 m yr^{-1}. This is comparable to other studies in the nearby Neuse River sub-estuary (-0.58 m yr^{-1}) and across the APES that found historical rates of change on the order of -0.5 m yr^{-1} (Chapter 3; Cowart et al. 2011; Riggs and Ames 2003). The rate of erosion for the wetland shorelines (swamp forest and marsh shores) is somewhat greater; swamp forest and marsh shorelines are eroding at an average rate of 0.6 m yr^{-1}. Over 70% of all natural (un-modified) shoreline

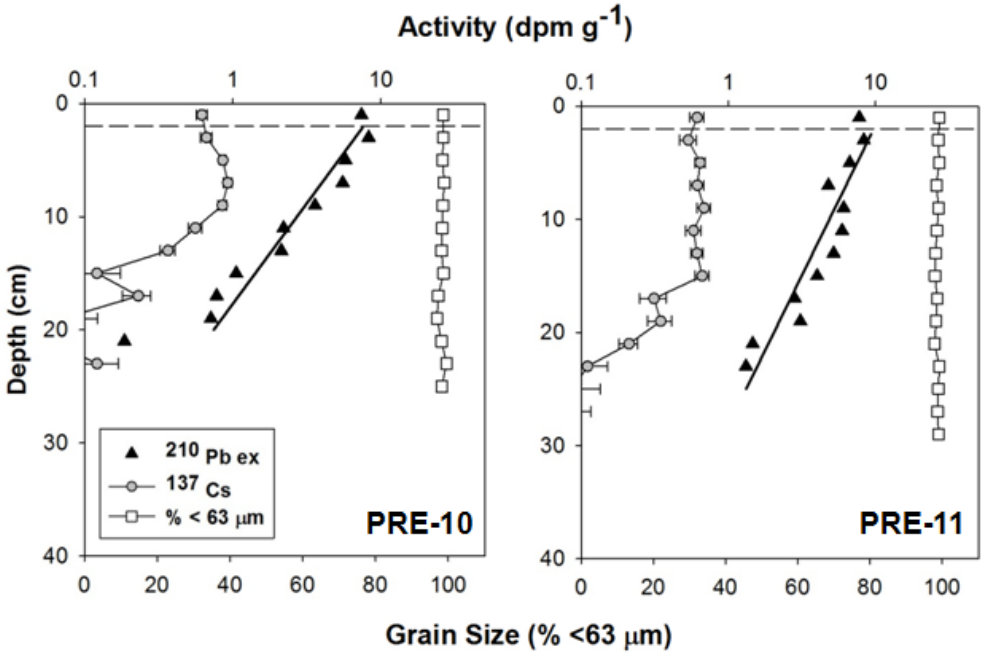

Fig. 5 Plots of radioisotope activity (excess ^{210}Pb and ^{137}Cs) and grain-size for the Lower PRE sites (PRE-10 and PRE-11). The dashed line on each plot denotes the depth of a surface mixed layer (when present).

transects were found to be eroding and only 28% accreting. All wetland shoreline transects were found to be eroding.

The predominant natural shoreline types in the PRE are marsh and sediment bank (31.4% and 33.9%, respectively), while swamp forest only accounts for 7.3% of PRE shoreline (Fig. 6; Table 4). Modified shorelines cover 27.4% of the estuary, and the amount increased significantly over the 1998-2007 era. A change in shore type was observed at 28% of the shoreline, with approximately half converted to modified (13.7%), most of which changed from sediment bank to modified (12.9% out of the 28%). In terms of shoreline length, this equates to an additional 15.7 km more of modified shoreline in 2007 (Table 4). This is evident in Figure 6, where a clear shift from sediment bank to modified shore-type can be seen along the northern bank and at several hot spots along the southern bank. Landward of these shorelines were observed to be either under development or already developed in 1998, but without shore protection structures. The remaining 14.3% of change in shoreline type was primarily due to the conversion of swamp forest to estuarine marsh in the Upper region of the sub-estuary (Fig. 6). However, due to the low resolution of the 1998 DOQQ imagery (1 m, in-contrast to 0.15 m for the 2007 imagery), it is possible that some of that 14.3% change may be error in the shoreline type attributing. It is not likely that modified shore types were incorrectly attributed, as their man-made geometry is easily identified. However, an increase of marsh shoreline types by almost 20 km over the decade (with an approximately 7 km loss of swamp forest) indicates there may be more error associated with digitizing natural shorelines.

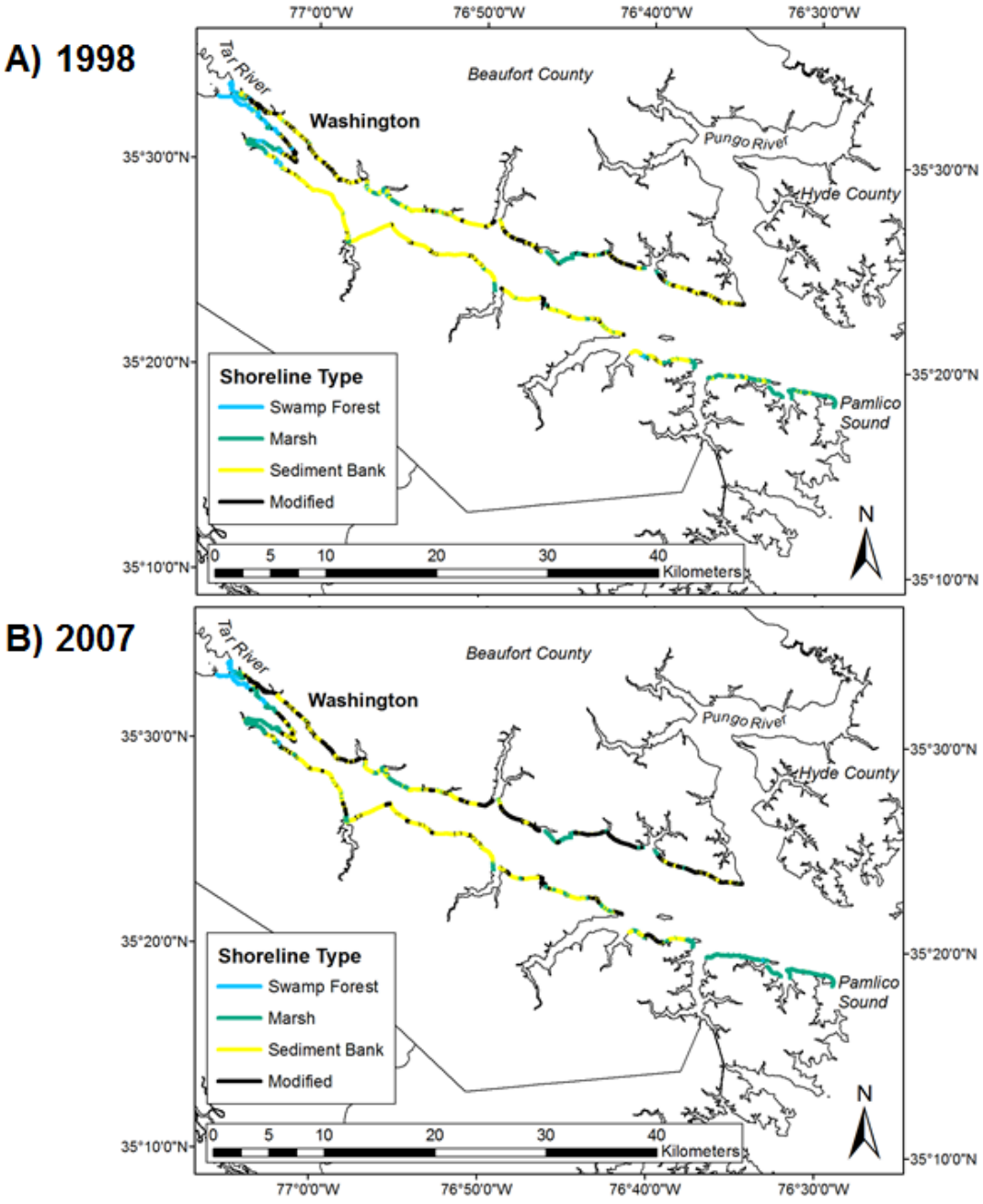

Fig. 6 Shoreline position and type for A) 1998, and B) 2007, in the trunk of the PRE. The black lines denote modified shorelines; the light blue and teal lines denote wetland shorelines, and the yellow lines denote sediment bank shorelines.

Table 4 Statistics for estuarine shorelines. The percentages reported by shoreline type from the ESMP Analysis Report and from this study are out of the total reported for each region (APES and PRE). For comparison, the percentage that each region contains of the total estuarine shoreline in North Carolina is reported in parentheses.

	Kilometers	**Percent**
Total Estuarine Shoreline in NC (ESMP; McVerry 2012):	**19,825.5**	**100 %**
Total APES Shoreline (ESMP Analysis Report; Walsh et al. 2013):	**7815.0**	**100 % (41.5 %)**
Swamp Forest	2426.9	31.0 %
Marsh	4025.0	51.5 %
Sediment Bank	904.4	11.6 %
Modified	439.3	5.6 %
PRE 2007 Shoreline:	**172.5**	**100 % (2.2 %)**
Swamp Forest	12.6	7.3 %
Marsh	54.3	31.4 %
Sediment Bank	58.4	33.9 %
Modified	47.3	27.4 %
PRE 1998 Shoreline:	**161.1**	**100 % (2.1 %)**
Swamp Forest	18.9	11.7
Marsh	36.9	22.9
Sediment Bank	73.6	45.7
Modified	31.6	19.6

4.4 Sediment Budget

A budget for fine sediments (<63 μm) in the PRE was constructed to examine the storage of fine sediment and the potential importance of shoreline erosion as a source of material. Suspended-sediment load from upstream was determined to be 0.96 x 10^5 t yr^{-1} in a previous study by Quafisi (2010). For the purpose of this budget it is assumed that the inorganic fraction of the suspended-sediment load is composed entirely of silt and clay and that the contribution from bedload transport is negligible.

Only wetland shorelines were considered in the budget calculation. The wetland shoreline features were subdivided into segments by intersecting the shoreline layer with a thiesson polygon layer that was created from a shoreline points file. The resulting segments were then intersected with their respective shoreline points so that each segment was attributed with the appropriate SCR, shoreline type, and other relevant characteristics. Shoreline elevation was determined using a digital elevation model (DEM) mosaic from 2001 with a horizontal resolution of 6.1 m (20 ft) and a vertical accuracy of 0.2 m (0.7 ft; http://www.ncfloodmaps.com). The DEM was modified using a mask layer to remove any negative values, then re-sampled using the Nearest-Neighbor method at a resolution of 25 m (one-half the transect spacing used for shoreline change analysis in AMBUR) in Arc GIS 10.1 to determine mean shoreline elevation along each shoreline segment. The shoreline segments were then intersected with the DEM to extract shoreline elevation. Any segments that were not covered in the DEM were automatically assigned a value of zero. A value of 0.6 m was added to the elevation of the shoreline segments to represent a mean depth or scarp height along eroding wetland shorelines based on field observations of the researcher and previous studies (Riggs and Ames 2003). The total contribution of material from shoreline erosion (S; t yr^{-1}) was then determined with the following equation:

$$S = \sum[\{(SCR \times E \times L)\} \times \{DBD\}] \quad \text{Equation 9}$$

where *SCR* is the shoreline erosion rate (m yr^{-1}); *E* is the total elevation including the 0.6 m adjustment (m); *L* is the length of each shoreline segment (m), and *DBD* is the dry bulk density for the shoreline material (g cm^{-3}).

For marsh soils a mean DBD value of 0.56 g cm^{-3} was used; for swamp soils a mean DBD of 0.86 g cm^{-3} (Anderson and Mitsch 2006; Bradley and Morris 1990; Childers and Day 1990; Craft et al. 1993; Craft 2007; Kabrick et al. 2005; Marcus and Kearney 1991; Richardson et al. 1988; Sanders 2002; Turner et al. 2006; Ward et al. 1998). These values are similar to DBDs utilized by Marciniak (2008) of 0.61 (marsh soils) and 0.98 (swamp soils) for a sediment budget in two creeks of the Neuse River estuary. To examine the impact of different DBD values on the budget, the shoreline contribution was determined for the mean DBD and for one standard deviation above and below the mean (0.56 ± 0.39 and 0.86 ± 0.48 for marsh and swamp soils, respectively). The mass of eroded shoreline material calculated from each of the three scenarios was 0.24 x 10^5, 0.63 x 10^5, and 1.16 x10^5 t yr^{-1} (i.e., minus one standard deviation, mean DBD, and plus one standard deviation, respectively). When the rest of the budget calculation remained constant, these scenarios resulted in the shoreline contribution representing 20.0%, 39.6%, and 54.8% of fine source material for the PRE.

The storage of mud was determined using the sediment accumulation rates from this study and a 30 m resolution bathymetric data layer. Grain-size data from this and previous studies were plotted on the bathymetry layer (1954; Fig. 7). While a direct correlation between depth and grain-size was not observed, most of the muddy sites were located in water depths greater than 2.5 m. Previous studies also have characterized shallow waters near shore as having

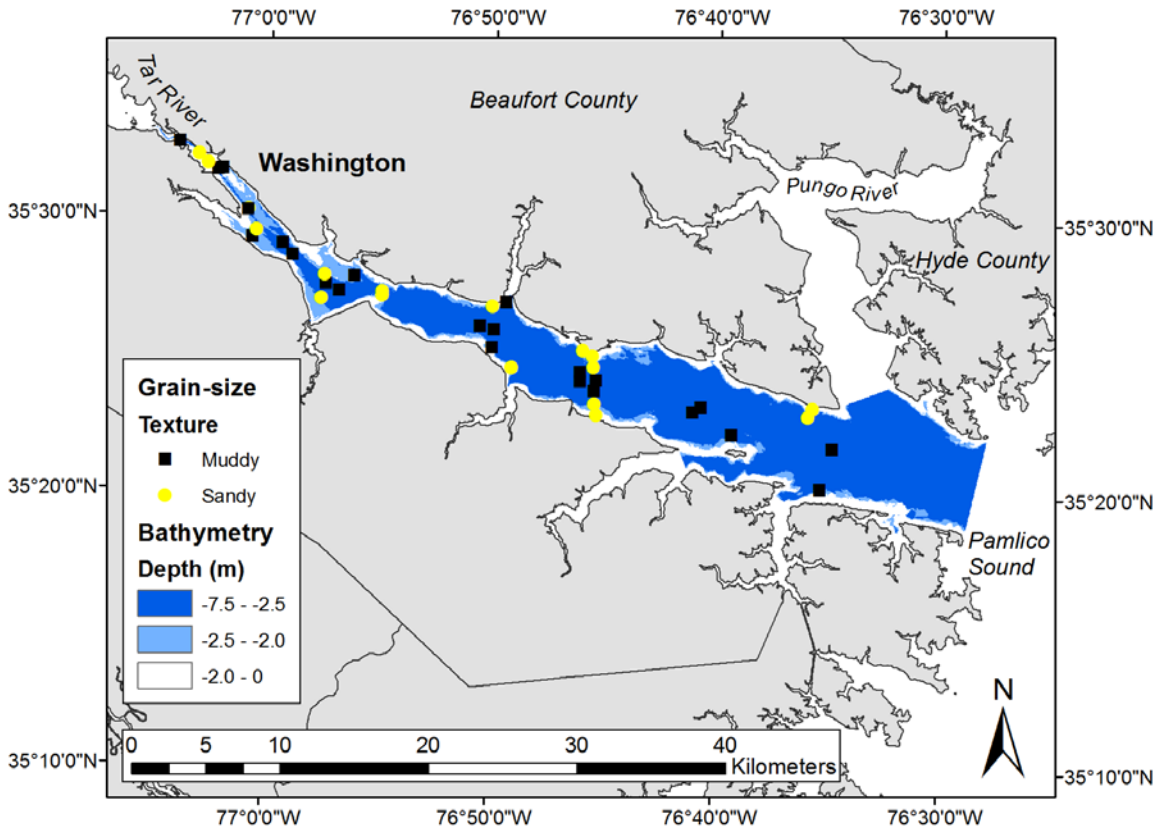

Fig. 7 PRE bathymetry and sediment texture. Bathymetry is divided into three depth bins based on seabed sediment texture; 0-2.0 m is shallow sandy sediment; 2.0-2.5 m is mixed sand and mud depending on location; >2.5 m is muddy sediment. Sediment texture was classified using grain-size analyses from this study and previous research (Bellis et al. 1975; Duane 1964; Wells and Kim 1989).

coarse to medium sandy sediments (Fig. 7; Bellis et al. 1975; Duane 1964; Wells and Kim 1989). Therefore, all cells with depth values shallower than 2.5 m were removed from the raster using a mask layer. The total area of potential fine sediment storage was calculated to be 196.5 km^2, or 33.7% of the 583 km^2 of the estuary (Table 5; Geise et al. 1979).

The resulting bathymetry raster was then converted into a polygon layer and divided into regions with each PRE site as the centroid for individual region polygon features (Fig. 8; Table 5). As site PRE-5 was not used to calculate a mass accumulation rate, a divide was placed at the PRE-5 location and the regions east and west were allocated to PRE-4 and PRE-6 (Fig. 8). The PRE-11 site was not utilized to calculate sediment storage as it was located past the mouth of the estuary. The downstream limit of calculated sediment storage was placed half-way between the PRE-10 and PRE-11 sites. A mass accumulation rate was uniformly applied to each region, and the regions were summed to quantify the total storage (Table 5):

$$Q = \sum[\{A\} \times \{MAR\}] \div [100] \qquad \text{Equation 10}$$

where A is the total area per region (m^2); MAR (g cm^{-2} y^{-1}) is the mass accumulation rate (previously determined for each site from Eq. 4), and the [100] is an adjustment factor for units (includes both a conversion from centimeters to meters, and grams to tonnes). The fine material not stored in the estuary is reported as exported from the system to Pamlico Sound. The sediment supplied from wetland erosion is calculated to be 0.63 x 10^5 t yr^{-1} from 219.2 km of shoreline (~43% of incoming fine sediments). The river supplies 0.96 x 10^5 t yr^{-1} (~57% of sediment; Fig. 9; Quafisi 2010). So, the total storage of fine sediment is 1.6 x 10^5 t yr^{-1}, or 93% of the total sediment supplied. Accounting for storage, this resultes in 0.3 x 10^4 t yr^{-1} (7%) of fine sediment exported to the adjacent Pamlico Sound (Fig. 9).

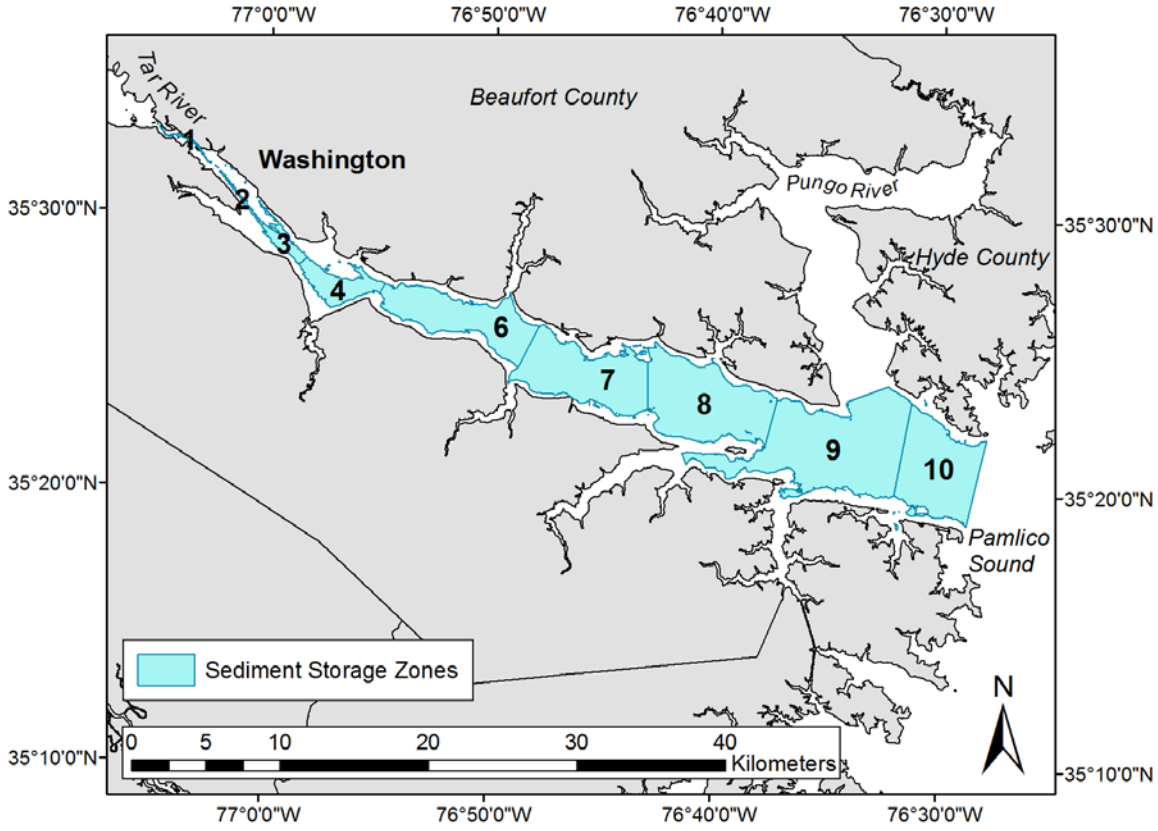

Fig. 8 The extent of the PRE muddy seabed (bounded by 2.5 m bathymetry contour). Storage of sediment was calculated for each area. Regions were divided at geographic mid-points between study sites.

Table 5 Sediment storage by zone. Water depth (m) is reported for each zone along with total area (km^2), mass of fine sediment (t yr^{-1}) stored, and the percent stored (out of total).

Site	Storage Zone	Water Depth (m)	Storage Area (km^2)	Mass Stored (t yr^{-1})	Percent Stored
PRE-1	1	2.3	0.5	655.0	0.4
PRE-2	2	2.0	0.6	117.9	0.1
PRE-3	3	3.3	3.0	1503.0	1.0
PRE-4	4	3.1	8.4	9278.4	6.0
PRE-6	6	4.1	25.6	30,693.6	19.7
PRE-7	7	4.7	31.6	25,270.4	16.2
PRE-8	8	4.1	37.9	26,532.7	17.0
PRE-9	9	4.3	30.7	46,516.6	29.6
PRE-10	10	6.2	58.1	15,354.7	9.8
Total Storage:		----	**196.5**	**155,922.3**	----

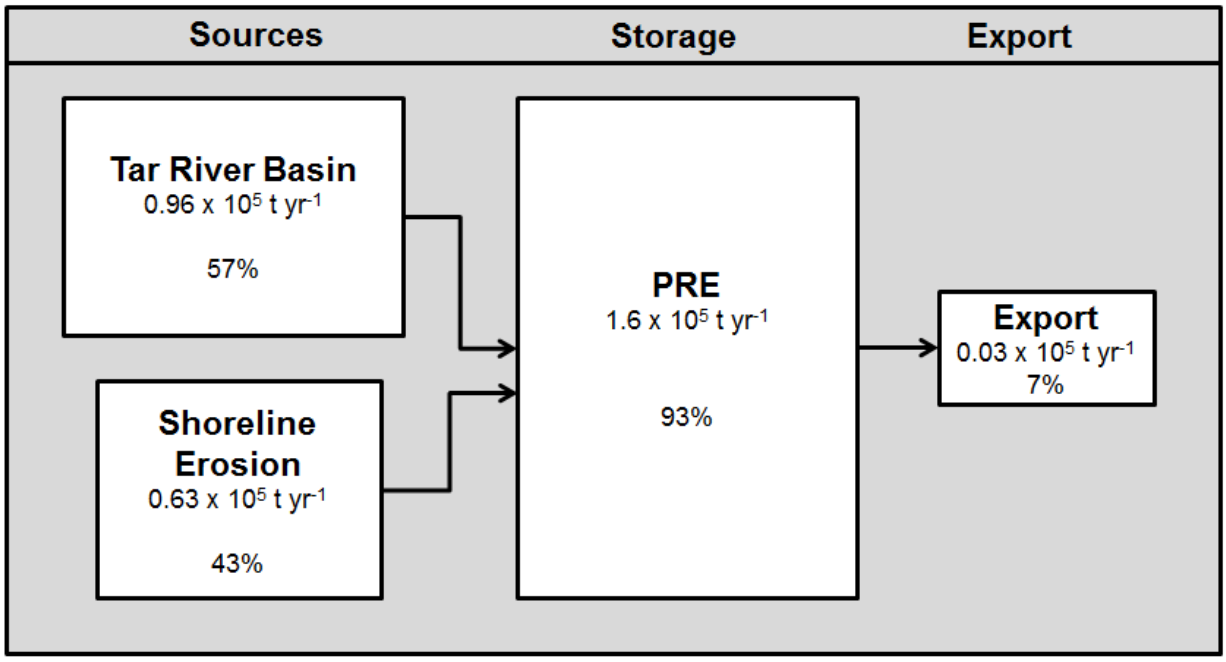

Fig. 9 Box model representing the fine sediment budget for the PRE. Sources of material include wetland shoreline erosion and sediment discharge from the Tar River. Storage represents the accumulation of material within the PRE. Box sizes are not to scale.

5.0 Discussion

5.1 Sedimentation in the Tar-Pamlico estuary

The sedimentological data and sediment accumulation rates presented in this study provide insights into the movement and storage of sediment across the Tar-Pamlico sub-estuary. The Upper region of the sub-estuary is characterized by a relatively thin layer (approximately 20 cm) of sandier sediments that overly a coarse deposit of shell, sand, and woody debris. These sites (located in the narrow channel at the head of the estuary where the Tar discharges into the PRE) are strongly influenced by freshwater discharge (e.g., river hydrodynamics; Fig. 1). The shallow activity profiles and average water depths (< 3 m) indicate a region of low or transient deposition at PRE-2 and PRE-3 (Fig. 10). Previous research by Giffin and Corbett (2003) observed a linear accumulation rate of 0.3 cm yr^{-1} at a site near PRE-3. They hypothesized the accumulation was due to the presence of a turbidity maxima in the region (Giffin and Corbett 2003). This study observed lower rates of accumulation (< 0.2 cm yr^{-1}) but supports the potential for short-term, transient, deposition at the site.

The Middle region is characterized by overall higher rates of fine sediment accumulation, (mud fraction greater than 95%; Table 1; Fig. 7). Inventories above atmospheric predicted deposition support this (> 26.5 dpm cm^{-2}; Benninger and Wells 1993). PRE-4 site, located in a small embayment, is characterized by high excess ^{210}Pb surface activity, inventory, and accumulation rate. Fine sediments delivered from the Tar River and eroded from nearby swamp and marsh shorelines are likely deposited in the shallow bay as the estuary widens and river flow decreases. However, at the south end of the embayment the estuary narrows abruptly to ~2.5 km across and deepens to over 5 m. Site PRE-5 was located in the channel of this narrow outlet from the embayment and the complex sediment record here probably reflects these conditions (Fig. 5; Table 2; Corbett et al. 2007; Tully 2004). Greater flow velocities as a function of the

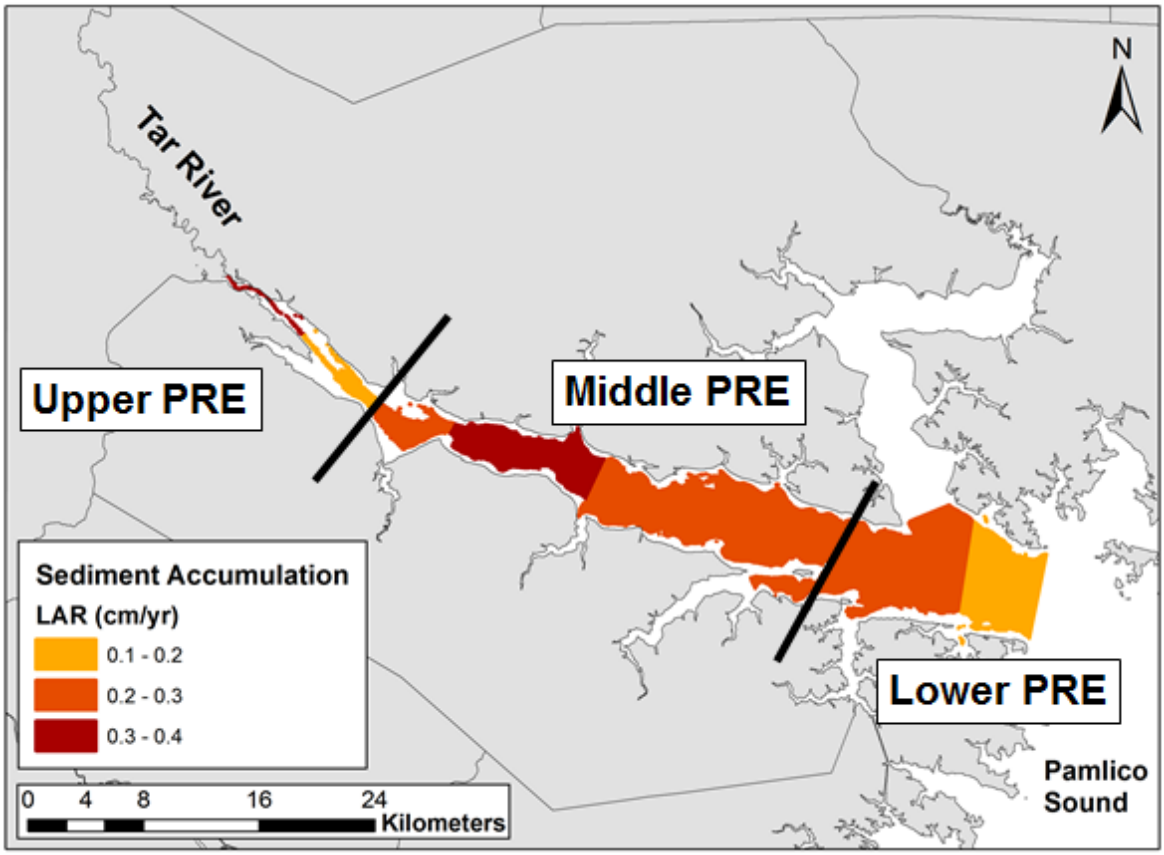

Fig. 10 Zones with estimated sediment storage rates, as determined from excess ^{210}Pb.

narrower channel likely increase scour of the seabed, resulting in increased water depth, coarser sediments, and variable radioisotope profiles. A study by Cooper et al. (2004) also found indications of alternating sediment conditions and properties (bulk density and loss on ignition) in this area.

The high radionuclide inventories and accumulation rates at PRE-6 indicate a focusing of sediment into a zone of rapid accumulation (Fig. 10). However, near vertical activity profiles of excess ^{210}Pb and ^{137}Cs in the first 10 cm suggest a thick surface mixed layer produced by biological mixing or physical reworking composed of clay-sized particles. The rest of the Middle region is characterized by greater than 95%, homogenous, muddy sediments, and thin surface mixed layers (~2 cm). This region is deeper than 4.5 m on average and is relatively uniform in estuary width (Figs. 1 and 2A). Together, these data indicate a large section of the lower Middle region is consistently accreting fine sediments with little re-working or erosion of deposited material (Fig. 10).

The Lower region indicates a zone at the mouth of the estuary (downstream of the confluence of the PRE and Pungo River tributary) of lower accumulation (Fig. 10). Channel narrowing, reduced sediment input, and greater wave exposure likely result in an area of low accumulation (Fig. 10). The vast majority of available fluvial sediment has probably deposited within the more landward (with enhanced settling rates from flocculation) PRE (84%), leaving less material available to accumulate at the PRE-11 site. In the sediment budget calculation, the PRE-11 region only represents approximately 9% of the total storage of fine material, whereas the Middle regions sites PRE-6, PRE-7, PRE-8, and PRE-9 contain 83% of the sediment stored in the estuary. Some material is likely exported to the adjacent Pamlico Sound through wave resuspension. Based on storage area (196.5 km^2) and total inputs, it is estimated than an average

sedimentation rate of 0.33 cm yr^{-1} (resulting in ~17 cm thick layer of sediments) would be required to store 93% of supplied sediment. In reality, rates of sedimentation vary across the estuary; however, this estimate is consistent with many of the study sites and previous work by Giffin and Corbett (2003).

5.2 Shoreline Change

For PRE shorelines, calculated over a 9-year-era, instead of the 50-year typically used to determine historical rates of change in studies, the mean SCR (-0.5 ± 0.9 m yr^{-1}) is comparable to both intermediate (decadal) and historical rates observed in the APES (Chapter 3; Cowart et al. 2011; Riggs and Ames 2003). Therefore, despite the proportionally large annualized error of ± 0.9 m yr^{-1}, this rate is representative of mean shoreline change across the PRE. This is important to note for subsequent discussion of the sediment budget.

Bellis et al. (1975) estimated a rate of shoreline hardening in the APES at13 km yr^{-1}. The recently completed Estuarine Shoreline Mapping Program (ESMP) estimates that approximately 5% of all shoreline in the twenty coastal counties of North Carolina are currently modified with structures (Table 4; McVerry 2012). In the PRE, this hardening is much higher; 27.4% of the shoreline along the trunk of the estuary is modified (Table 4). Over the 1998 to 2007 era examined in this study, there was an increase of 15.7 km (7.8%) of modified shoreline, primarily by conversion of sediment bank shores to structures (Table 4). By converting the net increase in modified shoreline (15.7 km) to an annualized rate, the rate hardening for the PRE is calculated to be 1.7 km yr^{-1}. As the ratio of modified to natural shoreline is several times greater in the PRE in comparison to other shorelines in the APES, this is likely greater than the actual rate of hardening and was far less than the Bellis et al. (1975) estimate. This estimate does not account

for spatial variability in shoreline modification or the influence of coastal management policies, or the types of shoreline structures that are constructed. While much of this modification was observed along sediment bank shores, which were not included in the final sediment budget, the overall increase in modified shorelines indicates the possibility of future impacts to sediment supply. Essentially, the supply of sediment from shoreline sources would be reduced as the amount of modified shoreline expands. A study in the Chesapeake Bay hypothesized that as river sources of sediment have decreased due to upstream dam construction, the significance of shoreline erosion to coastal sediment budgets has increased (Marcus and Kearny 1991). Therefore, human activities along estuarine shorelines may impact future sediment supply.

5.3 Sediment Budget

A sediment budget was constructed for the Tar-Pamlico sub-estuary to examine sediment storage and the contribution of shoreline erosion. The budget focuses specifically on fine sediments (grain size <63 μm), as rates of sedimentation for sandy areas of the seabed were not quantified. A previous study by Quafisi (2010) quantified the storage of sediment on the floodplain of the Tar River and estimated a load of sediment to the estuary of 0.96×10^5 t yr^{-1}. As reported in Table 5, shoreline erosion can account for almost 43% of the total supply of muddy sediment to the system, while the Tar River input equals 57% of the material. The percent of sediment contributed from shoreline erosion is less than reported in other studies, including the Neuse River estuary and tributaries of the Chesapeake Bay (Benninger and Wells 1993; Marcus and Kearny 1991; Pachineelam et al. 1999; Yarbro et al. 1983). However, it should be noted that these previous studies addressed a total sediment budget (including erosion from all shoreline types in the region of interest) instead of a budget solely for fine sediments. In the PRE, 33.9 % of the shoreline is sediment bank and therefore not included in this budget.

These shorelines are expected to primarily contribute sandy sediment to nearshore shoals and shallow margins (< 2.5 m depth; Bellis et al. 1975; Wells and Kim 1989).

The shoreline contribution (in this budget) varies significantly depending on the DBD and scarp height values ranging from 20% to 55%. As a result, the amount of fine material potentially exported from the PRE extends from negative values to 0.72 x 10^5 t yr^{-1} or 32%. Future refinements of this budget should therefore include DBD values derived from sediment sampling of the shorelines located within the estuary, instead of literature-derived values.

Previous studies have indicated that the Tar-Pamlico and Neuse River sub-estuaries provide sediment to Pamlico Sound (Benninger and Wells 1993; Tully 2004). However, other studies of estuarine systems found that the vast majority of material is stored within the drowned-river tributary (Donoghue et al. 1989; Marcus and Kearney 1991; Phillips and Slattery 2006; Schubel and Carter 1970; Wells and Kim 1991). This sediment budget calculated that a maximum 7% of supplied fine material leaves PRE system. In sediment budgets for the Chesapeake Bay, and previous work in the Albemarle-Pamlico system, over 80% of supplied material is stored within either creek or drowned-river tributaries of these large, complex, estuarine systems (Donoghue et al. 1989; Hobbs et al. 1992; Marciniak 2008; Marcus and Kearney 1991; Phillips 1987; Phillips 1989; Phillips and Slattery 2006; Schubel and Carter 1970). These studies, and the research presented here, also support the significance of shoreline erosion as a source of sediments to estuarine systems. With increased sea-level rise (SLR), greater accommodation space may further reduce transport to the sound.

6.0 Summary and Conclusions

This study examined measures of radionuclide tracers and sedimentological characteristics at 11 sites across the Tar-Pamlico sub-estuary, North Carolina. Rates of shoreline

change for the decade of 1998-2007 were used to examine the significance of shoreline erosion as a source of fine sediment to the system. Finally, a preliminary sediment budget for fine sediments was constructed.

Measures of grain-size and dry bulk density illustrate the distribution of sediments across the system. Fine sediments were generally observed in areas where water depth was greater than 2.5 m, and the greatest percentages of mud were seen along the Middle region. Spatial variability in inventories of excess ^{210}Pb and rates of sediment accumulation indicate depositional centers in the Middle region (sites PRE-4 and PRE-6). Moderate rates of accumulation were extended to the Lower region sites. Rates of shoreline change were comparable to other studies within the APES (-0.5 ± 0.9 m yr^{-1}), and changes in shoreline type indicate an increase in modified shores by 7.8%. A rate of hardening of 1.7 km yr^{-1} was estimated for the PRE, significantly less than earlier estimates.

The preliminary sediment budget indicates erosion may contribute almost one-half (43%) of incoming fine sediment to the sub-estuary. A total of 93% of incoming fine sediment is apparently stored within the estuary (primarily in the Middle region), while only 7% is thought to be exported to nearby Pamlico Sound. These findings are comparable to previous studies in both the Chesapeake Bay and Albemarle-Pamlico estuarine systems.

These data illustrate the complexity of fine sedimentation in even a small sub-set of the large Albemarle-Pamlico Estuarine System and highlight the potentially increasing importance of shorelines as a source of sediment to coastal systems.

REFERENCES

Allen, D.W., 1964. Clay minerals of Tar-Pamlico River sediments. M.S. Thesis (unpublished), University of North Carolina, Chapel Hill.

Amein, M., and Airan, D.S., 1976. Mathematical modeling of circulation and hurricane surge in Pamlico Sound. NC Sea Grant, UNC-SG-76-12, Raleigh, NC.

Anders, F.J., and Byrnes, M.R., 1991. Accuracy of Shoreline Change Rates as Determined from Maps and Aerial Photographs. Shore and Beach 59, 17-26.

Anderson, C.J., and Mitsch, W.J., 2006. Sediment, carbon, and nutrient accumulation at two 10-year-old created riverine marshes. Wetlands 26(3), 779-792.

Appleby, P.G., 1997. Sediment records of fallout radionuclides and their application to studies of sediment-water interactions. Water, Air and Soil Pollution 99, 573-586.

Appleby, P.G., 2008. Three decades of dating recent sediments by fallout radionuclides: a review. The Holocene 18(1), 83-93.

Appleby, P.G., and Oldfield, F., 1978. The calculation of Lead-210 dates assuming a constant rate of supply of unsupported ^{210}Pb to the sediment. Catena 5, 1-8.

Appleby, P.G., and Oldfield, F., 1992. Application of lead-210 to sedimentation studies. In: Ivanovich, M., and Harmon, R.S. (editors), Uranium-series disequilibrium: applications to earth, marine, and environmental problems, Claredon Press, Oxford, UK, 731-778.

Arfi, R., and Bouvy, M., 1995. Size, composition and distribution of particles related to wind-induced resuspension in a shallow tropical lagoon. Journal of Plankton Research 17(3), 557-574.

Bellis, V., O'Conner, M.P., and Riggs, S.R., 1975. Estuarine shoreline erosion in the Albemarle-Pamlico region of North Carolina. UNC Sea Grant Publication, Raleigh, North Carolina.

Benninger, L.K., and Wells, J.T., 1993. Sources of sediment to the Neuse River estuary, North Carolina. Marine Chemistry 43, 137-156.

Bradley, P.M., and Morris, J.T., 1990. Physical characteristics of salt marsh sediments: ecological implications. Marine Ecology Progress series 61, 245-252.

Cable, J., Burnett, W., Moreland, S., and Westmoreland, J., 2001. Empirical assessment of gamma ray self-absorption in environmental analyses. Radioactivity and Radiochemistry 12, 30-39.

Childers, D.I., and Day, J.W., 1990. Marsh-water column interactions in two Louisiana estuaries. 1. Sediment dynamics. Estuaries 13(4), 393-403.

Cloern, J.E., 1987. Turbidity as a control on phytoplakton biomass and productivity in estuaries, Continental Shelf Research 7(11/12), 1367-1381.

Coakley, J.P., and Syvitski, J.P.M., 1991. SediGraph technique. Principles, methods, and application of particle size analysis, Cambridge University Press, Cambridge, NY, 129-142.

Corbett, D.R., Vance, D., Letrick, E., Mallinson, D., and Culver, S., 2007. Decadale-scale sediment dynamics and environmental change in the Albemarle Estuarine system, North Carolina. Estuarine, Coastal and Shelf Science 71, 717-729.

Corbett, D.R., Walsh, J.P., *in-press*. ^{210}Lead and ^{137}Cesium - Establishing a Chronology for the Last Century. Handbook of Sea Level Research. John Wiley & Sons, Ltd.

Cowart, L., Corbett, D.R., and Walsh, J.P., 2011. Shoreline Change along Sheltered Coastlines: Insights from the Neuse River Estuary, NC, USA. Journal of Remote Sensing 3, 1516-1534.

Craft, C.B., Seneca, E.D., and Broome, S.W., 1993. Vertical accretion in microtidal regularly and irregularly flooded estuarine marshes. Estuarine, Coastal and Shelf Science 37, 371-386.

Craft, C., 2007. Freshwater input structures soil properties, vertical accretion, and nutrient accumulation of Georgia and U.S. tidal marshes. Limnology and Oceanography 52(3), 1220-1230.

Crowell, M., Leatherman, S.P., and Buckley, M.K., April 1993. Shoreline Change Rate Analysis: Long Term Versus Short Term Data. Shore and Beach, 13-20.

Curray, J.R., 1965. Late Quaternary history, continental shelves of the United States. In: Wright, H.E., and Frey, D.G. (editors), The Quaternary of the United States. Princeton University Press, 723-735.

Cutshell, N.H., Larsen, I.L., and Olsen, C.R., 1983. Direct analysis of ^{210}Pb in sediment samples: self-adsorption corrections. Nuclear Inst. Methods 206, 309-312.

Dadey, K.A., Janecek, T., and Klaus, A., 1992. Dry-bulk density: its use and determination. Proceedings of the Ocean Drilling Program, Scientific Results 126, 551-554.

DeLaune, R.D., Patrick, W.H., and Buresh, R.J., 1978. Sedimentation rates determined by ^{137}Cs dating in a rapidly accreting salt marsh. Nature 275, 395.

Donoghue, J.F., Bricker, O.P., and Olsen, C.R., 1989. Particle borne radionuclides as tracers for sediment in the Susquehanna River and Chesapeake Bay. Estuarine, Coastal and Shelf Science 29, 341.

Duane, D.B., 1964. Significance of skewness in recent sediment, Western Pamlico Sound, North Carolina. Journal of Sedimentary Petrology 34, 864-874.

Dyer, K.R., 1997. Estuaries: a physical introduction. New York, John Wiley & Sons.

Fletcher, C.H., Rooney, J.J., Barbee, M., Lim, S.C., and Richmond, B.M., 2003. Mapping shoreline change using digital orthophotogrammetry on Maui, Hawaii. Journal of Coastal Research SI 38, 106-124.

Folk, R.L., 1954. The distinction between grain size and mineral composition in sedimentary rock nomenclature. Journal of Geology 62(4), 344-359.

Geis, S., and Bendell, B., 2010. Charting the Estuarine Environment: A methodology spatially delineating a contiguous, estuarine shoreline of North Carolina. Division of Coastal Management, Raleigh, NC.

Geise, G.L., Wilder, H.B., and Parker, G.G., 1979. Hydrology of major estuaries and sounds of North Carolina. USGS Publication 2221.

Giffin, D., and Corbett, D.R., 2003. Evaluation of sediment dynamics in coastal systems via short-lived radioisotopes. Journal of Marine Systems 42, 83-96.

Hibma, A., Stive, M.J.F., and Wang, Z.B., 2004. Estuarine morphodynamics. Coastal Engineering, 51, 765-778.

Hobbie, J.E., 1970. Hydrography of the Pamlico River Estuary, NC. WRRI, University of North Carolina, Chapel Hill.

Hobbs, C.H., Halka, J.P., Kerhin, R.T., and Carron, M.J., 1992. Chesapeake Bay sediment budget. Journal of Coastal Research 8(2), 292-300.

Horton, B.P., Peltier, W.R., Culver, S.J., Drummond, R., Engelhard, S.E., Kemp, A.C., Mallinson, D., Thieler, E.R., Riggs, S.R., Ames, D.V., and Thomson, K.H., 2009. Holocene sea-level changes along the North Carolina coastline and their implications for glacial isostatic adjustment models. Quaternary Science Reviews 28, 1725-1736.

Jackson, C.W., C.R. Alexander, and D. M. Bush. 2012. Application of the AMBUR R package for spatio-temporal analysis of shoreline change: Jekyll Island, Georgia, USA. Computers and Geosciences 41**,** 199-207.

Jaeger, J.M., Mehta, A., Faas, R., and Grella, M., 2009. Anthropogenic impacts on sedimentary sources and processes in a small urbanized subtropical estuary, Florida. Journal of Coastal Research 25(1), 30-47.

Kabrick, J.M., Dey, D.C., Van Sambeek, J.W., Wallendorf, M., and Gold, M.A., 2005. Soil properties and growth of swamp white oak and pin oak on bedded soils in the lower Missouri River floodplain. Forest Ecology and Management 204, 315-327.

Kemp, A.C., Horton, B.P., Culver, S.J., Corbett, D.R., van de Plassche, O., Gehrels, W.R., Douglas, B.C., and Parnell, A.C., 2009. Timing and magnitude of recent accelerated sea-level rise (North Carolina, United States). Geology 37, 1035-1038.

Kirshnaswamy, S., Lal, D., Martin, J.M., and Meybeck, M., 1971. Geochronology of lake sediments. Earth and Planetary Science Letters 11, 401-414.

Leuttich, R.A., Carr, S.D., Reynolds-Fleming, J.V., Fulcher, C.W., and McNinch, J.E., 2002. Semi-diurnal seiching in a shallow, micro-tidal lagoonal estuary. Continental Shelf Research 22, 1669-1681.

Mallinson, D., Riggs, S., Thieler, E.R., Culver, S.J., Foster, D.S., Corbett, D.R., Farrell, K., and Wehmiller, J.F., 2005. Late Neogene and Quaternary evolution of the northern Albemarle embayment (mid-Atlantic continental margin, U.S.A.). Marine Geology 217, 91-117.

Mallinson, D., Culver, S., Riggs, S., Thieler, E.R., Foster, D., Wehmiller, J., Farrell, K., and Pierson, J., 2010. Regional seismic stratigraphy and controls on the Quaternary evolution of the Cape Hatteras region of the Atlantic passive margin, USA. Marine Geology 268, 16-33.

Marciniak, K.J., 2008. Sediment dynamics in tributaries of the Neuse River Estuary, North Carolina. Un-published thesis, East Carolina University, Greenville, NC.

Marcus, W.A., and Kearney, M.S., 1991. Upland and coastal sediment sources in a Chesapeake Bay estuary. Annals of the Association of American Geographers 81(3), 408.

McVerry, K., 2012. North Carolina estuarine shoreline mapping project: statewide and county statistics. North Carolina Division of Coastal Management, 1-145.

Meade, R.H., 1969. Landward transport of bottom sediments in estuaries of the Atlantic coastal plain. Journal of Sedimentary Petrology 39(1).

Meade, R.H., 1972. Transport and deposition of sediments in estuaries. Environmental Framework of Coastal Plain Estuaries.

Nichols, M.M., 1989. Sediment accumulation rates and relative sea-level rise in lagoons. Marine Geology 88, 201-219.

Nichols, M.M., and Poor, G., 1967. Sediment transport in a coastal plain estuary. Journal of the Waterways and Harbors Division WW4, 83.

Nichols, M.M., Johnson, G.H., and Peebles, P.C., 1991. Modern sediments and facies model for a microtidal coastal plain estuary, the James Estuary, Virginia. Journal of Sedimentary Petrology 61(6), 883.

Nittrouer, C.A., Sternberg, R.W., Carpenter, R., and Bennett, J.T., 1979. The use of Pb-210 geochronology as a sedimentological tool – application to the Washington Continental Shelf. Marine Geology 31(3-4), 297-316.

North Carolina Floodplain Mapping Program. http://www.ncfloodmaps.com.

Park, B.K., 1971. Mineralogy of recent sediment so North Carolina sounds and estuaries. Ph.D. Thesis (unpublished), University of North Carolina, Chapel Hill.

Patchineelam, S.M., Kjerfve, B., and Gardner, L.R., 1999. A preliminary sediment budget for the Winyah Bay estuary, South Carolina, USA. Marine Geology 162, 133-144.

Perillo, G.M.E., 1995. Definitions and geomorphic classifications of estuaries. Geomorphology and Sedimentology of Estuaries, G.M.E. Perillo (editor), New York, Elsevier, 53.

Pethick, J., 1984. An introduction to coastal geomorphology. London, Edward Arnold Ltd.

Phillips, J.D., 1986. The utility of the sediment budget concept in sediment pollution control. Professional Geographer 38(3), 246-252.

Phillips, J.D., 1989. River discharge and sediment deposition in the upper Pamlico estuary. In: Neilson, B.J., Kuo, A., and Brubaker, J. (editors), Estuarine Circulation, Humana, Clifton, N.J.

Phillips, J.D., 1997. A short history of a flat place: three centuries of geomorphic change in teh Croatan National Forest. Annals of the Association of American Geographers 87(2), 197-216.

Phillips, J.D., 1991a. Fluvial sediment delivery to a coastal plain estuary in the Atlantic drainage of the United States. Marine Geology 98, 121-134.

Phillips, J.D., 1991b. Fluvial sediment budgets in the North Carolina Piedmont. Geomorphology 4, 231-241.

Phillips, J.D., 1992. The source of alluvium in large rivers of the lower coastal plain of North Carolina. Catena 19, 59-75.

Phillips, J.D., and Slattery, M.C., 2006. Sediment storage, sea-level, and sediment delivery to the ocean by coastal plain rivers. Progress in Physical Geography 30(40), 513.

Pritchard, D.W., 1967. Observations of circulation in coastal plain estuaries. Estuaries, American Association of Advanced Science Publication 83, 3-5.

Quafisi, D., 2010. Assessment of modern sediment storage in the floodplain of the lower Tar River, North Carolina. M.S. Thesis, East Carolina University, Greenville, North Carolina.

Richardson, C.J., Walbridge, M.R., and Burns, A., 1988. Soil chemistry and phosphorus retention capacity of North Carolina coastal plain swamps receiving sewage effluent. NC-WRRI-88-241.

Riggs, S.R., Cleary, W.J., and Snyder, S.W., 1995. Influence of inherited geologic framework on barrier shoreface morphology and dynamics. Marine Geology 126, 213-234.

Riggs, S.R., and Ames, D.V., 2003. Drowning the North Carolina coast: sea-level rise and estuarine dynamics. North Carolina Sea Grant, UNC-SG-03-04, 1-152.

Ritchie, J.C., and McHenry, J.R., 1990. Application of radioactive fallout Cesium-137 for measuring soil erosion and sediment accumulation rates and patterns: a review. Journal of Environmental Quality 19, 215-233.

Robbins, J.A., and Edgington, D.N., 1975. Determination of recent sedimentation rates in Lake Michigan using Pb-210 and Cs-137. Geochimica et Cosmohimica Acta 39, 285-304.

Rosati, J.D., 2005. Concepts in sediment budgets. Journal of Coastal Research 21(2), 307-322.

Rusnak, G.A., 1967. Rates of sediment accumulation in modern estuaries. Estuaries 83, 180.

Sanders, R., 2002. Sedimentation rates and metal retention in an urban Louisiana swamp. M.S. Thesis (unpublished), Louisiana State University, LA.

Soetaert, K., and Middelburg, J.J., 2009. Modeling eutrophication and oligotrophication of shallow-water marine systems: the importance of sediments under stratified and well-mixed conditions. Hydrobiologia 629, 239-254.

Swarzenski, P.W., Porcelli, D., Andersson, P.S., and Smoak, J.M., 2008. The behavior of U- and Th- series nuclides in the estuarine environment. Radioactivity in the Environment, Elsevier, Chapel Hill, North Carolina.

Tully, L.S., 2004. Evaluation of sediment dynamics using geochemical tracers in the Pamlico Sound estuarine system, North Carolina. M.S. Thesis (unpublished), East Carolina University, Greenville, NC.

Turner, R.E., Milan, C.S., and Swenson, E.M., 2006. Recent volumetric changes in salt marsh soils. Estuarine, Coastal and Shelf Science 69, 352-359.

Ward, L.G., Kearney, M.S., and Stevenson, J.C., 1998. Variations in sedimentary environments and accretionary patterns in estuarine marshes undergoing rapid submergence, Chesapeake Bay. Marine Geology 151, 111-134.

Wells, J.T., and Kim, S.Y., 1989. Sedimentation in the Albemarle-Pamlico Lagoonal System: synthesis and hypotheses. Marine Geology 88, 263.

Wells, J.T., and Kim, S.Y., 1991. Trapping and escape of fine-grained sediments: Neuse River estuary, NC. Coastal Sediments, 775-788.

Yabro, L.A., Carlson, P.R., Fisher, T.R., Chanton, J.P., and Kemp, W.M., 1983. A sediment budget for the Choptank River Estuary in Maryland, USA. Estuarine, Coastal, and Shelf Science 17, 555-570.

CHAPTER 5

Estuarine Shoreline Change: Implications for Coastal Zone Management in North Carolina

1.0 Introduction and Context

Shoreline change is a process that is influenced by natural (e.g., storm waves and currents) and anthropogenic activities (e.g., bulkheading), and these dynamics threaten ecosystems, human developments, and economic sustainability (Rabenold 2013; Charlier and De Meyer 1998; French 2003). In 2003 it was estimated that 53% of the United States' population lived in a coastal county (NOAA 2004). Loss of property from erosion and sea-level rise will reach over $500 million per year over the next several decades (Heinz 2000; Rabenold 2013). According to the IPCC, eustatic sea-level rise is 2-3 mm yr^{-1}, resulting in an increase of mean sea-level (MSL) of 0.2-0.6 m by the year 2100 (IPCC 2007). In North Carolina, a report by the Coastal Resources Commission (CRC) indicates rates of relative sea-level (RSL) rise of 2.0-4.3 mm yr^{-1} (DCM 2010; Horton et al. 2009; Kemp et al. 2009; NOAA 2004). While there is much debate regarding the exact rate, sea-level rise will impact many coastal communities around the world (Horton et al. 2009; Kemp et al. 2009; NOAA 2004; Poulter et al. 2009). This has the potential to exacerbate the problem of shoreline erosion. Indeed, storms such as hurricanes also affect rates of shoreline erosion depending on their timing and intensity (Day et al. 2007; List et al. 2006; Phillips et al. 1999).

Despite the potential risks, coastal counties are continuing to grow in population (Crossett 2013; Rabenold 2013). Nationwide, it is estimated that over the last ~50 years there has been an average increase of 70% in the populations of coastal counties (Wilson and Fischetti 2010). Crossett (2013) predicts a growth of 8% over the next 7 years. In North Carolina, counties such as Brunswick, Currituck, and Dare exhibited an over 400% increase in total population, with Dare County ranking 17th in the nation for percent increase in population (Wilson and Fischetti 2010). The accompanying increase in development has been shown to

decrease the capacity of coastal environments to respond to natural processes such as sea-level rise, erosion, and storms (Kittinger and Ayers 2010).

One way that increased population and development impact natural coastal processes is through the construction of shoreline protection structures, or "armoring" of the shoreline (Douglass and Pickel 1999). A study in Mobile Bay, Alabama, found that by 1997 only 70% of the shoreline was still classified as natural, while the remainder was armored with either bulkheads or revetments (Douglass and Pickel 1999). In other states, such as New Jersey, the amount of armored shoreline is reportedly as high as 75% (Erdle et al. 2006). In North Carolina, the total amount of shoreline armoring is approximately 5% across the twenty coastal counties; however, in Carteret County as much as 15% of the county's shoreline is modified (McVerry 2012). To meet both the demands of development and protect coastal habitat, natural processes such as erosion need to be taken into account when formulating management plans for the estuarine shorezone.

The issue of estuarine shoreline erosion is not unique to North Carolina, and approaches to everything from measuring erosion to managing development vary by state. Furthermore, a lack of unifying policies at the federal level has hindered the creation of more comprehensive and comparable management plans for the coastal zone (Eichbaum 1994). Policies targeting different aspects of coastal management exist at all levels of government and commonly overlap in jurisdiction (Eichbaum 1994). Currently, the main federal legislation facilitating coastal management is the Coastal Zone Management Act (CZMA), which was enacted in 1972 as an attempt to consolidate efforts and provide a supporting framework for management at the federal level (Christie 1994; Hershman et al. 1999; Kittinger and Ayers 2010). The objective of the CZMA was to "…preserve, protect, develop, and where possible, to restore or enhance, the

resources of the Nation's coastal zone for this and succeeding generations" (Christie 1994; CZMA 1972; Hershman et al. 1999). This was to be accomplished by supporting the implementation of state coastal management programs.

North Carolina was the first state to enroll in the Coastal Management Program (NCDENR 2011; NOAA 2010). The state passed its Coastal Area Management Act (CAMA) in 1974, and the National Oceanic and Atmospheric Administration (NOAA) approved their Coastal Management Plan (CMP) in 1978 (NCDENR 2011; NOAA 2010). Key to the execution of the NC CAMA is the central authority of the NC Coastal Resources Commission (CRC) (Kittinger and Ayers 2010). In a 1975 revision of the CAMA, the CRC was created as a central governing body that would; "…designate areas of environmental concern [AECs], adopt rules and policies for coastal development within those areas, and certify local land-use plans." (Fig. 1; DCM 2007). The CRC provides not only oversight to agency and local government management plans and policies but also provides minimum guidelines that all coastal counties are required to abide (Kittinger and Ayers 2010). The CRC is supported by the DCM and the Coastal Resources Advisory Council (CRAC). The DCM is responsible for land-use planning and all the associated permitting and enforcement that accompany coastal development in the State's 20 CAMA counties (DCM 2010). Of specific relevance to this thesis, the DCM is also tasked with the permitting and regulation of estuarine shoreline modification.

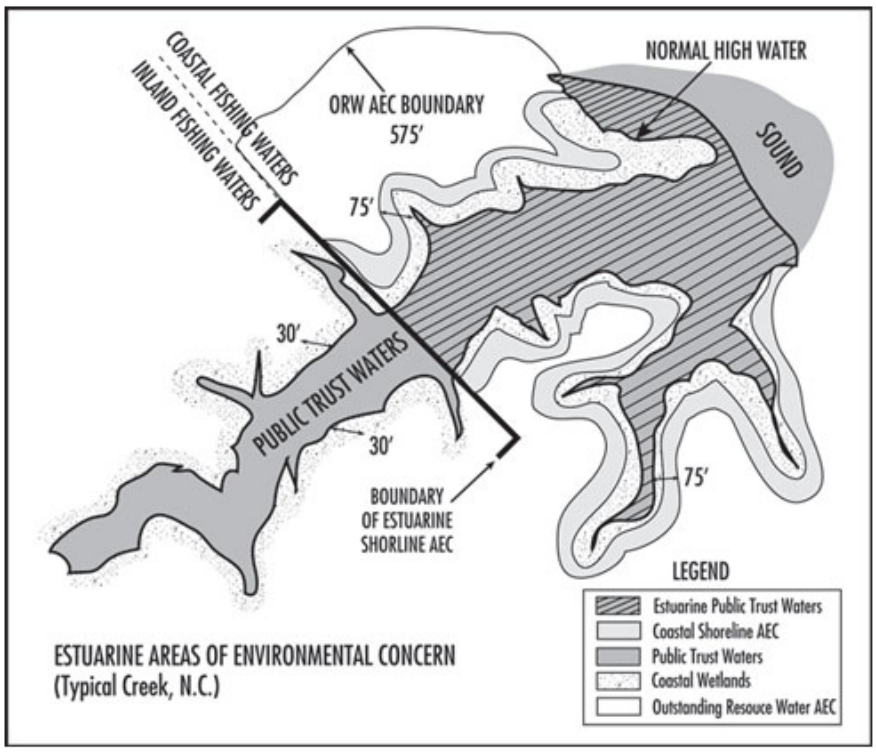

Fig. 1 Map illustrating the boundaries and setbacks of the AECs as they are defined by the North Carolina CAMA (DCM 2010).

The overall objective of this thesis was to examine estuarine shoreline dynamics in the large, shallow, Albemarle-Pamlico Estuarine system (APES) of North Carolina. Specifically, this thesis investigated: 1) estuarine shoreline change and its drivers over varying temporal and spatial scales, 2) the role of shoreline erosion in a sediment budget, and 3) the potential impacts of shoreline hardening on the functioning of the system. This was accomplished using a combination of field and laboratory methods, as well as the application of remote sensing and computer modeling techniques. This chapter summarizes the results of this dissertation, and explores the implications of this study's results on future estuarine shoreline management in North Carolina.

2.0 Summary and Management Implications

Shoreline change was found to be highly variable over different timescales and by site. The average historical (50yr era) rate of shoreline change, for all of the study sites, was -0.5 m yr^{-1}. This is comparable with previous studies of estuarine shorelines in North Carolina (Cowart et al. 2010; Cowart et al. 2011; Riggs and Ames 2003). Rates of shoreline change were also determined for discrete time periods comprising the fifty-year-era; however, no clear trend of accelerating shoreline erosion was observed. For the 1998-2007 period, shoreline change was investigated in-detail for the Tar-Pamlico estuary (PRE; which included the GCP site), as well as for the other four individual sites (GRG, KHW, OCR, and PPP). The shoreline change rate ranged from -0.03 ± 0.5 to -1.0 ± 0.9 m yr^{-1} with sites GCP and KHW being the end members. While there was little change in shoreline position observed at the GCP site for this era (H4; within error), the mean SCR for the entire PRE estuary trunk was -0.5 m yr^{-1}.

To observe these changes in the shorezone at a higher frequency and resolution, the combination of Real-time Kinematic GPS (RTK-GPS) surveys and balloon-aerial photography (Aerostat) were utilized (Eulie et al. 2013). The two methods facilitate rapid, high-accuracy, and cost-effective shoreline surveys in the field. This study found that Aerostat-mapped shoreline positions were comparable in accuracy to the RTK-GPS (Eulie et al. 2013). However, the former required the latter, i.e., RTK-GPS is necessary to provide highly accurate control points with which to georeference the Aerostat imagery (Eulie et al. 2013). The imagery is valuable as it provides contextual information that is useful for analyzing the process and drivers of change in coastal environments (Eulie et al. 2013). Despite the use of high-accuracy methods such as the RTK-GPS and Aerostat, the range of change uncertainty was greater for the sub-annual than for longer estimates of shoreline change due to annualizing the error (even a lower error) from the shorter survey periods. This is one reason that previous shoreline change studies, and management plans, focus on the historical rate of change (i.e., over many decades). Only in recent years has the accuracy of field and remote sensing mapping techniques increased to the point where these finer-scale changes can be resolved with certainty. As the cost of these technologies decreases, and the accuracy increases, they should be utilized more often to examine fine-scale variability in shoreline position, in the larger context of the historical trend.

As stated, these methods were employed to examine sub-annual (S1-S5; bi-monthly) change in shoreline position at the individual study sites. The greatest variability, both between sites and eras, was observed in the sub-annual SCRs. At some sites the annualized rate of change was significant and clearly exceeded the error (e.g., PPP and GCP), at others (e.g., KHW, GRG, and OCR) much of the measured shoreline change fell within error. However, during the S2 era, the SCR for the GRG site also exceeded the error. Erosion-accretion cycles were also

observed at the PPP and GCP sites for consecutive eras; this was likely a response to differences in wave energy.

Waves were modeled for individual events and the entire sub-annual time period using a coupled hydrodynamic-wave model. The model was validated using observations of wave height from two storm events in the APES prior to running the simulations for the sub-annual eras. Wave heights were simulated for three meteorological events that occurred during the S2 era, including the passage of Hurricane Earl. A wind ramp simulation was also run to examine the role of wind direction on wave energy and shoreline erosion at the sites, and the results from the ramp were utilized to hind-cast wave height for the sub-annual periods (S1-S5). The simulations indicate that, while the greatest significant wave heights did occur during the S2 era, they occurred at different times during the era, at the respective sites. This is largely due to differences in wind direction and shoreline orientation at the sites. Also, the erosion-accretion cycle from S2 to S3 at the PPP and GCP sites was observed to correspond with differences in wave energy over the sub-annual eras. The greatest wave heights (and energy) were simulated to occur during the eras of greatest erosion. At the PPP site, the 16% of simulated wave heights >0.4 m occurred during the S2, S4, and S5 eras, when the rate of erosion was high, but accounted for 60% of total wave energy simulated over the sub-annual time period.

Coastal storms have been highlighted in previous studies as important mechanisms for the shoreline erosion (Camfield and Morang 1996; Dolan et al. 1978; List et al. 2006; Phillips 1999), and the research here provide quantified evidence. The present study simulated significant wave heights of 0.6 – 1.5 m that corresponded to significantly higher rates of erosion at the sites. At the GRG site, rates of -8.6 to -9.7 m yr^{-1} were observed. During Hurricane Earl, the annualized SCR at the PPP site was almost -20 m yr^{-1}. But it is notable, that while the SCR

at the PPP site was significantly greater, post-storm recovery in the form of several meters of accretion was also observed during the next era (S3).

Sediment bank shorelines such as the PPP or GCP sites, and oceanfront shores, have the potential to recover through the transport of sediment back onto the shore face during from lower energy waves; whereas, for marsh shorelines such as the GRG site, the post-storm shoreline position represents the new marsh edge. Therefore, the contribution of coastal storms or other high-energy wave events, likely has a greater impact on the long-term rate of change along wetland shorelines such as marshes. This response to storms could impact development in North Carolina's coastal counties where 65% of the estuarine shoreline is composed of marsh, and in some counties, such as Currituck and Hyde, over 80% of the shoreline is marsh (McVerry 2013). Finally, when the current rate of sea-level rise (2.0-4.3 mm yr^{-1}) is also factored into the scenario, there is an even greater potential for the net loss of marsh shorelines due to the combination of shoreline erosion, inundation, and the presence of development that impedes the landward transgression of these systems (Brinson et al. 1995; Horton et al. 2009; Kemp et al. 2009; NOAA 2004; Voss 2009). This is important because future loss of wetland habitat from erosion and inundation may impact the resilience of coastal communities to impacts such as storm surge (Barbier et al. 2013). While the protection provided by wetlands from wave energy and storm surge is widely known, a recent study in the Mississippi River Delta by Barbier et al. (2013) quantified the cost savings in damages from having more wetland cover. They found that damage costs from storm surge could be reduced by over $700,000 (or the equivalent of saving 3-5 properties) at a single marsh transect if there was as little as a 1% increase in the marsh-water ratio along that transect (Barbier et al. 2013).

Erosion from wetland shorelines also represents an important source of fine sediments to the larger estuarine system. Within the Tar-Pamlico estuary, wetlands (marshes and swamp) represent 40% of the total shoreline (not including small tributary creeks), and 53% of all natural shoreline. A fine sediment budget was constructed during this study to examine the contribution of shoreline material to larger estuarine system. The budget was constructed using data from previous research in the APES by Marciniak (2008), Quafisi (2010), and others, as well as from the present study. While the contribution of fine sediment was found to vary significantly depending on characteristics such as dry bulk density (DBD) and scarp height, the final budget presented in Chapter 4 estimated 43% of the fine material was incoming from shoreline erosion. This is less than the 85-98% of material estimated by other studies in the Neuse River estuary and Chesapeake Bay (Benninger and Wells 1993; Marcus and Kearny 1991; Pachineelam et al. 1999; Yarbro et al. 1983). However, as the discharge from coastal rivers is increasingly impacted by the presence of dams, shoreline erosion is hypothesized to become a more important source of material (Marcus and Kearny 1991). Given this hypothesis, the rate and extent to which estuarine shorelines are modified with structures will impact the supply of sediment to systems such as the APES.

As part of the sediment budget, rates of sediment accumulation and the storage of fine material were calculated. This was used to determine the percent of supplied material to the Tar-Pamlico that was stored, and the percent that was available for export to the adjacent Pamlico Sound. Rates of sediment accumulation were determined through the use of the radionuclides ^{137}Cs and ^{210}Pb. Linear rates of sediment accumulation ranged from 0.1 to 0.4 cm yr^{-1} across the Tar-Pamlico estuary. Sedimentation in the Upper region of the Tar-Pamlico is likely controlled by river hydrodynamics and is characterized by mostly lower (<0.2 cm yr^{-1}) rates of

accumulation. The Trunk region of the estuary is characterized by higher rates of accumulation (0.2 to 0.4 cm yr^{-1}), with the greatest rate of accumulation seen at PRE-6, located in the center of the Middle region. Along the Middle, sedimentation appears to be controlled by a combination of estuary geometry and hydrology. Fine sediments supplied by the Tar River and eroded from the marshes and swamps are potentially deposited in the shallow bay around site PRE-4. However, at the southern end of the embayment the estuary narrows considerably, and radionuclide activity profiles for a site located there indicate scouring of the seabed due to greater flow speeds. As the estuary widens again, material is accumulated in the regions around sites PRE-6 to PRE-9. This area represents the primary sediment depocenter for the Tar-Pamlico estuary, where over 80% of the supplied material is stored. Overall, this study estimates that 93% of all fine sediment supplied to the Tar-Pamlico is ultimately stored within the system, with only a small fraction (7%) potentially exported to Pamlico Sound. This is comparable with other studies in the APES and Chesapeake Bay.

3.0 Implications for Estuarine Shoreline Management in North Carolina

Under ideal conditions, coastal management and waterfront development plans would account for natural processes such as waves and currents, the local sediment budget, shoreline migration and sea-level rise (Charlier and De Meyer 1998; Roman and Nordstrom 1996). Effective coastal management should strive to address problems and conflicts in advance (Charlier and De Meyer 1998; Kittinger and Ayers 2010). Instead, most responses to shoreline erosion are reactive and without advanced planning (Charlier and De Meyer 1998). Problems are addressed on a case-by-case basis and dealt with as they occur. Another issue is that management programs can overlap in jurisdiction and management agencies often have

conflicting or competing objectives when it comes to resource management (Charlier and De Meyer 1998; Kittinger and Ayers 2010). Federal programs such as the CZMA have attempted to minimize these problems but have certainly not eliminated them (Charlier and De Meyer 1998; Christie 1994; Kittinger and Ayers 2010). However, partnerships for addressing coastal and ocean issues, such as the Governors South Atlantic Alliance (GSAA), the Southeast Coastal Ocean Observing Regional Association, and the Chesapeake Bay Program, show how coastal management can become more integrated and improve in the future. It is recommended that states foster these partnerships and that support be provided at the federal level (NOAA already supports some of the aforementioned programs) to promote these efforts and assist in regional and inter-state coordination.

Online portals that facilitate the timely and affordable, dissemination of information to managers, scientists, and the public are also becoming important tools. Products such as: the NC DCM's online portal (i.e., the Estuarine Shoreline Stabilization Decision Tree), the NC ONEMAP, the NC Coastal Atlas, Maryland's coastal Atlas (i.e., Shorelines), and Virginia's Coastal GEMS. These tools provide data and educate the public on the coastal zone and provide regulatory and permitting information (MDDNR 2012; DCM 2010; VADEQ 2012). Maryland's portal is a good example; it enables users to look at historical and modern erosion rates, hazard and vulnerability data, storm surge and sea-level rise projections, policies and regulations, inventories of shoreline engineering and other projects as well as environmental data, base maps, and aerial images (MDDNR 2012).

Realistically, the variable response of estuarine shorelines to episodic events and wave energy creates an even more complex management situation for North Carolina and the CRC and DCM. All of the shorelines discussed in this dissertation fall within the Estuarine System AEC

as designated by the CRC (DCM 2010; Heath and Owens 1994). Currently, the Estuarine Shoreline AEC extends from a baseline of normal high water, or normal water level, to a distance of 75 ft (22.9 m) inland (Fig. 1; DCM 2010). This zone is extended to 575 ft (175.3 m) where adjacent to designated Outstanding Resource Waters (Fig. 1; DCM 2010). There are currently no erosion set-backs for development within this AEC, such as for the Ocean AEC; however, there is a standard 30 ft (9.1 m) buffer required between new development and the baseline (DCM 2010).

According to NOAA (2012a), most estuarine shorelines in the United States lack sufficient data to establish set-back erosion rates, as is done for many oceanfront shorelines. In North Carolina, there is potential within the existing regulatory framework (i.e., the AECs) to implement set-backs or a system of rolling easements, but regulatory actions such as this must consider socioeconomic impacts as well as environmental factors (e.g., erosion rates). With the recent completion of the DCM's Estuarine Shoreline Mapping Project (ESMP), the first continuous digital map of the entire estuarine shoreline of North Carolina is now available (McVerry 2012). The DCM plans to produce new estuarine shoreline maps on a regular cycle, similar to the current method of mapping oceanfront erosion rates (every 5 years; DCM 2013). With additional shoreline position data, North Carolina will be able to produce detailed maps of estuarine shoreline erosion. Results from this dissertation research, and other on-going research efforts will help understand and evaluate the observed dynamics. As observed in this dissertation, erosion rates can vary greatly between shoreline types and locations. The continued mapping effort by the DCM will provide the level of detail necessary to apply erosion set-backs to the State's estuarine shorelines, although the environmental, economic, and social ramifications will need further attention.

For implementation, the DCM could utilize the existing estuarine AEC baseline, or the line of stable vegetation (as utilized for the ESMP to designate the shoreline), to set a baseline for measuring erosion set-backs or defining an erosion easement. For clarity, it would make sense that the resulting set-back lines are comparable to the oceanfront system's which are based on erosion rates and structure size. Based on the findings in this and other work, shoreline type should be considered in the estuarine system. For example, the South Carolina DHEC recommended the implementation of set-back lines based on the erosion rates of different types of estuarine shorelines (NOAA 2012a; SCDHEC-OCRM 2010). Across the vast NC coastal zone, a hybrid approach of applying set-back rates based on erosion along shorelines with the most data, or most prone to erosion (based on shoreline type), and a standard set-back for other shorelines could be applied. This type of approach is currently utilized in Minnesota for shorelines along Lake Superior (NOAA 2013a). Minnesota's North Shore Management Plan (NSMP) applies a set-back of "50 times the annual erosion rate plus 25 feet" where enough shoreline data is available, and applies a standard set-back of 125 ft for all other shorelines (NOAA 2013a). This type of hybrid approach could facilitate the implementation of an overall estuarine shoreline set-back system in North Carolina now, with more site-specific set-backs where adequate data on shoreline erosion already exists. In addition to set-backs, efforts could be considered to encourage the use of more "soft" shoreline protection strategies such as vegetative plantings or oyster sills, which can provide protection for estuarine shorelines from erosion, and benefit nearby development. These methods have been shown to attenuate erosive energy from waves and storm surge, while still allowing an exchange of water and sediment between the shoreline and adjacent estuary (Hardaway and Byrne 1999; Nordstrom 1992; NRC 2007; Rogers and Skrabal 2001).

However, more study of estuarine shorelines would be necessary before implementing any of the measures discussed here. In particular, ecological and socioeconomic issues must be evaluated. Coastal managers will need to consider how set-backs and hardening limitations might alter ecosystem services or property values. Additionally, the efficacy of shoreline erosion mitigation measures (i.e., engineering approaches) should be further investigated. From a geoscience standpoint, there is limited knowledge on the processes that control estuarine shoreline change, and how current and future human activities (e.g., development), or sea-level rise may alter those processes over varying temporal and spatial scales. In conclusion, this research has examined and identified some of the processes and factors influencing estuarine shoreline change, as well as how shoreline dynamics can affect the sedimentary functioning of the larger estuarine system. Additional interdisciplinary investigation is essential to improve our understanding of estuarine system behavior and potential management implications.

REFERENCES

CAMA, 1974. Coastal Area Management Act, 113A.

CZMA, 1972. Coastal Zone Management Act.

Barbier, E.B., Georgiou, I.Y., Enchelmeyer, B., Reed, D.J., 2013. The value of wetlands in protecting southeast Louisiana from hurricane storm surges. PLoS ONE 8(3), 1-6.

Benninger, L.K., and Wells, J.T., 1993. Sources of sediment to the Neuse River estuary, North Carolina. Marine Chemistry 43, 137-156.

Byrne, J.P., 2010. Rising seas and common law baselines: a comment on regulatory takings discourse concerning climate change. Georgetown Law Faculty Publications and Other Works, Georgetown University.

Camfield, F.E., Morang, A., 1996. Defining and interpreting shoreline change. Ocean and Coastal Management 32(3), 129-151.

Charlier, R.H., De Meyer, C.P., 1998. Coastal Erosion: Response and Management. Springer, New York.

Christie, D.R., 1994. Coastal and Ocean Management Law. West Publishing, St. Paul.

Christie, D.R., 2009. Of beaches, boundaries, and SOBs. Journal of Land Use and Environmental Law 25, 1-75.

Cowart, L., Corbett, D.R., Walsh, J.P., 2011. Shoreline change along sheltered coastlines: insights from the Neuse River Estuary, NC, USA. Remote Sensing 3, 1516-1534.

Crossett, K.M., Culliton, T.J., Wiley, P.C., Goodspeed, T.R., 2004. Population trends along the coastal United States: 1980-2008.

Day, J.W., Boesch, D.F., Clairain, E.J., Kemp, G.P., Laska, S.B., Mitsch, W.J., Orth, K., Mashriqui, H., Reed, D.J., Shabman, L., Simenstad, C.A., Streever, B.J., Twilley, R.R.,

Watson, C.C., Wells, J.T., Whigham, D.F., 2007. Restoration of the Mississippi Delta: Lessons from Hurricanes Katrina and Rita. Science 315(5819), 1679-1684.

DCM, 2010. The Coastal Area Management Act. http://portal.ncdenr.org/web/cm/coastal-area-management-act1.

DCM, 2013. Oceanfront Shorelines: Erosion and Oceanfront Development. http://portal.ncdenr.org/web/cm/what-you-should-know-about-erosion-and-oceanfront-development.

Dolan, R., Hayden, B., Heywood, J., 1978. Analysis of coastal erosion and storm surge hazards. Coastal Engineering 2, 41-53.

Douglass, S.L. and Pickel, B.H., 1999. The effect of bulkheads on urban bay shorelines. Shore and Beach 67, 19-25.

Eichbaum, W., 1994. Coastal Management and Policy, in: Commission on Geosciences, E., and Resources (Ed.), Environmental Science in the Coastal Zone: Issues for further research.

Erdle, S.Y., Davis, J.L.D., Sellner, K.G., 2006. Management, Policy, Science, and Engineering of Nonstructural Erosion Control in the Chesapeake Bay. Living Shoreline Summit, Williamsburg, Virginia.

Eulie, D.O., Walsh, J.P., Corbett, D.R., 2013. High-resolution Analysis of Shoreline Change and Application of Balloon-based Aerial Photography, Albemarle-Pamlico Estuarine System, North Carolina, USA. Limnology and Oceanography: Methods 11, 151-160.

French, P.W., 2003. Coastal and Estuarine Management. Routledge, London.

Hardaway, C.S., Byrne, R.J., 1999. Shoreline management in Chesapeake Bay. Virginia Institute of Marine Sciences, Gloucester Point, Virginia.

Heath, M.S., Owens, D.W., 1994. Coastal management law in North Carolina: 1974-1994. North Carolina Law Review: Coastal Management 72, 1413-1451.

Hershman, M.J., Good, J.W., Bernd-Cohen, T., Goodwind, R.F., Lee, V., Pogue, P., 1999. The effectiveness of coastal zone management in the United States. Coastal Management 27, 113-138.

Horton, B.P., Peltier, W.R., Culver, S.J., Drummond, R., Engelhard, S.E., Kemp, A.C., Mallinson, D., Thieler, E.R., Riggs, S.R., Ames, D.V., and Thomson, K.H., 2009. Holocene sea-level changes along the North Carolina coastline and their implications for glacial isostatic adjustment models. Quaternary Science Reviews 28, 1725-1736.

Kemp, A.C., Horton, B.P., Culver, S.J., Corbett, D.R., van de Plassche, O., Gehrels, W.R., Douglas, B.C., and Parnell, A.C., 2009. Timing and magnitude of recent accelerated sea-level rise (North Carolina, United States). Geology 37, 1035-1038.

Kittinger, J.N., Ayers, A.L., 2010. Shoreline armoring, risk management, and coastal resilience under rising seas. Coastal Management 38, 634-653.

List, J.H., Farris, A.S., Sullivan, C., 2006. Reversing storm hotspots on sandy beaches: spatial and temporal characteristics. Marine Geology 226, 261-279.

Marciniak, K.J., 2008. Sediment dynamics in tributaries of the Neuse River Estuary, North Carolina. Un-published thesis, East Carolina University, Greenville, NC.

Marcus, W.A., and Kearney, M.S., 1991. Upland and coastal sediment sources in a Chesapeake Bay estuary. Annals of the Association of American Geographers 81(3), 408.

McVerry, K., 2012. North Carolina estuarine shoreline mapping project: statewide and county statistics. North Carolina Division of Coastal Management, 1-145.

NOAA, 2010. Ocean and Coastal Management in North Carolina. Office of Ocean and Coastal Resource Management.

NOAA, 2012a. Construction setbacks. Office of Ocean and Coastal Resource Management. http://coastalmanagement.noaa.gov/initiatives/shoreline_ppr_setbacks.html.

NOAA, 2012b. Erosion Control Easements. Office of Ocean and Coastal Resource Management. http://coastalmanagement.noaa.gov/initiatives/shoreline_ppr_ easements.html.

Nordstrom, K.F., 1977. Bayside beach dynamics: implications for simulation modeling on eroding, sheltered, tidal beaches. Marine Geology 25, 333-342.

Nordstrom, K.F., 1992. Estuarine Beaches. Elsevier Applied Science, New York.

NRC, 2007. Mitigating Shoreline Erosion along Sheltered Coasts. National Academies Press, Washington.

Patchineelam, S.M., Kjerfve, B., and Gardner, L.R., 1999. A preliminary sediment budget for the Winyah Bay estuary, South Carolina, USA. Marine Geology 162, 133-144.

Phillips, J.D., 1999. Event timing and sequence in coastal shoreline erosion: Hurricanes Bertha and Fran and the Neuse Estuary. Journal of Coastal Research 15, 616.

Poulter, B., Feldman, R.L., Brinson, M.M., Horton, B.P., Orbach, M.K., Pearsall, S.H., Reyes, E., Riggs, S.R., Whitehead, J.C., 2009. Sea-level rise research and dialogue in North Carolina: creating windows for policy change. Ocean and Coastal Management 52, 147-153.

Quafisi, D., 2010. Assessment of modern sediment storage in the floodplain of the lower Tar River, North Carolina. M.S. Thesis, East Carolina University, Greenville, North Carolina.

Rabenold, C., 2013. Coastal zone management: Using no-build areas to protect the shorefront. Coastal Management 41(1), 294-311.

Riggs, S.R., Ames, D.V., 2003. Drowning the North Carolina coast: sea-level rise and estuarine dynamics. North Carolina Sea Grant, North Carolina.

Rogers, S., Skrabal, T.E., 2001. The Soundfront Series: Managing erosion on estuarine shorelines. UNC-SG-01-12, North Carolina.

Roman, C.T., Nordstrom, K.F., eds., 1996. Estuarine Shores: Evolution, Environments and Human Alterations. John Wiley & Sons, London.

SCDHEC-OCRM, 2010. Adapting to shoreline change: A foundation for improved management and planning in South Carolina. Shoreline Change Advisory Committee.

Wilson, S.G., Fischetti, T.R., 2010. Coastline population trends in the United States: 1960 to 2008. U.S. Department of Commerce, Economics, and Statistics Administration, U.S. Census Bureau.

Yabro, L.A., Carlson, P.R., Fisher, T.R., Chanton, J.P., and Kemp, W.M., 1983. A sediment budget for the Choptank River Estuary in Maryland, USA. Estuarine, Coastal, and Shelf Science 17, 555-570.

APPENDIX A: PERMISSION LETTER

Devon Olivola Eulie
605 Bracken Fern Road
Wilmington, NC 28405

April 11, 2014

Dr. Paul Kemp
1000 Pope Road
Honolulu, HI, 96822

Dear Dr. Paul Kemp:

I am completing a doctoral dissertation at East Carolina University entitled "Examination of Estuarine Sediment Dynamics: Insights from the Large, Shallow, Albemarle-Pamlico Estuarine System, NC, U.S.A." I would like your permission to reprint in my dissertation the following published work, of which I am the lead author:

Eulie, D.O., Walsh, J.P., and Corbett, D.R., 2013. High-resolution analysis of shoreline change and application of balloon-based aerial photography, Albemarle-Pamlico Estuarine System, North Carolina, USA. *Limnology and Oceanography: Methods*, 11, 151-160.

The published work will be reproduced in a Microsoft Word format as Chapter 2 of my doctoral dissertation.

The requested permission extends to any future revisions and editions of my dissertation, including non-exclusive world rights in all languages, and to the prospective publication of my dissertation by UMI. These rights will in no way restrict republication of the material in any other form by you or by others authorized by you. Your signing of this letter will also confirm that you own [or your company owns] the copyright to the above-described material.

If these arrangements meet with your approval, please sign this letter where indicated below and return it to me by email (eulied@uncw.edu) or fax (910-962-7634). Thank you very much.

Sincerely,

[Devon Olivola Eulie]

PERMISSION GRANTED FOR THE USE REQUESTED ABOVE:

[Dr. Paul Kemp]

4/11/14
Date